

ANALYZING THE IMPACT OF ENERGY STORAGE CAPACITY ON
RENEWABLE ENERGY GENERATION USING WIND POWER: THE CASE OF
TURKEY

by

Aykut Gül

B.S., Industrial Engineering, Yaşar University, 2018

Submitted to the Institute for Graduate Studies in
Science and Engineering in partial fulfillment of
the requirements for the degree of
Master of Science

Graduate Program in Industrial Engineering

Boğaziçi University

2021

ACKNOWLEDGEMENTS

First of all, I would like to thank my thesis supervisor Aybek Korugan for introducing me this topic. He was very helpful and gave valuable instructions during my thesis. I really enjoyed working together and learned so much from him. I am also very grateful for Emre Kalkan's support during the thesis. He provided me very useful information and I saved considerable amount of time by accessing the information needed quickly, thanks to him. I would like to express my gratitude to Hande Gizem Yaman for being my mentor since very first day of my master's journey. She always supported and encouraged me with her broad vision. I would like to thank my loved ones, my family and my girlfriend, who have supported me during entire process. They always pushed me against each challenge and raised my morale. I will be grateful forever for their love. I would like to express deep gratitude to Kerem Şurğun and Burak Derecik. As a roommate, Kerem really helped me during my first year in İstanbul. We took 3 courses together with Burak and could not count the hours as we try to catch deadlines. Special thanks go to all friends and my professors. I learned a lot from each person I met and enjoyed my time at Boğaziçi.

ABSTRACT

ANALYZING THE IMPACT OF ENERGY STORAGE CAPACITY ON RENEWABLE ENERGY GENERATION USING WIND POWER: THE CASE OF TURKEY

Renewable energy sources (RES) are expected to be dominant in near future. However, RES suffer from unavailability and intermittency that causes unreliable energy output due to daily or hourly weather conditions. (Liserre et al., 2010) As the share of renewables increases, electricity systems must gain more flexibility and reliability. Battery energy storage systems (BESS) stand as powerful tools to accelerate transition to sustainable energy. They can help reducing the variability between electricity generation and consumption by storing the excess energy at off-peak period and discharging the energy at peak periods. (Beltran et al., 2013) We considered a hypothetical question on the efficiency of wind power. We coupled wind power generation with BESS to see the impact of storage capacity on this problem. Our ultimate goal is to provide efficiency of wind power using storage. We aimed to determine the hourly optimal storage capacity for one year to utilize wind more and obtain smooth electricity production in national scale. We developed an optimization model that analyzes the system on hourly basis. We modeled BESS as inventory of energy. Using national data, statistical models were developed to capture the uncertainty of both wind energy and demand. We fitted probability distributions for both energy supply and demand. Using probability distributions, we generated different datasets that reflect the hourly energy supply and demand. We ran the optimization model with all possible combinations of supply and demand pairs. This way, we achieved the robustness in optimal storage capacity, utilization level of wind turbines and other resources. The analysis was extended to various scenarios considering different system configurations.

ÖZET

ENERJİ SAKLAMA KAPASİTESİNİN TÜRKİYE'DEKİ YENİLENEBİLİR ENERJİ ÜRETİMİNE ETKİSİNİN ANALİZİ: TÜRKİYE SENARYOSU

Yenilenebilir enerji kaynaklarının (YEK) yakın gelecekte yaygınlaşması beklenmektedir. Ancak, saatlik veya günlük hava koşulları YEK'den güvenilir olmayan enerji arzına neden olmaktadır. (Liserre vd., 2010) Enerji sistemlerindeki YEK'in payı arttıkça, enerji sistemlerinin daha esnek ve güvenilir olması gerekmektedir. Batarya enerji depolama sistemleri (BEDS), sürdürülebilir enerjiye geçişi hızlandırmak için etkili bir araç olabilir. Üretilen fazla enerji, talebin yoğun olmadığı dönemlerde depolanır ve talebin yoğun dönemlerde bu enerji kullanarak elektrik üretimi ve tüketimi arasındaki sapma azaltılabilir. (Beltran vd., 2013) Bu çalışmada, rüzgar enerjisinin verimliliği ile ilgili kurgusal bir sistem dikkate alınmıştır. Rüzgar enerjisi ve BEDS'ler birlikte ele alınmış ve depolama kapasitesinin rüzgar enerjisi verimliliğine etkisi incelenmiştir. Ana amacımız, BEDS ile rüzgar enerjisinin verimliliğinin artırılmasıdır. Bu çalışma, rüzgarı daha verimli kullanmak ve ulusal ölçekte sürekli elektrik üretimi elde etmek için bir yıl boyunca saatlik optimum depolama kapasitesini belirlemeyi hedefler. Bu amaçla, doğrusal optimizasyon modeli geliştirmiştir. BEDS, bir enerji envanteri olarak ele alınmıştır. Hem enerji arzı hem de enerji talebindeki belirsizliği yansıtmak için ulusal veriler kullanarak istatistiksel model geliştirilmiştir. Enerji arzı ve talebi yansıtan olasılık dağılımları belirlenmiştir. Bu dağılımlar kullanılarak, bir yıllık saatlik enerji arzı ve talebini yansıtan çeşitli veri kümeleri oluşturuldu. Tüm olası arz ve talep veri kombinasyonları optimizasyon modelinde kullanıldı. Böylelikle, optimal depolama kapasitesi, rüzgar türbinlerinin kullanım oranı vb. gibi karar değişkenlerinde sağlamlığa erişildi ve sonuçlar raporlandı. Çalışma, farklı sistem kurguları doğrultusunda genişletildi.

TABLE OF CONTENTS

| | |
|--|------|
| ACKNOWLEDGEMENTS | iii |
| ABSTRACT | iv |
| ÖZET | v |
| LIST OF FIGURES | viii |
| LIST OF TABLES | x |
| LIST OF SYMBOLS | xv |
| LIST OF ACRONYMS/ABBREVIATIONS | xvii |
| 1. INTRODUCTION | 1 |
| 2. LITERATURE REVIEW | 5 |
| 2.1. BESS Sizing Methods Literature | 5 |
| 2.1.1. Probabilistic Models | 5 |
| 2.1.2. Deterministic Models | 7 |
| 2.2. BESS Modelling Environment Literature | 8 |
| 2.2.1. Distributed Renewable Energy Systems | 9 |
| 2.2.2. Standalone Hybrid Renewable Energy Systems | 10 |
| 2.2.3. Microgrid | 11 |
| 2.2.4. Renewable Energy Power Plant | 12 |
| 2.2.5. National Scale | 13 |
| 3. PROBLEM DEFINITION and OBJECTIVES | 16 |
| 3.1. Model Assumptions and Methodology | 19 |
| 3.2. Mathematical Model | 21 |
| 3.2.1. Sets | 22 |
| 3.2.2. Parameters | 22 |
| 3.2.3. Decision Variables | 23 |
| 3.2.4. Objective Function | 26 |
| 3.2.5. Constraints | 29 |
| 3.3. Statistical Model | 30 |
| 3.3.1. Hourly Potential Wind Data Distribution Fitting | 33 |

| | |
|--|----|
| 3.3.2. Hourly Electricity Demand Data Distribution Fitting | 38 |
| 4. SCENARIO ANALYSIS | 41 |
| 4.1. Parameter Selection | 41 |
| 4.2. Definition of Scenarios | 43 |
| 4.3. Base Scenario | 44 |
| 4.3.1. Global Base Scenario | 44 |
| 4.3.2. Turkish Base Scenario | 50 |
| 4.4. Battery Technology Scenario | 52 |
| 4.4.1. Long Life Scenario | 52 |
| 4.4.2. Efficiency Scenario | 56 |
| 4.5. No LWSPS Scenario | 57 |
| 5. CONCLUSION | 60 |
| REFERENCES | 65 |
| APPENDIX A: OPTIMIZATION MODEL ROBUST RESULTS | 75 |
| APPENDIX B: ARENA DISTRIBUTION FITTING SUMMARIES | 80 |

LIST OF FIGURES

| | | |
|-------------|---|----|
| Figure 3.1. | Monthly Real-Time Electricity Generation by Wind Energy in Turkey in 2019 (EPIAS, 2020). | 17 |
| Figure 3.2. | Hourly Demand Fluctuation between 7-13 January 2019 (EPIAS, 2020). | 17 |
| Figure 3.3. | Hourly Electricity Generation by Wind and Scaled Load Demand between 7-13 April 2019 (EPIAS, 2020). | 18 |
| Figure 3.4. | Flowchart of robustness operation. | 21 |
| Figure 3.5. | Structure of total system cost. | 27 |
| Figure 3.6. | Real Time Electricity Demand through 2019 in Turkey (EPIAS, 2020). | 32 |
| Figure 3.7. | Fluctuation of Real Time Electricity Demand through 2019 in Turkey (EPIAS, 2020). | 32 |
| Figure 3.8. | Hourly Demand Fluctuation between 7-20 January 2019 (EPIAS, 2020). | 39 |
| Figure 4.1. | Hourly storage level while LWPSP=0.3 in base scenario. | 45 |
| Figure 4.2. | Hourly storage level while LWPSP=0.2 in base scenario. | 45 |
| Figure 4.3. | Monthly energy balance while LWPSP=0.2 in base scenario. | 47 |

| | | |
|--------------|---|----|
| Figure 4.4. | Installed BESS capacity and cumulative emission level for different LWPSP in base scenario. | 48 |
| Figure 4.5. | Installed BESS capacity, cumulative emission and wind utilization level for different LWPSP in base scenario. | 48 |
| Figure 4.6. | Total number of BEV's required for base scenario. | 49 |
| Figure 4.7. | Installed BESS capacity and cumulative emission level for different LWPSP in Turkish energy portfolio scenario. | 51 |
| Figure 4.8. | Average cumulative emission level comparison between base and Turkish energy portfolio scenario. | 51 |
| Figure 4.9. | Hourly storage level with first threshold range while LWPSP=0.22. | 53 |
| Figure 4.10. | Hourly storage level with second threshold range while LWPSP=0.22. | 54 |
| Figure 4.11. | Hourly storage level with third threshold range while LWPSP=0.22. | 54 |
| Figure 4.12. | Total number of BEV's required for long life scenario under full availability assumption. | 55 |
| Figure 4.13. | Hourly storage level with low efficient battery while LWPSP=0.2. | 56 |
| Figure 4.14. | Hourly storage level with ideal battery while LWPSP=0.2. | 57 |
| Figure 5.1. | Installed BESS capacity and wind efficiency under different LWPSP levels. | 62 |

LIST OF TABLES

| | | |
|-------------|---|----|
| Table 3.1. | IC, AIC and RTEG for wind energy in 2 February, 2019 (EPIAS, 2020). | 36 |
| Table 4.1. | Cost parameters of the storage system. | 41 |
| Table 4.2. | Efficiency parameters of LIB technology. | 42 |
| Table 4.3. | Electricity generation costs with different energy sources. | 42 |
| Table 4.4. | Emission factors for electricity generation sources. | 43 |
| Table 4.5. | Financial parameters. | 43 |
| Table 4.6. | Scenarios and their definitions. | 43 |
| Table 4.7. | Base scenario and brief definition. | 44 |
| Table 4.8. | Battery technology scenarios and their definitions. | 52 |
| Table 4.9. | Minimum and maximum allowable SOC for long life scenario. | 53 |
| Table 4.10. | Efficiency configurations for efficiency scenario. | 56 |
| Table 4.11. | Performance measure results for “no LWPSP” scenario. | 58 |
| Table 4.12. | 95% confidence interval for “No LWPSP” scenario. | 59 |

| | | |
|-------------|---|----|
| Table A.1. | Minimum, maximum and average capacity results in global base scenario. | 75 |
| Table A.2. | 3 sigma limits for average capacity results in global base scenario. . | 75 |
| Table A.3. | Minimum, maximum and average capacity results for 1. threshold range. | 76 |
| Table A.4. | 3 sigma limits of average capacity with 1. threshold in long life scenario. | 76 |
| Table A.5. | Minimum, maximum and average capacity results for 2. threshold range. | 76 |
| Table A.6. | 3 sigma limits of average capacity with 2. threshold in long life scenario. | 77 |
| Table A.7. | Minimum, maximum and average capacity results for 3. threshold. | 77 |
| Table A.8. | 3 sigma limits of average capacity with 3. threshold in long life scenario. | 77 |
| Table A.9. | Minimum, maximum and average capacity for low efficiency scenario. | 78 |
| Table A.10. | 3 sigma limits of average capacity in low efficiency scenario. | 78 |
| Table A.11. | Minimum, maximum and average capacity for ideal battery scenario. | 78 |
| Table A.12. | 3 sigma limits of average capacity in ideal battery scenario. | 79 |
| Table B.1. | Arena PDF fitting summary for wind energy supply in January. . . | 81 |

| | | |
|-------------|--|----|
| Table B.2. | Arena PDF fitting summary for wind energy supply in February. . . | 82 |
| Table B.3. | Arena PDF fitting summary for wind energy supply in March. . . . | 83 |
| Table B.4. | Arena PDF fitting summary for wind energy supply in April. . . . | 84 |
| Table B.5. | Arena PDF fitting summary for wind energy supply in May. | 85 |
| Table B.6. | Arena PDF fitting summary for wind energy supply in June. | 86 |
| Table B.7. | Arena PDF fitting summary for wind energy supply in July. | 87 |
| Table B.8. | Arena PDF fitting summary for wind energy supply in August. . . . | 88 |
| Table B.9. | Arena PDF fitting summary for wind energy supply in September. . . | 89 |
| Table B.10. | Arena PDF fitting summary for wind energy supply in October. . . . | 90 |
| Table B.11. | Arena PDF fitting summary for wind energy supply in November. . . . | 91 |
| Table B.12. | Arena PDF fitting summary for wind energy supply in December. . . . | 92 |
| Table B.13. | Arena PDF fitting summary for weekday energy demand in January. . . . | 93 |
| Table B.14. | Arena PDF fitting summary for weekday energy demand in February. . . . | 94 |
| Table B.15. | Arena PDF fitting summary for weekday energy demand in March. | 95 |
| Table B.16. | Arena PDF fitting summary for weekday energy demand in April. | 96 |
| Table B.17. | Arena PDF fitting summary for weekday energy demand in May. | 97 |

| | | |
|-------------|---|-----|
| Table B.18. | Arena PDF fitting summary for weekday energy demand in June. . | 98 |
| Table B.19. | Arena PDF fitting summary for weekday energy demand in July. . | 99 |
| Table B.20. | Arena PDF fitting summary for weekday energy demand in August. | 100 |
| Table B.21. | Arena PDF fitting summary for weekday energy demand in September. | 101 |
| Table B.22. | Arena PDF fitting summary for weekday energy demand in October. | 102 |
| Table B.23. | Arena PDF fitting summary for weekday energy demand in November. | 103 |
| Table B.24. | Arena PDF fitting summary for weekday energy demand in December. | 104 |
| Table B.25. | Arena PDF fitting summary for weekend energy demand in January. | 105 |
| Table B.26. | Arena PDF fitting summary for weekend energy demand in February. | 106 |
| Table B.27. | Arena PDF fitting summary for weekend energy demand in March. | 107 |
| Table B.28. | Arena PDF fitting summary for weekend energy demand in April. | 108 |
| Table B.29. | Arena PDF fitting summary for weekend energy demand in May. . | 109 |
| Table B.30. | Arena PDF fitting summary for weekend energy demand in June. . | 110 |
| Table B.31. | Arena PDF fitting summary for weekend energy demand in July. . | 111 |
| Table B.32. | Arena PDF fitting summary for weekend energy demand in August. | 112 |

| | |
|---|-----|
| Table B.33. Arena PDF fitting summary for weekend energy demand in September. | 113 |
| Table B.34. Arena PDF fitting summary for weekend energy demand in October. | 114 |
| Table B.35. Arena PDF fitting summary for weekend energy demand in November. | 115 |
| Table B.36. Arena PDF fitting summary for weekend energy demand in December. | 116 |

LIST OF SYMBOLS

| | |
|------------------|--|
| A | Useful lifetime of the system |
| bat_util | Overall battery utilization |
| cap | Installed battery capacity |
| chg_eff | Charging efficiency |
| chg | Energy charged to the storage units |
| c_min | Minimum state of charge |
| c_max | Maximum state of charge |
| dischg | Energy discharged from the storage |
| dischg_eff | Discharging efficiency |
| emiss_fact | Unit emission factor |
| emiss_lev | Total cumulative emission level |
| i | Discount rate |
| load_dem | Hourly electricity demand |
| r_stor | Hourly storage level |
| self_dischg | Self discharge rate |
| tot_fos_cost | Total fossil cost |
| tot_INV_cost | Total investment cost |
| tot_MAIN_cost | Total maintenance cost |
| tot_OPE_cost | Total operation cost |
| tot_RE_cost | Total renewable energy generation cost |
| tot_REP_cost | Total replacement cost |
| tot_stor_cost | Total storage cost |
| unit_RE_gen_cost | unit cost of electricity generation by wind energy |
| unit_fos_cost | unit cost of electricity generation by natural gas |
| unit_INV_cost | unit investment cost of storage units |
| unit_OPE_cost | unit operation cost of storage units |
| unit_MAIN_cost | unit maintenance cost of storage units |
| unit_REP_cost | unit replacement cost of storage units |

| | |
|-----------|--|
| util_lev | utilization level of wind energy |
| used_wind | Hourly actual electricity generation by wind |
| wind_out | Hourly forecasted electricity generation by wind |

LIST OF ACRONYMS/ABBREVIATIONS

| | |
|-----------------|--|
| AIC | Available Installed Capacity |
| BESS | Battery Energy Storage Systems |
| BEV | Battery Electric Vehicle |
| BNEF | Bloomberg New Energy Finance |
| CISO | California Independent System Operator |
| CO ₂ | Carbon Dioxide |
| COV | Coefficient of Variation |
| CRF | Capital Recovery Factor |
| CTRAN | Climate Transparency |
| DRES | Distributed Renewable Energy Systems |
| EIA | Energy Information Administration |
| EP | Energy Portal |
| EPIAS | Turkish Energy Markets Operation Company |
| EUD | Electricity Producers Association |
| GAMS | General Algebraic Modeling System |
| GHG | Green House Gas |
| IC | Installed Capacity |
| kton | Kiloton |
| KWh | Kilo Watt Hours |
| LCOE | Levelized Cost of Energy |
| LIB | Lithium-Ion Battery |
| LP | Linear Programming |
| LWPS | Loss of Wind Power Supply |
| LWPSP | Loss of Wind Power Supply Probability |
| MENR | Ministry of Energy and Natural Resources |
| MGM | Turkish State Meteorological Service |
| MILP | Mixed Integer Linear Programming |
| MW | Mega Watt |

| | |
|------|----------------------------------|
| MWh | Mega Watt Hours |
| PHEV | Plug-in Hybrid Electric Vehicle |
| PV | Photovoltaic |
| RES | Renewable Energy Systems |
| RTEG | Real Time Electricity Generation |
| SOC | State of Charge |
| TJ | Tera Joule |
| UNCC | United Nations Climate Change |
| USD | United States Dollars |
| WB | World Bank |
| WEC | World Energy Council |
| WWF | World Wildlife Fund |

1. INTRODUCTION

The global warming crisis and climate change caused by unprecedented CO₂ emission levels across globe create a major threat for civilization's future. The emission levels are caused by economic activities such as transportation, power generation, agricultural and industrial production based on conventional resources. Nowadays, there is a scientific consensus on CO₂ and other greenhouse gases emitted as a result of burning fossil fuels increase the average global temperatures, change the climate patterns and damage the natural balance. This global challenge has created a significant awareness in the public. Scientific community, researchers and policy makers are seeking new ways to find possible solutions in order to tackle this challenging problem. To overcome this issue, member countries gathered in United Nations Climate Change Conference in Paris in 2015. Vast majority of the member countries built a consensus about the urgency of the problem and signed the Paris Climate Agreement. The agreement defines a framework for transition to sustainable energy generation to prevent the disastrous outcomes of the climate change. In other words, the agreement urges countries to accelerate the transition to low carbon future with swift actions and investments. Decarbonisation in industrial activities, transportation, residential and commercial buildings play a crucial role. From this perspective, renewable energy penetration in power generation is a key goal for each country in the world.

RES are expected to be dominant energy providers in the future to obtain sustainability in energy generation (Evans *et al.*, 2012). They are abundant in nature and are also eco-friendly. However, RES have undesired characteristics such as unavailability and intermittency (Vazquez *et al.*, 2010). These characteristics cause the variation in actual energy output from these resources. According to the report by International Renewable Energy Agency, this situation is defined as variable renewable energy (IRENA, 2017). The variability of RES can be due to climate patterns, daily or even hourly weather conditions (Liserre *et al.*, 2010). For instance, inconsistent solar irradiance leads to unstable energy output from solar panels.

Regarding wind, highly variable energy is generated by wind turbines due to irregular wind speed profiles. This leads to uneven and intermittent electricity generation from renewable sources which creates a significant challenge for system operators since energy imbalance occurs between renewable energy supply and electricity demand.

In some cases, the wind generation and electricity demand follows the same pattern during the day, as both of them increase or decrease simultaneously. However, the exact opposite can be also valid. There might be cases such that they are negatively correlated. There are two possible outcomes if they are negatively correlated. The first is the unsatisfied demand if energy supply is less than demand. The second case is the curtailment application of wind turbines while there is not enough load demand. Currently, the curtailment operation is not applicable in Turkey. The system operators buy the total amount of energy that was generated by wind.

As the renewables' share in energy systems reaches significant levels, the variation and fluctuation characteristics will be more severe regarding energy supply. Under these circumstances, the electricity systems must be transformed by being more flexible and reliable. This transformation can be achieved by deploying storage units in electricity networks both in small scale and large scale. Battery energy storage systems (BESS) can reduce the variability between electricity generation and consumption by storing the excess energy at off-peak period and discharging this energy at peak periods (Beltran *et al.*, 2013) In general, they are able to store the excess energy for hours, days or even months. This feature of storage systems provide flexibility to networks as they can respond to sudden changes in the electricity system. BESS have huge potential in terms of flexibility and system reliability of electricity networks. They can increase the stability level of RES combined with conventional resources (Sørensen, 2017). This mechanism can smooth the electricity generation by enabling energy generators to work at optimal capacity (Condon *et al.*, 2018). Due to these factors, RES can't be entirely utilized in energy systems without BESS. This leads BESS to gain significant importance (Li, 2015).

Turkey's demand for electricity is growing due to its economic activity and population increase. According to World Energy Council, rising trend of Turkey's electricity demand will continue due to GDP growth, industrial activities and urbanization exercises (World Energy Council, 2016). A report published by World Wildlife Fund (WWF) claimed that Turkey has a potential to meet nearly 50% of its electricity demand from renewables by 2030 (WWF, 2014). The increase of RES coupled with BESS can allow Turkey to obtain more green energy generation with lower emission, reduce the money spent of imported fossil fuels and protect its economy from energy price fluctuation and speculation. Therefore, Turkey can secure the energy supply. Additionally, BESS penetration makes Turkey to be less dependent to foreign energy. Turkey supplies 75% of its primary energy need by imports (WWF, 2014). Therefore, the penetration of renewable energy coupled with BESS is crucial in terms of continuous energy supply considering the expected economic growth and population increase.

The effect of storage mechanism on renewable integration in national scale is an important topic to address. However, the literature lacks enough research that is implemented in this framework. To the best of our knowledge, no previous research has investigated the effect of storage units to the wind power efficiency in Turkey based on national data. From this perspective, this thesis aims to fill this gap in the literature.

Many questions remain unanswered such as whether or not storage mechanisms can enhance the share of renewables in energy generation or are BESS useful in increasing the grid reliability with high renewable energy integration. Another topic to address is whether or not BESS can increase the utilization and efficiency of wind energy.

We aimed to determine the hourly optimal storage capacity for one year in order to utilize wind more efficiently and obtain smooth renewable energy production in national scale. For this purpose, an optimization model that considers BESS was developed on hourly basis for one year.

The influence of LIB as BESS on the uncertainty of wind energy was addressed. A statistical model was developed to capture the uncertainty of wind energy and load demand. As a statistical model, we fitted the probability distributions that predicts both hourly wind energy supply and load demand. Based on probability distributions, different datasets that reflect the hourly wind energy supply and load demand for one year were generated. After, we run the optimization model with all possible combinations of supply and demand data to capture the uncertainty of both sides. Then, we tried to obtain the robustness in optimal storage capacity and utilization level of wind turbines etc. The analysis was supported with different scenarios considering different system configurations.

The organization of the thesis is as follows. The literature review is in chapter 2. Explanation of both mathematical and statistical model with detailed problem definition was presented in chapter 3. Scenario analysis and results were discussed in chapter 4. Finally, the conclusion and future work were presented in chapter 5.

2. LITERATURE REVIEW

BESS sizing problems deal with determining the optimal capacity of BESS in a specific environment. The analyzed system generally consists of one or multiple energy generators, demand technologies and a storage system. Energy generation portfolio can consist solely of renewable energy, such as solar and wind, or combination of conventional generators with renewable energy. In BESS sizing problems, renewable energy generation and electricity demand must be predicted as much precise as possible. The main objective is to obtain the optimal BESS capacity with different sizing criteria while ensuring the energy demand satisfaction.

BESS sizing has been widely studied in the literature. Extensive amount of work can be found that discusses the sizing problem. In this thesis, literature review will be addressed in the framework of BESS sizing methods and system modeling context.

2.1. BESS Sizing Methods Literature

2.1.1. Probabilistic Models

Probabilistic methods rely on historical data to fit probability distributions in order to generate simulated datasets regarding renewable energy. Solar irradiance data or wind speed profile can be given as good examples. Researchers also benefited from distributions which was used in previous publications. Renewable energy supply and load demand can be predicted using statistical models. This way, stochastic nature of renewable energy can be captured.

According to Yang *et al.* (2018), probabilistic approaches are very advantageous for situations in which there is limited data. However, they tend to lose their benefits for cases in which various performance measures must be optimized. From this perspective, they are not favored for detailed system optimization problems.

Probabilistic methods were widely preferred by authors in the literature. Firstly, Cervone *et al.* (2016) used discrete time Markov chains to generate solar irradiance data for 20 years to forecast photovoltaic (PV) power generation. The system consists PV and storage systems. The authors analyzed 3 different battery technologies, in terms of variability reduction and economic perspective. They showed that the deployment of storage systems significantly reduce the variation in renewable power generation, nearly 34% decrease in the variability compared to system without any storage capacity.

Wu *et al.* (2014) applied statistical methods to model the forecast errors of wind power estimation. For this purpose, authors developed a mixed distribution based on normal and Laplace distribution. Using probabilistic optimization, optimal size of BESS was determined considering daily total cost of the storage system.

Tan *et al.* (2010) proposed stochastic simulation using Monte Carlo approach. The authors optimally sized the batteries in building integrated PV systems to meet two objectives simultaneously. These are demand shifting at peak electricity cost period and outage protection. Based on the building's load profile, weather data and historical outage distribution, the simulation estimates PV energy generation, required backup energy and required demand shifting energy. The battery sizing was decided based on the desired probability of sustaining supply through an interruption.

Dragičević *et al.* (2014) applied robust mixed integer linear problem (MILP) to minimize the total investment cost of the system in a remote telecommunication station. The proposed system consists of PV panels, wind turbine, batteries and fuel cells. The robust optimization model yields a set of optimal solutions which represent different optimal renewable energy capacity and storage capacity. Then, the authors tested these results against different outcomes as they aimed to resemble future activity of the system.

Bahramiadi *et al.* (2012) presented a MILP to optimally size an energy storage system in a microgrid framework in their work.

In their study, the objective function aims to minimize the total cost which is the summation of the BESS investment cost and system operation cost. It has been shown that larger sized BESS does not always mean more economic benefit. There exists a trade-off mechanism between BESS size and total operating cost of the microgrid. Case studies revealed that the optimal size of BESS is nearly 5 MWh with the minimum total cost.

Saboori *et al.* (2015) implemented particle swarm optimization to optimally size an BESS in electrical distribution networks. The proposed model is developed based on mixed-integer nonlinear programming with the objective aiming to minimize energy not supplied cost and BESS system cost. Results of the study indicated that BESS is very effective on increasing network reliability.

As stated before, probabilistic methods can be advantageous to address the unpredictability of renewable energy. In this thesis, we benefited from probabilistic approaches to illustrate the stochastic nature of wind energy and load demand.

2.1.2. Deterministic Models

These models require known data input and known initial parameters such as BESS energy capacity or power capacity. Based on a specific performance criteria, the optimization was carried out. Performance criteria can be either technical or financial. BESS sizing can be made following this approach.

According to Yang *et al.* (2018), deterministic models perform better in returning more accurate results. While optimizing combinations of multiple performance criterion, deterministic model are powerful than probabilistic models. However, optimization interval must be selected carefully. It is very likely that one can miss the exact result if optimization interval is not defined well.

Malheiro *et al.* (2015) analyzed an isolated hybrid system. The system consists of wind turbines, PV modules, diesel generators and batteries. The system was modeled as MILP with objective function that aims to minimize the levelized cost of energy (LCOE). The authors implemented various scenarios with different system configurations. According to the results of the reference scenario, the optimal battery size is 558.4 KWh.

Ru *et al.* (2013) studied the battery storage size determination problem that is implemented in grid-connected PV systems by developing an efficient algorithm with mixed integer linear model. The main objective is to minimize the electricity cost and the cost occurred due to loss of battery capacity while satisfying the load demand. The authors found the battery size as 16.714 KWh for residential load and 13.816 KWh for commercial load with the minimum cost.

Diaf *et al.* (2007) tried to optimally size components in hybrid system consisting PV panels, wind turbine and battery storage. Linear optimization model was developed in order to minimize the LCOE while achieving the desired system reliability.

2.2. BESS Modelling Environment Literature

Hyrid RES can include different system components such as both renewable and conventional energy generation units. The term “hybrid” refers to the fossil generation part of the system. The main objective of the hybrid RES is to satisfy the load demand on a continuous basis (Rekioua, 2020). However, renewable energy generators solely are not able to provide constant power delivery against load demand due to their stochastic features. Regarding this issue, non-renewable generators and storage systems are indispensable in terms of stability and security of the constant energy supply.

Yang *et al.* (2018) divided hybrid RES into four categories based on the operation framework. We benefited from the categorization implemented by Yang *et al.* (2018).

2.2.1. Distributed Renewable Energy Systems

Distributed renewable energy systems (DRES) are special structures in which the energy is generated and distributed independent of the centralized energy systems, in other words grid. They can be considered as a substitute to centralized energy systems (REN21, 2017).

Wang *et al.* (2013) proposed a basic method to integrate BESS to a wind farm. The basic method is based on minimizing the square of the differences between the original wind power generator output and the desired output which the BESS conjunction with the wind power generator. The results showed that an BESS with capacity of 3.72–8.31 KWh is the optimal setting.

Yang *et al.* (2014) proposed a sizing strategy for BESS to be used in distribution networks with high PV integration. In the study, li-ion phosphate battery is selected for storage purpose. The proposed method was used for peak load shaving and voltage regulation purposes such as voltage stability. BESS size is determined as a result of cost-benefit analysis. The results illustrated that the storage sizing must be in the interval of 1.5-3 hour of peak load.

Zheng *et al.* (2014) presented a BESS sizing method for operation of distribution companies to utilize the energy storage systems effectively and reduce the operational risk of price volatility. In the study, LIB and lead-acid batteries are selected as BESS technologies. Cost-benefit analysis is applied to optimally size the BESS. Sizing criteria includes maximizing benefit of distribution companies and minimizing the power loss. The authors verified the results with case studies.

Schneider *et al.* (2016) analyzed a DRES consisting of PV modules and BESS. The storage system was deployed to minimize the total system cost which includes the energy generation cost and total storage system cost. According to simulation results, the optimal battery capacity ranged from 26 to 37 KWh under different system settings.

2.2.2. Standalone Hybrid Renewable Energy Systems

Standalone hybrid RES are very effective in terms of supplying electricity in remote areas. Initially, diesel generators were mainly used as a power source in these areas. However, increasing fuel cost and environmental concerns supported the spread of renewable energy generators.

Standalone systems can also include fossil generation units such as diesel generators. Deploying a BESS is required in all standalone hybrid RES. Yang *et al.* (2018) highlighted that the main logic of installing a BESS in standalone systems is to avoid the imbalance problem of renewable energy supply and electricity demand.

Shang *et al.* (2016) described a method for storage sizing with the objective of minimizing the annual levelized cost of electricity which consists of annualized investment cost, annual operation cost and fuel cost. In the study, the hybrid renewable energy system consists of wind turbines, PV panels and diesel generators. The authors also analyzed various level of renewable integration in the system using penetration level. For this purpose, a particle swarm optimization algorithm is developed.

Luo *et al.* (2014) focused on isolated grids by developing an energy storage sizing approach that considers the reliability level. The optimality was handled by genetic algorithm and sequential simulation with the objective of minimum annualized cost. The authors also compared the technical characteristics of current storage technologies. The results illustrated that the optimal battery size is 36.4 MWh.

Dragičević *et al.* (2014) proposed a method to minimize the total investment cost. Energy is solely provided by renewable energy sources such as PV modules and wind turbines. The systems also consist of energy storage systems including fuel cells, lithium-ion batteries and valve-regulated lead–acid batteries. The solution procedure is based on a robust MILP. The results indicated that the optimal battery sizes are 18.04 KWh and 14.65 KWh for valve-regulated lead–acid battery and LIB, respectively.

Alex *et al.* (2014) studied hybrid system consisting of PV modules, wind turbine and lead acid battery bank as BESS. For this purpose, two different simulation was performed. The first one aims to utilize wind and solar generation together with batteries while the second simulation only utilizes solar power with battery banks. The authors concluded that required battery capacity is 114.5 KWh for PV and battery system whereas 49.8 KWh battery capacity is required for hybrid system with PV, wind and BESS.

2.2.3. Microgrid

Microgrid is a local energy network with two main modes such as grid-connected mode and autonomous mode. A microgrid can work in the grid-connected mode as well as it can operate in autonomous mode during extraordinary times such as storms or major breakdowns in grid. This mode is also called as islanded mode. In such cases, the microgrid produces its own renewable energy and consumes against electricity demand.

Firouzi and Abarghoee (2014) proposed improved bat algorithm to optimally size an energy storage system in a microgrid. The system includes micro turbine, PV panels, wind turbines and storage systems such as fuel cells and LIB. The main objective is to minimize total energy and operating cost of the microgrid. The results showed that installing a 150 kWh storage system in the microgrid can lower the total cost nearly 40% compared to microgrid without installing BESS.

Chen *et al.* (2012) developed a method to optimally size an BESS in a microgrid. The method comprises cost-benefit analysis. Analyzed system consists of wind turbines, PV panels, micro turbines, fuel cells and LIB. Two optimization models were developed for both islanded and grid-connected modes. The mathematical model was developed as MILP. Case studies validated the efficiency of the proposed method. The results indicated that optimal battery size is 500 kWh and 1400 kWh for the grid-connected scenario and the islanded scenario, respectively.

Khorramdel *et al.* (2015) proposed a method for microgrids that is integrated to wind turbines. The analyzed microgrid includes wind turbines and storage units. The proposed system was analyzed for both grid-connected case and stand-alone mode. According to the results, the optimal battery size ranged from 400 to 1100 KWh to obtain the maximum total benefit. On the other hand, 1400-1600 kWh sized battery must be installed to minimize the total cost.

Nguyen *et al.* (2015) analyzed a microgrid system consisting of PV panels, diesel generator and BESS. The authors specifically focused on vanadium redox battery. Dynamic programming algorithm was developed to determine the optimal battery storage capacity with the minimum total system cost. Results illustrated that optimal battery capacity was 65 KWh and 5 KWh for the islanded mode and grid-connected mode, respectively.

2.2.4. Renewable Energy Power Plant

Renewable energy suffers from high variation of actual energy generation. Eventually, the variation problem of renewable energy cause system operators not to forecast the energy production precisely. This problem becomes more severe especially in large scale renewable energy power plants. BESS are promising solutions against this situation. They can be deployed with large scale renewable power generators to compensate the production forecast error.

Cervone *et al.* (2016) analyzed the storage systems to decrease the costs due to energy imbalance. Imbalance penalty cost is defined in case of actual PV power output is different than expected output. The authors generated irradiance data for 20 years' time series using discrete-time Markov chains to estimate PV power generation. Different battery technologies are analyzed to obtain optimal battery size by considering PV power production variability and economic framework. The results showed that the optimal sizes are 100 KWh, 80 KWh and 90 KWh for lead acid, sodium sulfur and LIB, respectively.

Brekken *et al.* (2011) studied sizing and control strategies in a wind farm context. They analyzed zinc-bromine flow battery as energy storage system. The objective is to minimize the cost of BESS and compensate the forecasting errors as BESS improves the predictability of wind power output. Based on the simulation results, the optimal battery size is 40 MWh.

Wang *et al.* (2008) analyzed a wind farm with a storage unit aiming to achieve steady power generation with the least capital cost. For this purpose, a simulation model on Matlab was developed to optimally size BESS. Results of the study highlighted that the optimal storage capacity is 0.68 MWh whereas the optimal power rating is 1.33 MW.

Korpaas *et al.* (2003) implemented dynamic programming to optimally schedule and operate BESS in wind power plants for one year. Simulation results confirmed that the optimal storage capacity is 150 MWh where the optimal power rating is 8 MW.

2.2.5. National Scale

Previous studies proposed system designs in small scale. In this thesis, we aimed to find optimal hourly storage capacity in Turkey. Therefore, literature review was extended further considering this fact.

Bogdanov and Breyer (2016) developed a linear optimization model that determines the optimal hourly energy supply using 100% renewable energy resources. The objective function minimizes the total annual energy system cost. The research was conducted in scope of Northeast Asian countries. In this study, batteries and gas storage systems are considered as storage technologies. The output of the model presents optimized total system cost, installed capacities, energy production profiles, hourly storage level etc. According to the results, the LCOE is ranged between 69.4 and 91.3 €/MWh while installed BESS capacities ranged between 1,511 and 4,225 GWh.

The transition to fully renewable energy based energy system was analyzed for Baltic Sea region countries by Child *et al.* (2018). The optimization model that was developed by Bogdanov and Breyer (2016) was adapted by the authors. Similarly, the system was handled in five year time periods starting from 2015 to 2050. The results indicated that LCOE is expected to drop from 60 €/MWh in 2015 between 45 €/MWh and 48 €/MWh in 2050. From storage perspective, the total BESS capacity is expected installed 50-60 GWh in 2050. The authors also claimed that an energy system which is powered by solely renewables is feasible before 2050 for those countries.

Child *et al.* (2018) performed comprehensive analysis regarding fully renewable energy transition pathway of various countries in Europe. Authors used Lappeenranta University of Technology energy system transition model. (Bogdanov and Breyer, 2016) This energy system transition model performs simulation of power systems throughout five year time periods starting from 2015 until 2050 based on linear optimization based with pre-specified limitations. The objective function is the minimization of the total annual energy system cost. The output of the model presents optimized total system cost, installed capacities, energy production profiles, hourly storage level and etc. (Bogdanov and Breyer, 2016) The current LCOE is assumed as 69 €/MWh in European countries, on average. According to the results, this number can be decreased to 51 €/MWh in 2050. For EU countries including Turkey, nearly 3,320 GWh of BESS must be installed until 2050.

Kilickaplan *et al.* (2017) analyzed the 100% renewable energy transition of Turkish energy system by applying the same optimization model developed by Bogdanov and Breyer (2016). The system is analyzed until 2050 within 5 year periods. The study was supported with 2 different scenarios namely power scenario and integrated scenario. The results of the research showed that installed BESS capacity is 561.9 GWh for power scenario and 771.7 GWh for integrated scenario in 2050 in Turkey. In addition, LCOE occurred as 56.7 and 50.9 €/MWh for power scenario and integrated scenario, respectively in 2050 in Turkey.

At this point, it will be useful to underline the main differences between the study done by Kilickaplan *et al.* (2017) and our study. They analyzed the Turkish energy system as they introduced various energy conversion technologies, demand technologies and different types of storage technologies. In this thesis, we consider the wind energy as the main energy source in the system. Different from Kilickaplan *et al.* (2017), we only focused on LIB as storage technology. We made prediction regarding energy supply and demand only for one year. Our aim is to investigate the impact of the storage technology to the overall efficiency of wind energy.

To sum up, we can conclude that the previous researches mainly focuses on the BESS sizing in relatively small scaled environments. Regarding Turkey, we only found one study that dealt with BESS sizing problem on a country scale. However, as stated before the authors analyzed the problem with a broader angle by taking into account different energy forms, demand technologies etc. We couldn't find any study that considers the overall efficiency of wind energy as a dominant supplier on national scale. In summary, we believe that our study is a strong candidate to fulfill this gap in the literature.

3. PROBLEM DEFINITION and OBJECTIVES

The share of renewables in the energy generation portfolio is expected to increase in global scale. Similar to other countries, Turkey has been putting significant effort for this purpose in-line with domestic and national energy policy of the country. According to Enerji Portalı (2021), the total installed capacity in Turkey is 97,070 MW by April, 2021. The share of wind in total installed capacity is nearly 9.64%, accounting to 9,367.5 MW. According to Turkey Wind Energy Potential Atlas, the total usable potential wind energy capacity is forecasted as 47,850 MW (Yeni Enerji, 2014). According to 2019-2023 strategic plan published by Ministry of Natural Resources (MENR), the country aims to increase its total installed capacity to 11,883 MW and to 10,000 MW for wind and solar energy, respectively (MENR, 2018).

Varying weather conditions and changing climate patterns highly affect the energy generation from renewable energy. For instance, solar panels rely on the sunlight in order to generate energy. This means cloudy or rainy days can significantly decrease the energy generation by panels.

Regarding wind, the wind speed profiles directly affect the energy generation from wind turbines. Wind energy shows seasonality effect. Performance of wind plant varies over the course of a year due to the highly seasonal wind patterns in the world (U.S Energy Information Administration, 2015). As an illustration, Figure 3.1 presents the monthly real-time electricity production by wind energy across Turkey in 2019.

All in all, it can be concluded that the renewable energy depends on weather and geographical conditions. Stochastic nature of wind energy is caused by random behavior of wind speed and seasonal wind patterns. These factors lead to unpredictable wind energy generation. However, this problem is not binding for energy generation using conventional resources such as coal and natural gas. As long as there is available fuel for the power plant to operate, the energy generation level is predictable.

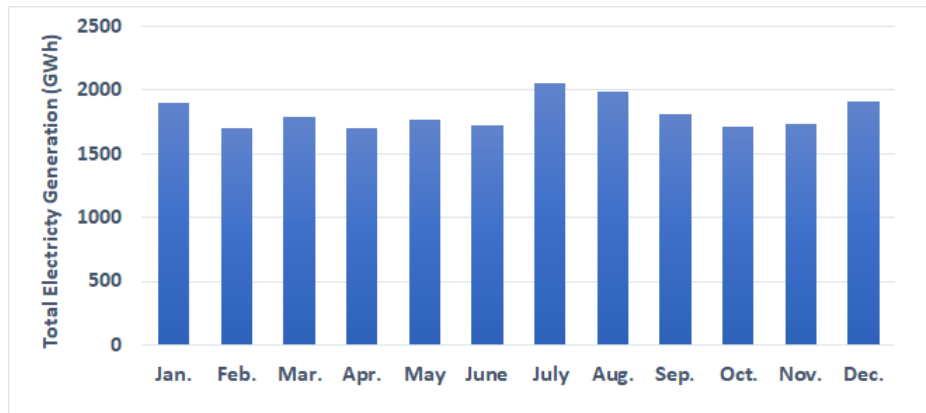


Figure 3.1. Monthly Real-Time Electricity Generation by Wind Energy in Turkey in 2019 (EPIAS, 2020).

Against the unpredictable nature of renewable energy supply, the electricity demand shows slightly predictable patterns. As an example, Figure 3.2 shows the hourly demand fluctuation between 7 January 2019,00:00-20 January 2019,23:00.

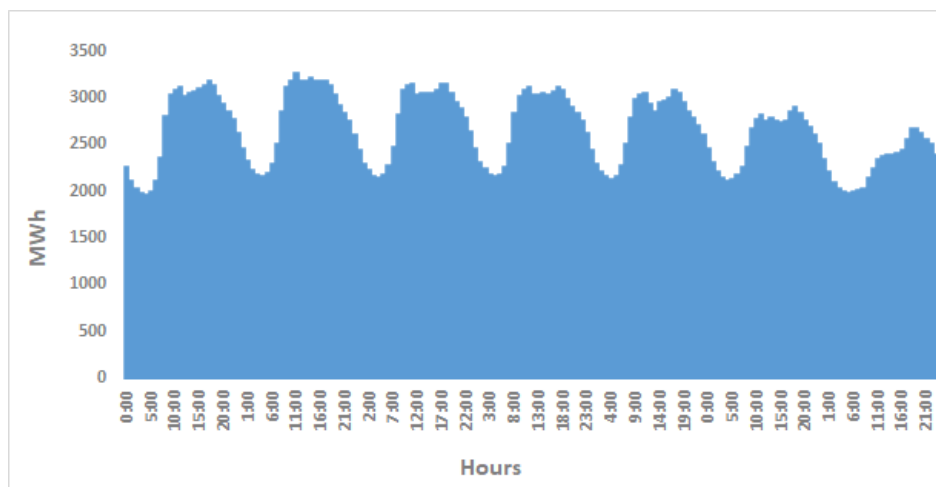


Figure 3.2. Hourly Demand Fluctuation between 7-13 January 2019 (EPIAS, 2020).

The overall pattern for the load demand in daily basis can be easily observed. In general, the demand steadily decreases between 00-04 due to night time. Afterwards, it starts to increase until 12.00. Then, it has tendency to stay constant until 18.00. Finally, it again stars to decrease until the end of the day.

At this point, the matching problem of wind energy supply with load demand arises naturally. There are 2 possible cases. The first case would be the risk of unsatisfied demand during low energy generation from wind energy while demand is high. The other case would be high energy generation during low demand periods. For this case, energy curtailment is necessary. So, overall utilization and efficiency of wind energy decreases due to curtailment applications. Figure 3.3 illustrates the mismatch between hourly wind energy supply and load demand between 7-13 April 2019 in Turkey.

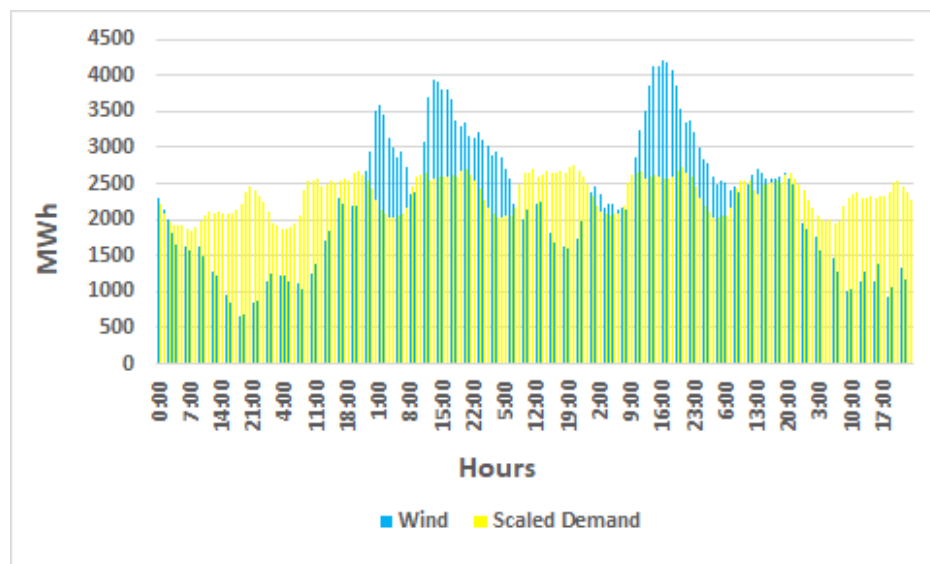


Figure 3.3. Hourly Electricity Generation by Wind and Scaled Load Demand between 7-13 April 2019 (EPIAS, 2020).

According to the Figure 3.3, the wind energy supply is lower than load demand during the first 44 hours. After, the wind generation starts to exceed the demand for next 36 hours. Following is the decrease in energy generation by wind for next couple of hours again. This pattern can repeat itself through the rest of the year.

Generally, macro energy optimization models handle the system without storage. They also assume a certain efficiency regarding wind power. As the share of renewables increases, the mismatch problem will be more severe. It is expected that the system operators will utilize the wind energy with different efficiency levels both in micro and macro systems.

Our main problem is to test the overall efficiency level of wind energy coupled with storage system. BESS can be effective solution to tackle this challenge as they can increase flexibility and reliability of national electricity networks (National Renewable Energy Laboratory, 2013). In short, renewable integration into energy portfolio in national scale stands as a significant problem for policy makers due to the intermittency problem of renewable energy.

The main objective of this research is to study the impact of storage systems in wind energy production and assess the efficiency level of wind under different system settings. A cost-benefit analysis was proposed that considers the hourly energy production and demand for one year. We analyze the effect of storage system to efficiency of wind energy production if wind energy would be the main driver in the system. For this purpose, the model aims to optimize each of the following: the amount of charged and discharged energy, hourly storage level in batteries, the generation level of renewable and fossil-fired electricity.

As usual in every optimization case, the model contains trade-offs. As an example, as long as the model decides to install storage capacity in the system, the objective function increases due to related cost components of the battery. However, if the model decides to serve the demand with fossil fuels, the objective function again increases due to the generation cost with fossil fuels. Therefore, making this distinction in the optimal way is the main task of the mathematical model.

Various assumptions were made within the general framework of the model. These assumptions will be described in detail through the next section.

3.1. Model Assumptions and Methodology

Inventory models were developed to find solutions to the problems related with production, in general. However, there are other areas in which the inventory models are applicable. Recent trend in inventory management is the energy modeling.

Marchi *et al.* (2019) stated that related topics with energy in literature include energy scheduling or sizing of BESS etc. Schneider *et al.* (2015) showed the similarities between inventory models and BESS. According to the authors, it is possible to reflect the intermittent energy supply and demand with stochastic supply and demand, respectively. Storing the energy during multiple periods refers to multi-period inventory model. Energy loss occurred in batteries corresponds to the inventory control of perishable goods. In batteries, a specific minimum level of energy must be kept to obtain long lifetime and good performance. This characteristic can be evaluated as safety stock.

Silva *et al.* (2019) also made similar comparison by determining the relations between their studied problem and inventory management context. The authors claimed that the battery can be addressed as a power stock. Moreover, power management can be viewed as production planning with particular inventory management policy. In this context, maximum battery capacity refers to inventory level with a limited capacity whereas the minimum battery capacity refers to safety stock. In this thesis, the model was developed under the same possible assumptions. These assumptions built the general structure of the mathematical model.

Although there are many similarities between two concepts, some different aspects also exist. As an example, the storage level decreases by time due to the self-discharge rate of the batteries. In a typical inventory environment, this situation is not valid since the inventory level of materials is steady through the planning period in case of no demand from the market. Another example would be the difference between transfer mechanism of the inventory. In a common inventory setting, the transfer of goods or materials to the customer, which is aiming to satisfy the demand, will be as the exact demand level of the customer. In other words, if the demand was 100 units, it is possible to produce exactly 100 units and ship them directly to the customer. However, in energy storage environment, if the demand was 100 units of energy, the charged and discharged level will not be exactly 100 units of energy due to the charging and discharging efficiency of the batteries.

The optimization model optimizes the decision variables through “n” period. In our case, this corresponds to one year. We optimize the model through 8,760 hours and energy balance between each time “t” and “t+1” was handled as “multi period inventory control problem”. Therefore, it has been shown that the principles of inventory management can be implemented in the context of energy storage modeling. Even though there are some aspects which differs between two approach, the similarities helped us significantly during determination of the problem solving methodology.

In the system, wind was assumed as the dominant energy provider to satisfy the demand in Turkey. If the wind energy insufficient, the model covers the remaining demand with either discharging the energy from batteries or burning NGA. Since we assumed the wind energy is the major energy source, we scaled the load demand to obtain more logical results. The scaling operation will be handled in the following sections.

In our experiments, we assume that the demand is inelastic. In simple words, we assumed that the energy demand does not change with the price. This is simply because we do not aim to remodel the price competition. We analyze the problem from the system decision makers’ point of view.

3.2. Mathematical Model

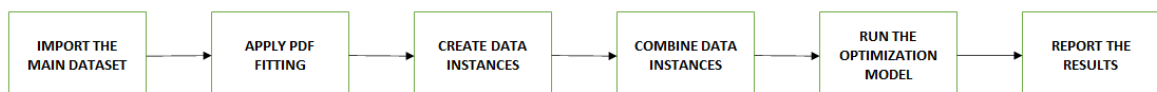


Figure 3.4. Flowchart of robustness operation.

The Figure 3.4 summarizes the importing the raw data, distribution fitting and obtaining robustness.

We developed a linear optimization model that determines the optimal hourly storage level, hourly energy generation level from wind and natural gas, hourly charged and discharged energy amount through one year. We run the optimization model under various of scenarios. Those scenarios will be based on different supply-demand data structures in Turkey. Those data structures will be obtained by fitting hourly real time electricity supply-demand data in Turkey. To that end, we used Monte Carlo simulation technique in order to generate 10 datasets for both supply and demand. For this purpose, R statistical software were used.

In this section, sets, parameters, decision variables, objective function and limitations of the mathematical model will be discussed in detail.

3.2.1. Sets

The model has only one set that defines the hours in one year.

- t : hours

In this study, the model was optimized through one year. Therefore, it is assumed that set “ t ” consists of 8760 instances. The number of instances were calculated as follows:

$$\frac{24 \text{ hours}}{\text{day}} * \frac{365 \text{ days}}{\text{year}} = 8760 \text{ hours}. \quad (3.1)$$

3.2.2. Parameters

Electricity generated by wind and load demand are predicted for each time period. Therefore, they are defined as parameter in the model. The unit of both parameters is MWh.

- $\text{wind_out}(t)$: the hourly forecasted electricity generation level by wind. (in MWh)

- $load_dem(t)$: the hourly forecasted electricity demand level. (in MWh)

As stated earlier, storage systems have chemical characteristics that determine the general efficiency of storage units. Efficiency parameters are defined in the model as;

- chg_eff : charging efficiency of the storage unit
- $dischg_eff$: discharging efficiency of the storage unit
- $self_dischg$: self-discharge rate of the storage unit
- c_min : minimum allowable SOC of the battery
- c_max : maximum allowable SOC of the battery

In this study, state of charge of the batteries at each time period is defined as the current fill percentage $r_stor(t)$ of overall storage capacity. It is calculated as follows:

$$SOC(t) = \frac{r_stor(t)}{cap}. \quad (3.2)$$

3.2.3. Decision Variables

The model has two types of decision variables in its structure. These are called as optimization variables and performance measures. As it is evident from the definition, optimization variables were defined to optimize the system configurations. On the other hand, performance measures were used for reporting purposes. Note that each decision variable was defined as continuous variable. Any integer or binary variable were not considered in this thesis.

For each time period, the model decides whether to charge the excess energy to the storage system or to discharge electrical energy from the batteries. The installed BESS capacity, hourly stored energy level in batteries, hourly generation level from wind and NGA were also decided by the optimization model.

- $chg(t)$: the amount of electricity charged to the storage (in MWh)
- $dischg(t)$: the amount of electricity discharged from the storage (in MWh)
- $r_stor(t)$: the level of electricity storage at time t (in MWh)
- $used_wind(t)$: the amount of electricity actually produced by wind in the system at time t (in MWh)
- $LWPS(t)$: loss of wind power supply at time t (in MWh)
- cap : the total installed BESS capacity (in MWh)

In the model, we assumed that the remaining demand was satisfied using NGA when the hourly demand exceeds the summation of wind energy supply and discharged energy amount. When the opposite is true, the excess energy is stored when there is enough capacity. The electricity generated by fossil fuels for each time corresponds to loss of wind power supply (LWPS).

Performance measures were used for reporting purposes. They consist of utilization level of batteries, LCOE, cumulative emission level, utilization level of wind and loss of power wind supply probability (LWPSP).

- $util_lev$: utilization level of forecasted wind energy. It is defined as percentage.
- bat_util : utilization level of storage system. It is defined as percentage.
- $emiss_lev$: the cumulative emission level in the system. The unit is kton of CO₂.
- $LWPSP$: loss of wind power supply probability.
- $LCOE$: levelized cost of energy. The unit is \$/MWh.

Loss of power supply probability was defined by Yang *et al.* (2007). Basically, it refers to the probability that the system is unable to satisfy the demand for operation horizon. In our study, we renamed this parameter as LWPSP. It simply refers to the probability that the overall proportion of the demand what was not satisfied by wind power. This probability was calculated as follows:

$$LWPSP = \frac{1}{8760} * \sum_{t=1}^{8760} \frac{LWPS(t)}{load_dem(t)}. \quad (3.3)$$

The utilization level of wind power was obtained by dividing real time generation over the predicted electricity generation. The calculation was provided as below.

$$util_lev = \frac{\sum_{t=1}^{8760} used_wind(t)}{\sum_{t=1}^{8760} wind_out(t)}. \quad (3.4)$$

Battery utilization level is calculated as follows:

$$bat_util = \frac{1}{8760} * \sum_{t=1}^{8760} \frac{r_stor(t)}{cap}. \quad (3.5)$$

Another performance measure is the total cumulative carbon emission occurred in a year due to the electricity generation by NGA. The cumulative emission level in the system was calculated as follows:

$$emiss_lev = emiss_factor * \sum_{t=1}^{8760} LWPS(t). \quad (3.6)$$

Levelized cost of energy is used in order to evaluate the different system designs from economic point of view. The LCOE was taken from Malheiro *et al.* (2015). It's unit is \$/MWh. It was calculated for each system design as follows:

$$LCOE = \frac{Total\ System\ Cost}{E_a} * CRF. \quad (3.7)$$

where

- E_a : annual energy demand (in MWh)
- CRF: capital recovery factor

Annual energy demand equals to the sum of electricity demand through a year.

$$E_a = \sum_{t=1}^{8760} load_dem(t). \quad (3.8)$$

Capital recovery factor (CRF) is used to distribute the results over the useful lifetime of the system. CRF considers a discount rate and useful lifetime. In this thesis, it is assumed that the cost occurred at each time is paid at the end of the year. We aim to optimize the present value of the total system cost. For this purpose, we used CRF to determine the present value of the total year-end cost. CRF was calculated as follows:

$$CRF = \frac{(1+i)^A * i}{(1+i)^A - 1}. \quad (3.9)$$

where

- i : discount rate
- A : useful lifetime of the system

3.2.4. Objective Function

The objective function aims to minimize the total system cost which includes the total renewable energy generation cost, the total storage cost and the total penalty cost.

$$\text{minimize } z = tot_RE_cost + tot_stor_cost + tot_fos_cost. \quad (3.10)$$

where

- tot_RE_cost : total cost of energy generation by wind.(in USD)
- tot_stor_cost : total cost of installed storage capacity. (in USD)
- tot_fos_cost : total cost of energy generation by fossil fuels. (in USD)

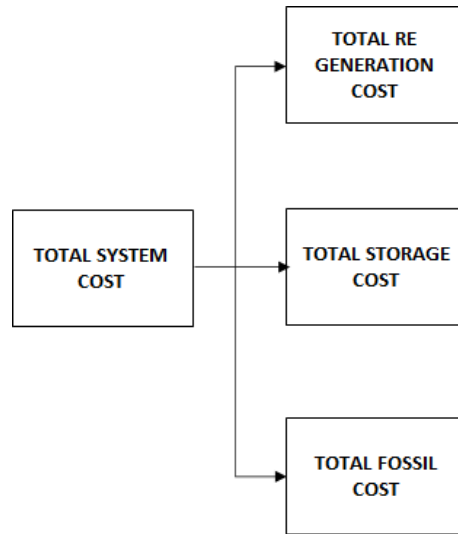


Figure 3.5. Structure of total system cost.

At each time period, production cost occurs due to energy generation by wind. In this study, we did not consider the investment cost of wind capacity. We assumed that The closed form of total energy generation cost is as follows:

$$total_RE_cost = \sum_{t=1}^{8760} unit_RE_gen_cost * used_wind(t). \quad (3.11)$$

where

- $unit_RE_gen_cost$: unit cost of electricity generation by wind in \$/MWh.
- $used_wind(t)$: the real-time electricity generation by wind in the system at time t . (in MWh)

In the proposed system, storage cost occurs due to battery capacity installation. It includes initial investment cost, operation cost, maintenance cost and replacement cost of batteries. Total storage cost was calculated as follows:

$$tot_stor_cost = tot_INV_cost + tot_OPE_cost + tot_MAIN_cost + tot_REP_cost. \quad (3.12)$$

where

- tot_INV_cost : total investment cost
- tot_MAIN_cost : total maintenance cost
- tot_REP_cost : total replacement cost
- tot_OPE_cost : total operation cost

Total investment cost was calculated as follows:

$$tot_INV_cost = unit_INV_cost * cap. \quad (3.13)$$

Total maintenance cost was calculated as follows:

$$tot_MAIN_cost = \frac{unit_MAIN_cost * cap}{CRF}. \quad (3.14)$$

Total replacement cost was calculated as follows:

$$tot_REP_cost = \frac{unit_REP_cost * cap}{CRF}. \quad (3.15)$$

Total operation cost was calculated as follows:

$$tot_OPE_cost = \frac{1}{CRF} * unit_OPE_cost * \sum_{t=1}^{8760} (chg(t) * chg_eff + dischg(t) / dischg_eff). \quad (3.16)$$

where

- $unit_INV_cost$: unit capital cost of batteries. (in \$/MWh)
- $unit_OPE_cost$: unit operation cost of batteries. (in \$/MWh)
- $unit_MAIN_cost$: unit maintenance cost of batteries. (in \$/MWh)
- $unit_REP_cost$: unit replacement cost of batteries. (in \$/MWh)

The remaining part of the objective function consists of total fossil cost.

Fossil cost occurs if the demand was satisfied by NGA. The total fossil cost is calculated as follows:

$$tot_fos_cost = \sum_{t=1}^{8760} fos_cost * LWPS(t). \quad (3.17)$$

where

- *fos_cost*: unit cost of electricity generation by NGA. (in \$/MWh)
- *LWPS(t)*: loss of wind power supply at period *t*. (in MWh)

These three cost types form the total system cost in the proposed model.

3.2.5. Constraints

In this section, the underlying limitations in the proposed model will be explained in detail. The constraints are as follows:

$$r_stor("1") = 0 \quad (3.18)$$

$$r_stor(t) \geq c_min * cap \quad (3.19)$$

$$r_stor(t) \leq c_max * cap \quad (3.20)$$

$$used_wind(t) + dischg(t) + LWPS(t) = load_dem(t) + chg(t) \quad (3.21)$$

$$used_wind(t) \leq wind_out(t) \quad (3.22)$$

$$LWPS \leq 0.2 \quad (3.23)$$

$$r_stor(t) \geq 0 \quad (3.24)$$

$$chg(t) \geq 0 \quad (3.25)$$

$$dischg(t) \geq 0 \quad (3.26)$$

$$used_wind(t) \geq 0 \quad (3.27)$$

$$r_{stor}(t) = r_{stor}(t - 1) * S + chg(t) * chg_eff - dischg(t)/dischg_eff. \quad (3.28)$$

where

- S: self discharge rate (in percentage)

Equation 3.18 specifies the initial storage level. In this study, it is assumed that there is no initial storage capacity in the system. We considered the batteries across the country as a single BESS. Thus, it is modeled as a single equivalent battery in the proposed system. Equation 3.19 and equation 3.20 ensure the minimum and maximum state of charge of the batteries through time window, respectively. Overall energy balance in the proposed system is ensured by equation 3.21. Equation 3.22 implies that used wind energy must be less than the total potential wind energy generation. In this thesis, an idealistic curtailment operation for wind energy is assumed. The detailed explanation of this concept is in the next chapter. Equation 3.23 implies a lower bound for the renewable energy penetration level in the system. For instance, equation 3.23 states that at most 20% of the demand can be satisfied by fossil fuels through one year. This simply means the penetration level of wind energy must be at least 80%. Starting from Equation 3.24 to Equation 3.27 ensure the non-negativity restrictions. Equation 3.28 refers to the battery energy balance between each consecutive period.

3.3. Statistical Model

Both wind energy and energy demand show stochastic characteristics. A statistical model was developed to reflect the stochastic nature. Hourly electricity generation and demand data were fitted to appropriate theoretical probability distributions. Arena 16.0 Input Analyzer was used for fitting operation.

Both energy supply and load demand data were imported from official website of EPIAS. The imported datasets reflect the hourly real time electricity generation by each energy source and hourly electricity demand in Turkey.

The available dataset belongs to time slots between 1 January 2016, 00.00 and 31 December 2019, 23.00. Therefore, raw dataset consists of total number of 35,062 instances. EPIAS offers the relevant electricity market data in terms of company's mission based on transparency (EPIAS, 2020).

Demand data shows the electricity consumption of the country in total. The demand data must be scaled in order to obtain feasible and logical results. In simple words, we assumed that the variation in the upper side of the demand is equal to 7.5% of the total electricity demand. In this study, we aimed to obtain hourly storage level against this variability. To mitigate the variation on the upper side, we propose installing the BESS in the system. The main reason behind scaling operation is the share of wind energy in total demand satisfaction. Our main logic was based on the most recent energy generation portfolio of Turkey against the real time electricity demand in the country. The share of wind in demand satisfaction has tendency to increase in Turkey. It was %5.59 in 2016 whereas the share of wind increased to %7.4 in 2019 (EPIAS, 2020). Considering this fact, the demand was scaled with 7.5% since we aim to reflect the most recent energy generation portfolio in Turkey. For this purpose, we scaled the demand with %7.5 by multiplying each demand instance with 0.075. In other words, 7.5% of total hourly electricity demand of Turkey forms the real time electricity demand in this study.

Figure 3.6 shows the real time electricity demand in Turkey from the beginning of 2019 until end of the year. It is easy to observe that the demand fluctuates on a regular basis. We can say that there is a baseline demand which is constant and steady throughout the year. In addition, there is continuous fluctuation. In this thesis, we assumed that 7.5% of the demand corresponds to this fluctuation. Figure 3.7 illustrates the fluctuated part of the demand in 2019 in Turkey

Our main goal is to determine the hourly optimal storage level for a year in order to smooth the wind energy generation against the demand by deploying storage units.

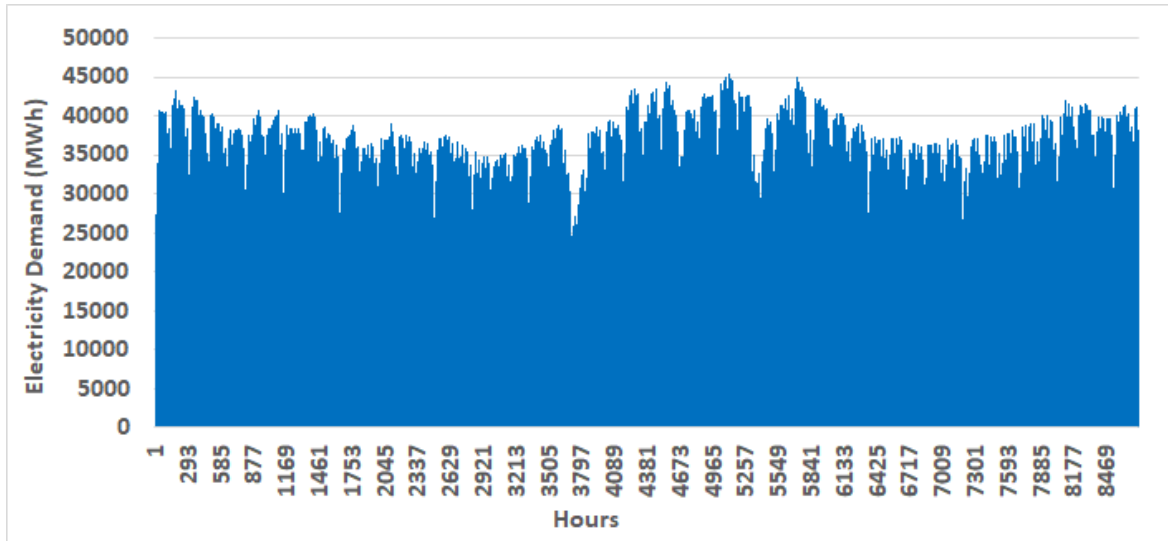


Figure 3.6. Real Time Electricity Demand through 2019 in Turkey (EPIAS, 2020).

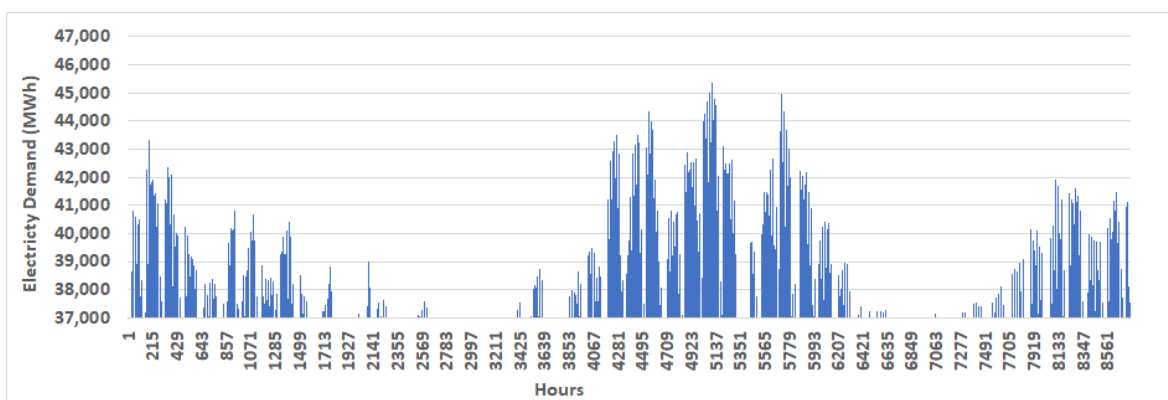


Figure 3.7. Fluctuation of Real Time Electricity Demand through 2019 in Turkey (EPIAS, 2020).

To achieve this, we selected the wind energy as the dominant energy provider which was supported with NGA to satisfy the demand. Batteries were also used in the proposed system.

Regarding distribution fitting for both wind energy generation and load demand side, we benefited the similar approach used by Ekren and Ekren (2009). The authors tried to find the optimal battery capacity in PV/wind hybrid energy conversion system. Arena Input Analyzer was used to obtain solar radiation, wind speed and load demand's probability distributions in order to calculate hourly solar and wind energy generation as well as hourly load demand. The fitting operation was carried out on hourly basis for each month of the year. In their study, seasonality effect was ignored for data fitting purposes. In other words, each data instance was assumed as independent. We assumed that this approach is also valid regarding distribution fitting for our study as well. We fitted theoretical distributions by assuming each data instance is independent. Normally, it can be said that the energy generated by wind at time "t+1" is dependent on the energy generated at time "t". The same is also valid for energy demand. However, since we run the model 100 times for each system configuration, we believe that this dependency can be ignored. It can be said that the dependency loses its effect, on average. On the other hand, one can take a different approach to the subject and can explain the dependency using time series methods. However, time series approaches are out of context of this study.

3.3.1. Hourly Potential Wind Data Distribution Fitting

The data which was provided by EPIAS reflects real-time electricity generation by wind across Turkey. EPIAS maintains the electricity generation data into three categories. These are as follows:

- Licenced Power Plant Investments
- Planning
- Ex-Post Generation

The first category provides the list of power plants which completed their provisional approval and activation by general directory of energy affairs. In planning category, the relevant data was provided into three sub-categories. These are;

- Final Daily Production Program
- Settlement Based Final Generation Plan
- Available Installed Capacity

Final daily production program presents the forecasted electricity generation level for the each operating day. Participants are subjected to inform the system operator about the predicted electricity production in the beginning of power balancing market. Settlement based final generation plan indicates the updated forecasted power generation final plan. Finally, available installed capacity (AIC) is the active power capacity which generators can supply to the system. Although EPIAS already presents the data, it must be underlined that AIC is calculated for wind energy as follows:

$$\text{Available Installed Capacity} = \text{Installed Capacity} * \text{Availability Factor}. \quad (3.29)$$

In general, availability factor is assumed nearly between 80% and 90% for wind energy. Availability factor is influenced by many factors including maintenance operations of wind turbines, unexpected breakdowns or repairs. Considering this fact, it can be concluded that installed capacity (IC) is a theoretical upper bound for AIC. This relationship was shown as below:

$$IC(t) \geq AIC(t). \quad (3.30)$$

As stated previously, the generation data also includes ex-post generation data. This section was further divided into two sub-categories. These are as follows:

- Real-Time Generation
- Injection Quantity

As it is evident from the definition, real-time generation data reflects the hourly and resource based electricity generation. Injection quantity data refers to the hourly injection of aggregate energy of injection units through a settlement period. It is worthwhile to mention about theoretical calculation of real time electricity generation (RTEG). RTEG was calculated as below:

$$RTEG(t) = AIC(t) * Capacity\ Factor(t). \quad (3.31)$$

In current situation, the capacity factor is always less than one. Therefore, available installed capacity can be considered as a theoretical upper bound for real-time electricity production. Calculation of capacity factor was shown as below:

$$Capacity\ Factor = \frac{RTEG(t)}{AIC(t)}. \quad (3.32)$$

Capacity factor basically refers to the actual hourly electrical energy output of a wind turbine over the maximum possible electricity generation. Regarding wind energy, it is calculated hourly. It does not have any unit. In addition, the capacity factor can be influenced by various of factors such as wind availability and the swept area of the turbines etc. Therefore, the variability and unpredictability of wind energy highly affect the capacity factor. On average, the capacity factor of typical wind farms varies between 25% and 45% (Clayton, 2015). As an illustration, the Table 3.1 shows the hourly IC, AIC and RTEG by wind energy in 2 February, 2019. The upper bound of capacity factor is 1. Therefore, AIC is greater than or equal to RTEG. This relationship was shown as below:

$$AIC(t) \geq RTEG(t). \quad (3.33)$$

Hence, Equation 3.34 is always true for wind turbines. It was shown as below:

$$IC(t) \geq AIC(t) \geq RTEG(t). \quad (3.34)$$

Table 3.1. IC, AIC and RTEG for wind energy in 2 February, 2019 (EPIAS, 2020).

| Hour | IC(MW) | AIC(MWh) | AF(%) | RTEG(MWh) | CF(%) |
|-------|----------|----------|-------|-----------|-------|
| 0:00 | 6,668.52 | 5,605.53 | 84.06 | 2,034.96 | 36.30 |
| 1:00 | 6,668.52 | 5,593.35 | 83.88 | 2,010.09 | 35.94 |
| 2:00 | 6,668.52 | 5,584.98 | 83.75 | 1,974.57 | 35.36 |
| 3:00 | 6,668.52 | 5,588.46 | 83.8 | 1,994.52 | 35.69 |
| 4:00 | 6,668.52 | 5,593.73 | 83.88 | 2,140.03 | 38.26 |
| 5:00 | 6,668.52 | 5,542.18 | 83.11 | 2,321.2 | 41.88 |
| 6:00 | 6,668.52 | 5,603.98 | 84.04 | 2,446.85 | 43.66 |
| 7:00 | 6,668.52 | 5,605.29 | 84.06 | 2,551.24 | 45.51 |
| 8:00 | 6,668.52 | 5,504.47 | 82.54 | 2,613.42 | 47.48 |
| 9:00 | 6,668.52 | 5,499.47 | 82.47 | 2,478.42 | 45.07 |
| 10:00 | 6,668.52 | 5,465.35 | 81.96 | 2,355.36 | 43.1 |
| 11:00 | 6,668.52 | 5,569.05 | 83.51 | 2,314.62 | 41.56 |
| 12:00 | 6,668.52 | 5,577.24 | 83.64 | 2,402.05 | 43.07 |
| 13:00 | 6,668.52 | 5,584.47 | 83.74 | 2,314.87 | 41.45 |
| 14:00 | 6,668.52 | 5,583.14 | 83.72 | 2,300.46 | 41.2 |
| 15:00 | 6,668.52 | 5,581.76 | 83.7 | 2,197.34 | 39.37 |
| 16:00 | 6,668.52 | 5,574.86 | 83.6 | 2,136.31 | 38.32 |
| 17:00 | 6,668.52 | 5,579.15 | 83.66 | 2,125.01 | 38.09 |
| 18:00 | 6,668.52 | 5,575.94 | 83.62 | 2,360.34 | 42.33 |
| 19:00 | 6,668.52 | 5,584.34 | 83.74 | 2,541.51 | 45.51 |
| 20:00 | 6,668.52 | 5,601.88 | 84 | 2,611.09 | 46.61 |
| 21:00 | 6,668.52 | 5,625.92 | 84.37 | 2,595.16 | 46.13 |
| 22:00 | 6,668.52 | 5,638.28 | 84.55 | 2,453.32 | 43.51 |
| 23:00 | 6,668.52 | 5,643.11 | 84.62 | 2,370.46 | 42.01 |

It can be concluded that the energy generation by wind turbines is dependent on the capacity factor of wind turbines and availability factor of wind energy.

Turkey showed significant effort to increase the share of renewable energy for the power generation in recent years. The renewable law which is introduced in 2005 aimed to increase the utilization of renewables in electricity generation, lower the GHG emission and diversify the energy sources (Official Gazette, 2005). This law is updated by the government in 2011. Basically, it is a mechanism that aims to build Turkish energy system in parallel with country's domestic and national energy policy. Wind, solar PV, geothermal, biomass, hydro and tidal energy are supported in this context (Enerji Portalı, 2018).

Therefore, EPIAS buys the total amount of generated electricity from the renewable energy power plants across the country. In other words, energy curtailment procedure was not applied in current situation due to small share of renewable energy in energy production. Curtailment means intentionally reducing the energy output of energy generators from the potential available production (California ISO, 2017). Curtailment can be applied to maintain system energy balance, not exceed the grid capacity and against low load demand. However, due to low share of renewable energy and country's more clean energy generation goals, curtailment applications is not performed by system operators in current situation in Turkey.

In this study, idealistic curtailment application is assumed. In Turkey, renewable energy producers such as solar and wind turbine participants have priority in selling generated electricity to EPIAS. According to the expert in MENR, this policy is in practice by EPIAS with parallel to country's widespread of renewable energy objectives. In other words, EPIAS promises the guarantee of purchasing the total amount of produced electricity which is provided by renewable energy power plants. Another reason of this procedure is the share of renewable energy in total electricity production is still relatively lower than conventional resources such as coal and natural gas.

As mentioned in previous sections, parameter “wind_out(t)” refers to the maximum potential electricity production by wind at time t . For current practices in Turkey, this parameter corresponds to the real time electricity generation. In simple words, real time electricity generation data which was imported from EPIAS refers to the parameter “wind_out(t)”. We developed our data fitting operation based on the RTEG.

We imported RTEG data starting from 2016 until the end of 2019. The fitting mechanism was carried out for supply side as follows. The first step was to segregate the supply data based on the months of the year. Secondly, the data was filtered again for each time hour in a day for each month. In this way, we applied the total number of 288 distribution fitting by implementing fitting procedure separately for 24 hours across 12 months. Hence, we can capture the hourly fluctuation in power generation for each month in a year. For distribution fitting process, the sample data must be independent and identically distributed. We enable this property by segregating the dataset through the hours for each month.

3.3.2. Hourly Electricity Demand Data Distribution Fitting

It is a common fact that electricity demand has high seasonality characteristic. For distribution fitting process, the sample data must be independent and identically distributed. However, in this case, the demand has strong hourly and daily circles. Figure 3.8 is very useful to illustrate this fact. It is easy to observe that demand shows similar patterns in daily basis. For instance, the demand steadily decreases between 0-4 am. Afterwards, it starts to increase until 12:00. Then, it has tendency to stay constant until 18 pm. Finally, it again starts to decrease until the end of the day. This pattern is illustrated by both figures above. This fact violates the “independent and identically distributed” assumption. Therefore, it is crucial to break the seasonality effect. The seasonality effect of the dataset recommends applying time series methods. However, time series analysis is out of context of this thesis.

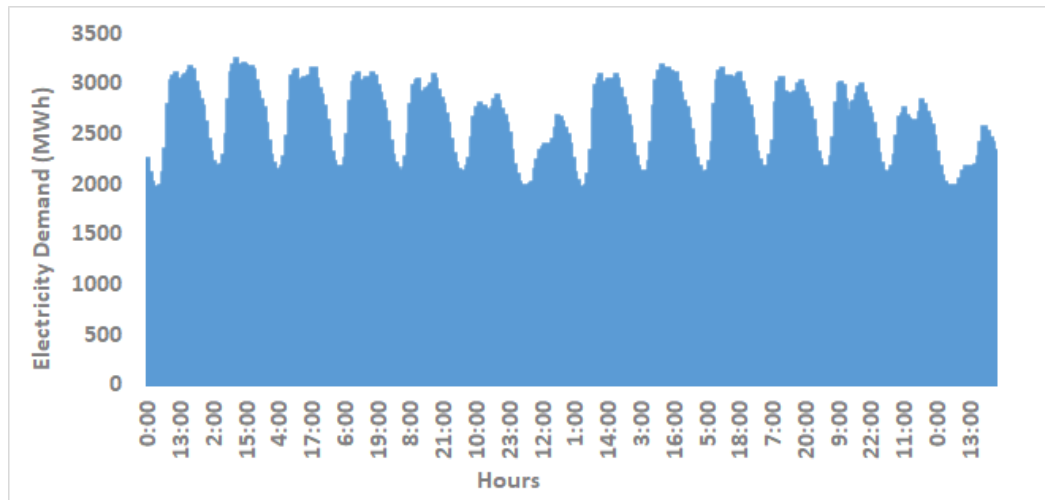


Figure 3.8. Hourly Demand Fluctuation between 7-20 January 2019 (EPIAS, 2020).

In order to overcome this problem, the following procedure was applied on the dataset. First, the data was split based on months of the year. Secondly, the data was filtered again for each time slot for each month. Finally, the data was filtered based on the working days and holidays. This has huge importance since there is a slight but enough decrease in the demand of electricity. One of the common reasons might be the decrease in industrial electricity consumption at weekends since it is not a working day. By applying this mechanism, we are able to capture the hourly demand fluctuation for each month through a year for both working days and holidays. It is important to note some exceptions. National holidays and religious festivals were considered as holidays even if they are in the weekdays. These data points were extracted from working days and used for distribution fitting of holidays.

Different than energy generation side, there are 3 filters that are applied on the load demand data. These are as follows:

- Month
- Weekday-Weekend
- Hour

After filtering operation, the seasonality effect of demand side was avoided. The next step is fitting the data to relevant probability distributions. Similar to energy generation side, the fitting operation is handled by Arena Input Analyzer. The same procedure with extra filter was applied on demand data. Therefore, distribution fitting operation was performed.

Uncertainty modeling plays a fundamental role in stochastic optimization to reflect the fluctuating characteristic of renewable energy. This is essential since each modeling method can reflect the system from differently. (Zakaria *et al.*, 2019). The optimization results would vary due to the several representations of the energy system. In this thesis, probability distribution function approximation technique is used to reflect the stochastic nature for renewable energy generation and load demand. The main logic behind the technique selection is we don't have perfect knowledge for both sides, as this method would be deterministic approach. Instead, we aim to approximate PDF's for each side, as we followed stochastic method. PDF approximation is implemented in hourly basis for both supply and demand side. Hourly PDF's were determined using Arena 16.0 Input Analyzer. The detailed explanation of distribution fitting operation will be presented in the following sub-sections.

After the uncertainties were modelled in the system, dataset generation step follows next. Broad representation of the current system can be achieved as a result of data generation. In this study, all simulations related with scenario generation were performed using R Studio Version 1.1.463.

10 datasets were generated for both energy supply and demand side by using Monte Carlo simulation based on 10 different seeds. The data generation process was carried out based on the pre-determined probability distributions. For 10 datasets for each side, total number of possible combinations of supply-demand pairs are equal to 100. We ran the optimization model for each combination of supply-demand pairs under different system configuration. As a consequence, we obtained the robustness for certain decision variables such as BESS capacity, utilization level etc.

4. SCENARIO ANALYSIS

4.1. Parameter Selection

Hourly energy supply and demand reflects the national data as it was taken from website of EPIAS. There isn't overall deployment of storage system in Turkey. Therefore, we can't obtained the national data. For this regard, we determined the parameters related with battery, such as cost structure and chemical efficiencies, based on literature review. As mentioned before, the total storage cost consists of investment cost, operation cost, maintenance cost and replacement cost of the batteries. Table 4.1 represents the cost parameters regarding with battery technology.

Table 4.1. Cost parameters of the storage system.

| Parameter | Value | Reference |
|-------------------------------------|---------|-------------------------------|
| Initial Unit Investment Cost | 350 | Lockhart <i>et al.</i> (2019) |
| Unit Operation Cost | 0.00047 | Malheiro <i>et al.</i> (2015) |
| Unit Maintenance Cost | 7.5 | Cole and Frazier (2019) |
| Unit Replacement Cost | 350 | Lockhart <i>et al.</i> (2019) |

Charging efficiency simply refers to the ratio of actual charged amount against transferred level during charging operation. Similarly, discharging efficiency indicates to the ratio of actual discharged amount against transferred level during discharging operation. On the other hand, self-discharge rate is the ratio of losing energy due to chemical structure of the battery units.

Jülch (2016) estimated and compared the overall efficiencies for different storage technologies and predicted the overall efficiency of LIB technology as 95%. In this study, the upper bound for efficiency parameters is assumed as 95%.

For the efficiency lower bound, we consider the study done by Abdin and Khalilpour (2019). In their work, the discharge efficiency is taken as 85%. Therefore, we assumed the lower bound for efficiency parameters as 85%. Chen *et al.* (2009) estimated the daily self-discharge rate between 0.1%-0.3%. In this study, we assumed the self-discharge rate similar to Chen *et al.* (2009). Table 4.2 represents the parameters related with battery technology.

Table 4.2. Efficiency parameters of LIB technology.

| Technology | Self-discharge Rate | Charging Eff. | Discharging Eff. |
|-------------------|----------------------------|----------------------|-------------------------|
| Li-ion | 0.1-0.3 | 85-95 | 85-95 |

Apart from storage cost, objective function also consists of renewable energy generation cost and penalty cost that occurs during serving the LWPS from NGA at each period. For this reason, electricity generation cost with different sources, for both fossil fuels and wind, must be defined, accordingly.

Table 4.3. Electricity generation costs with different energy sources.

| Source | Generation Cost | Reference |
|--------------------|------------------------|--------------------------------------|
| Wind | 50.1 | (Elektrik Üreticileri Derneği, 2018) |
| Natural Gas | 94 | (Yeşil Ekonomi, 2020) |

In the proposed model, CO₂ is released to the environment due to electricity generation from NGA. The unit of emission level is kton CO₂/MWh. For this reason, emission factors for different generation sources are defined. Table 4.4 represent the average emission factors. The emission factors of different fuels are taken from Turkish Green House Gas Inventory Report. Note that, the values in Table 4.4 is in ton CO₂/TJ. However, in our calculations, the unit change is implemented. In this thesis, the unit is kton CO₂/MWh.

Table 4.4. Emission factors for electricity generation sources.

| Source | Average Value | Unit | Reference |
|--|---------------|--------------------------|--|
| NGA | 55.6 | ton CO ₂ /TJ | (Turkish Greenhouse Gas Inventory, 2018) |
| Turkey's Average CO ₂ Emission Rate | 0.497 | ton CO ₂ /MWh | (Climate Transparency, 2017) |

National Renewable Energy Laboratory (2019) assumed discount rate as 10%-15%. In this study, discount rate is assumed as 10%. In addition, we assumed the useful lifetime of the system as 20 years.

Table 4.5. Financial parameters.

| Parameter | Value | Reference |
|-----------|----------|-------------------------------|
| i | 10%-15% | Lockhart <i>et al.</i> (2019) |
| A | 20 years | Lockhart <i>et al.</i> (2019) |

4.2. Definition of Scenarios

The scenarios are divided into three main categories. The relevant analysis for each category was carried out. The results of the analysis will be explained later.

Table 4.6. Scenarios and their definitions.

| Scenario | Definition |
|------------------------------------|---|
| Base | Run the model with base parameters |
| Battery Technology Scenario | Run the model with different efficiency and safety stock parameters |
| NO LWSP | Remove wind penetration constraint from the model |

Base scenarios reflect the optimization model with business as usual assumptions. Battery technology scenarios analyzes the situation with different parameters regarding battery technology. Finally, “NO LWSP” scenario analyzes the model if there is no restriction regarding wind energy penetration in the system.

4.3. Base Scenario

In this section, the results of base scenario will be presented and discussed. Base scenario are divided into 2 categories namely as “Global Base” and “Turkish Base”. Scenarios and their simple explanations were given in Table 4.7

Table 4.7. Base scenario and brief definition.

| Scenario | Definition |
|---------------------|--|
| Global Base | Business-as-usual assumptions. |
| Turkish Base | Emission intensity is based on Turkish energy portfolio. |

4.3.1. Global Base Scenario

The loss of wind power supply was satisfied with NGA and we assumed that there is infinite storage capacity to install in the system. Discount rate was considered as 10% and the lifetime of the proposed system was taken as 20 years. Both charging and discharging efficiency of the batteries were assumed as 90%. Fully charging and discharging of the batteries are allowed in the base model. Finally, the total BESS capacity is unrestricted. We assumed that there is no upper bound in terms of total BESS capacity in the system.

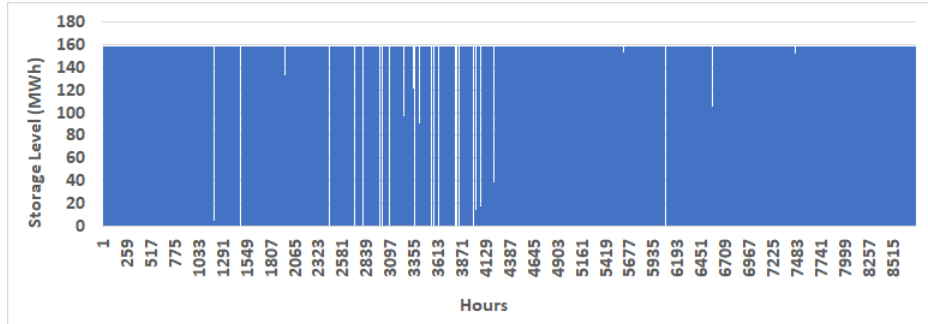


Figure 4.1. Hourly storage level while LWPSP=0.3 in base scenario.

As an example from optimization runs, Figure 4.1 represents the hourly storage level while LWPSP equals to 30%. Under these settings, the optimal battery capacity is 158.24 MWh. LCOE is found as 10.32 \$/MWh while the overall wind energy utilization is 83.66%. The cumulative CO₂ emission is 1,298.3 kton. For this case, battery utilization was as 20.48%. The batteries were empty %72 of the course year.

Figure 4.2 represents the hourly storage level if we force the model to deploy more wind energy. In other words, we select the minimum level of LWPSP as 20%. This time, 7,203.13 MWh battery capacity is found as an optimal solution. LCOE is found as 137.49 \$/MWh whereas the overall wind energy utilization is 98.36%. The cumulative CO₂ emission is 865.54 kton. The substantial increase of BESS capacity can be observed.

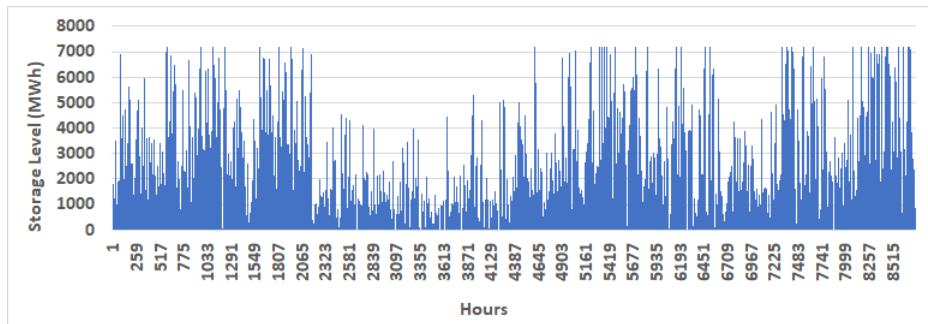


Figure 4.2. Hourly storage level while LWPSP=0.2 in base scenario.

To compensate the variation of wind energy and satisfy the wind energy penetration constraint, the model yielded a significantly higher BESS capacity. In the meantime, the LCOE has also increased in parallel with increment in storage unit capacity. To reach the desired renewable penetration in the system, the model utilized more wind energy nearly full.

For this case, `bat_util` equals to 15.38%. If we compare with previous case, the overall utilization decreased even if we force the model to deploy more wind energy. Normally, someone would expect the positive correlation between battery utilization and level of wind energy penetration. However, installed battery capacity outweighs the overall utilization even if lower LWSP. It can be concluded that the batteries have stored lower amount of inventory relative to its total capacity for second case. Regarding the percentage of empty inventory, the batteries were empty 47% through the year. If we compare with the previous case, the model charges and discharges more frequently regardless of overall decrease in utilization. Obviously, this is the expected outcome with lower LWSP in the system. That is due to the increased variance.

It must be noted that the minimum level for LWSP is 0.2 for the base scenario. After this value, the optimization model starts to yield infeasible solutions. This is due to the maximum utilization level of wind energy. In order to obtain LWSP as 20% in the system, the model used 97.91% of the wind energy. This is the average of 100 runs. If we force the model to decrease LWSP further, the wind can't satisfy the demand since it is fully utilized. At this point, the demand also can't be satisfied by natural gas since upper bound for LWSP in the system is restricted by Equation 3.23. Therefore, infeasibility occurs in the model.

As an example of model results with a specific supply-demand pair, Figure 4.3 illustrates the monthly energy balance while LWSP is equal to 20%. From the graph above, we can observe the seasonality characteristic of wind energy. We can observe the steady trend during first 3 months of the year. From April, there is steady increasing trend until the end of summer. Following is the decreasing trend again until October.

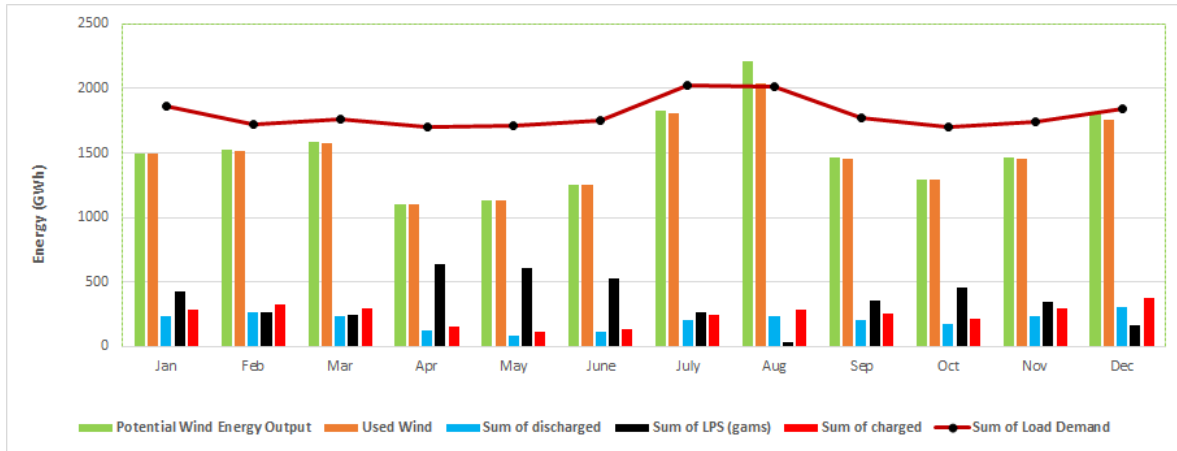


Figure 4.3. Monthly energy balance while LWPSP=0.2 in base scenario.

For the rest of the year, the overall wind energy output tends to increase again. This stands as a good example of the variation and unreliable characteristic of wind energy. It is apparent from this graph that the fossil fuels were used most in April since the renewable energy generation has the lowest level during the same month. The model decided to use more fossil fuels as well as utilizing the wind energy possible to satisfy the demand and obtain the energy balance. However, a small amount of energy was reserved to charge the batteries. Regarding energy balance, batteries also supported the supply side as they recharge during the month.

The least amount of fossil fuels were burnt in August. This situation is due to the highest achievable renewable energy generation during this month. Utilized wind energy was almost enough to satisfy the electricity demand in August. This is why the fossil fuels were used less in August than remaining months. It is also noticeable that the model depended on fossil fuels in each month to achieve demand satisfaction. The main reason of this situation is that additional capacity is required to satisfy the demand with wind. However, since the battery technology is more expensive than burning fossil, the model decided to install BESS on optimal level and utilize fossils, instead. Otherwise, the objective function would increase significantly. Therefore, it can be concluded that dependence on fossil fuels would still continue unless the relevant cost parameters will drop for LIB technology.

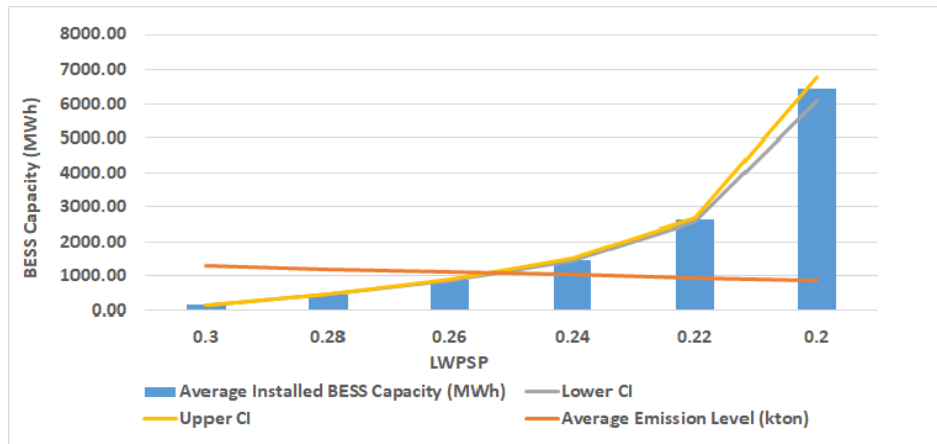


Figure 4.4. Installed BESS capacity and cumulative emission level for different LWPSP in base scenario.

As a result of 100 runs with global base scenario, Figure 4.4 represents relationship between average installed battery capacity with average of yearly cumulative emission level under different wind penetration levels. As it can be easily observed, the intersection point reflects the situation in which LWPSP equals 24%.

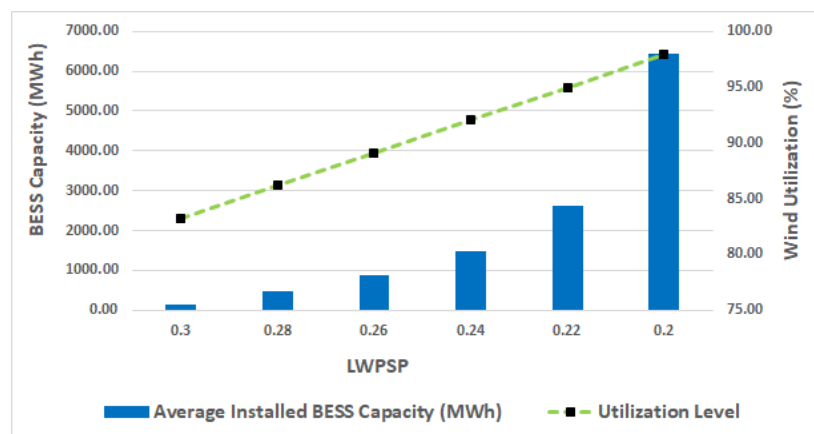


Figure 4.5. Installed BESS capacity, cumulative emission and wind utilization level for different LWPSP in base scenario.

According to the results of 100 runs with global base scenario, Figure 4.5 exhibits the relationship between average installed battery capacity under increasing wind energy penetration levels. The graph also illustrates the overall utilization level of wind energy by different LWPSP values. The steady increment of wind utilization level can be easily observed. The wind energy is utilized more each time we force to achieve a higher renewable portion while satisfying the demand. It must be noted that the model yields infeasibility if we would like to achieve LWPSP lower than 20%. The wind energy is almost fully utilized while LWPSP is 20% in the system.

The starting point of LWPSP is 30% since the wind power itself can satisfy the 70% of the demand without any storage capacity, on average. As we force the optimization model to obtain lower LWPSP value, the installed battery capacity in the system increases. Obviously, this is an expected outcome. The main reason of this situation is that the model decides to apply less curtailment on wind energy, produce more renewable energy and charge the batteries with the excess production. However, as long as we decrease the share of fossil fuels in the system, the model decides to produce more electricity using wind. As a result, the utilization level of wind increases as expected. This illustrates the penetration of renewable energy in the grid as we obtain more smooth production in supply side.

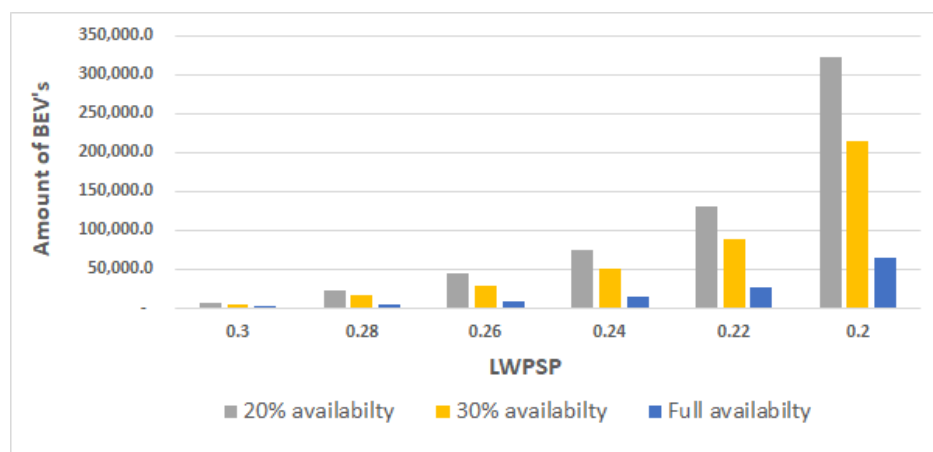


Figure 4.6. Total number of BEV's required for base scenario.

Figure 4.6 illustrates the relationship between LWSP and required number of BEV's under different availability assumptions. In order to calculate the required number of BEV's, we assumed that 1 BEV has 100 KWh battery capacity. Regarding availability of BEV's, we assumed 3 different availability values. These are 20%, 30% and 100%. For instance, we assumed that 20% of the BEV's are available for charging-discharging purposes. The remaining 80% were assumed as unavailable which means they were using for transportation purposes. Under full availability assumption, the system requires nearly 1,400 BEV's while LWSP equals 30%. If we aim to increase the wind penetration up to 80%, the system requires nearly 65,000 BEV's. While LWSP equals to 30%, if we assumed 30% availability total 4,800 BEV's are required whereas it increases 7,000 BEV's under 20% availability. While LWSP equals to 20%, the required BEV's were 214,000 and 321,000 for 30% and 20% availability assumptions, respectively.

4.3.2. Turkish Base Scenario

In this scenario, we run the model according to the current energy portfolio of Turkey. This is nearly double of the world average. According to Climate Transparency (2017), the average emission level due to power generation of Turkish energy portfolio is 0.497 ton CO₂/MWh. In simple words, whenever the energy is generated by burning NGA, 0.497 ton emission per MWh is released. In base scenario, it is assumed that the LWPS is served with only burning NGA. According to Turkish Greenhouse Gas Inventory (2018), the emission factor for NGA due to energy generation is 55.6 ton CO₂/TJ. After applying the unit change, it is resulted as 0.25 ton CO₂/MWh which is nearly the half of average emission rate in Turkey.

Figure 4.7 illustrates the average of storage unit capacity and average of yearly cumulative emission level under different LWSP values. Different from the base scenario, the intersection point reflects the situation in which LWSP equals 22%.

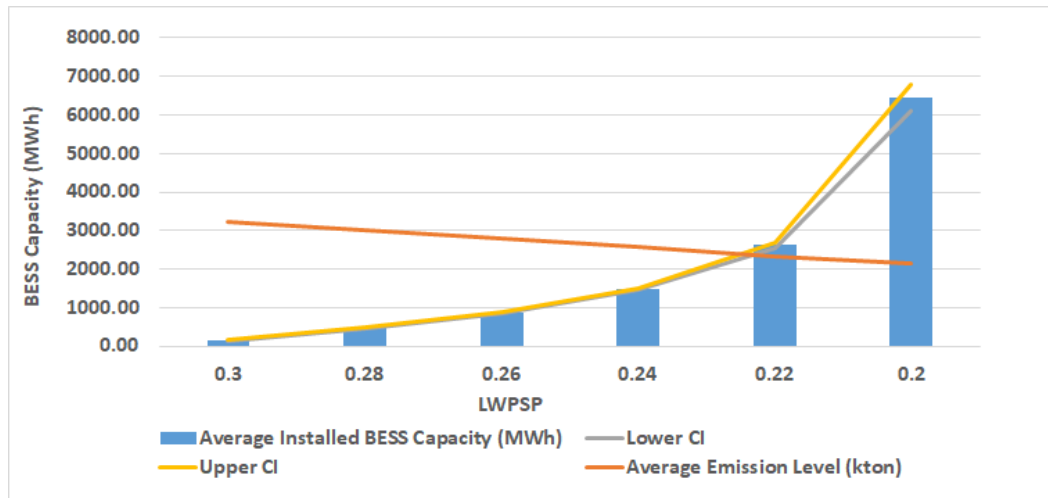


Figure 4.7. Installed BESS capacity and cumulative emission level for different LWSP in Turkish energy portfolio scenario.

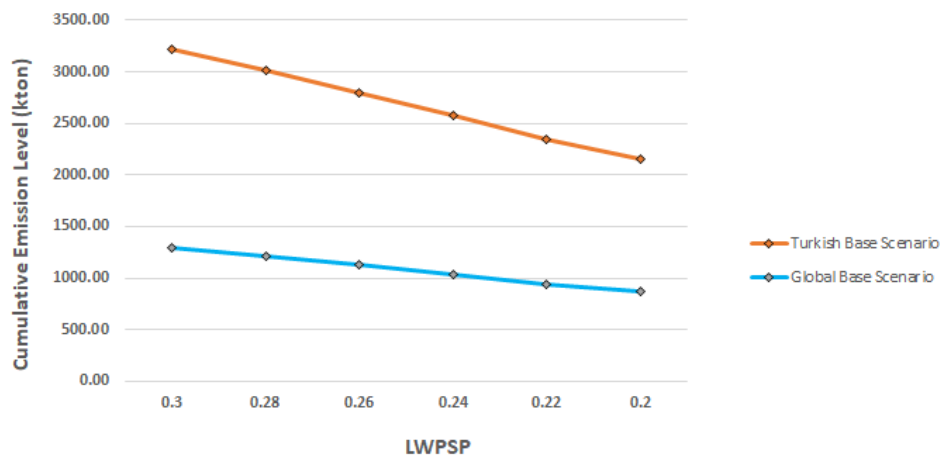


Figure 4.8. Average cumulative emission level comparison between base and Turkish energy portfolio scenario.

Figure 4.8 compares the average of yearly cumulative emission levels between base scenario and Turkish energy portfolio scenario. The orange line indicates the trend of the average of yearly cumulative emission based on Turkish energy portfolio whereas the blue one exhibits the change in average of yearly cumulative emission level based on emission factor of NGA. As it can be seen, the Turkish portfolio releases almost double emission against by only burning NGA.

4.4. Battery Technology Scenario

Battery technology scenarios are divided into two categories. These are as follows:

Table 4.8. Battery technology scenarios and their definitions.

| Scenario | Explanation |
|-------------------|---------------------------------|
| Long Life | Run with safety stock parameter |
| Efficiency | Change efficiency parameters |

Regarding long life scenario, different c_{min} and c_{max} values were defined as threshold values. The main purpose of this scenario is to show how much additional capacity was required if we would like to obtain long battery lifetime.

In efficiency scenarios, we tried to analyze how model output can be effected with different battery charging-discharging efficiency and self discharge rate. As the LIB technology matures with growing research and development studies, overall efficiency of the LIB technology is expected to increase. Therefore, we aimed to observe how model reacts against maturing battery technology.

4.4.1. Long Life Scenario

Fully charging and complete discharging are usually not recommended by battery manufacturers to obtain long operational life of battery.

Considering this fact, we added additional constraints to the global base scenario. 3 different threshold values for allowable SOC were obtained to analyze how much installed battery capacity is required.

Table 4.9. Minimum and maximum allowable SOC for long life scenario.

| Threshold Range | c_min | c_max |
|-----------------|-------|-------|
| 1 | 5% | 95% |
| 2 | 10% | 90% |
| 3 | 15% | 85% |

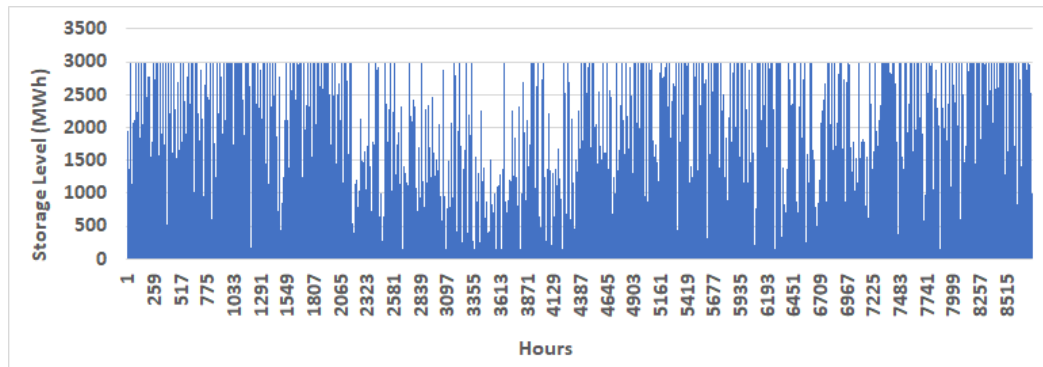


Figure 4.9. Hourly storage level with first threshold range while LWPSP=0.22.

Figure 4.9 represents the hourly storage level of the battery with threshold range 1 while LWPSP equals to 22%. Under these settings, the optimal battery capacity is 3,128.92 MWh. LCOE results as 63.84 \$/MWh while the overall wind energy utilization is 95.42%. The cumulative CO₂ emission is 952.09 kton. Note that $\min(r_{\text{storage}})=156.44$ and $\max(r_{\text{storage}})=2,972.48$. In other words, that fully discharging and fully charging is avoided by the model.

As an example from experiments, Figure 4.10 represents the hourly storage level of the battery with threshold range 2 while LWPSP equals to 22%. The optimal BESS capacity is 3,521.77 MWh.

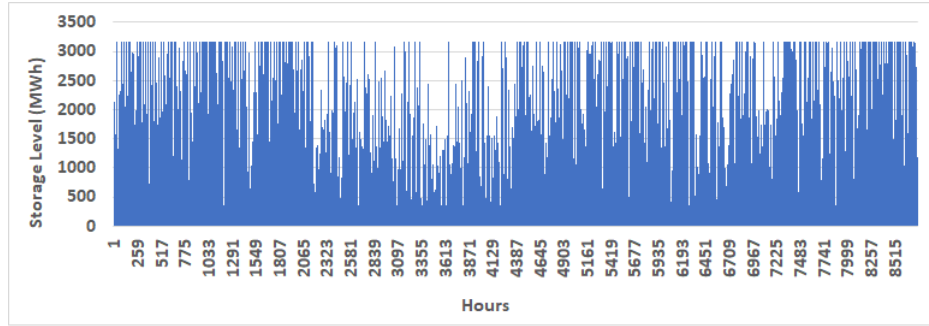


Figure 4.10. Hourly storage level with second threshold range while LWPSP=0.22.

If we compare the results with first threshold values, nearly 13% additional capacity is required. This results is expected due to additional unused capacity and inefficiency of storage units. LCOE resulted as 70.95 \$/MWh while the overall wind energy utilization is 95.43%. The cumulative CO₂ emission is 952.09 kton. Note that $\min(r_{\text{storage}})=352.17$ and $\max(r_{\text{storage}})=3,169.59$. This proves that required safety stock is provided due to the selection of threshold values as 10% and 90%.

As an example from carried experiments, Figure 4.11 represents the hourly storage level of the battery with 2. threshold level while LWPSP equals to 22%. For this case, the optimal battery capacity is 4,027.422 MWh. If we compare the results with first threshold values, nearly 29% additional capacity is required. LCOE resulted as 80.09 \$/MWh while the overall wind energy utilization is 95.43%.

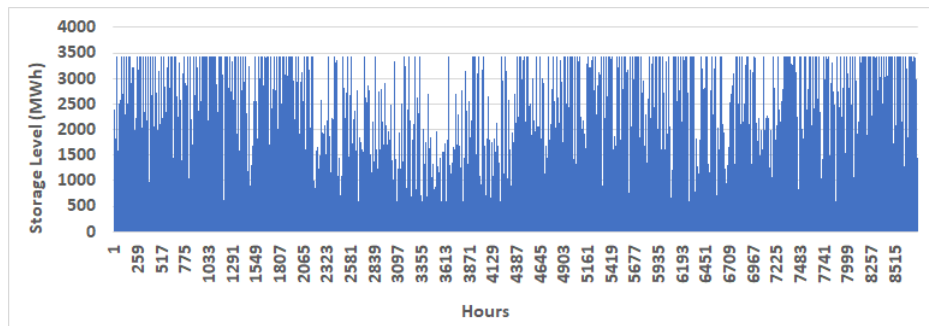


Figure 4.11. Hourly storage level with third threshold range while LWPSP=0.22.

Note that $\min(r_{\text{storage}}) = 604.11$ and $\max(r_{\text{storage}}) = 3,423.3$. This proves that required safety stock is provided due to the selection of threshold values as 15% and 85%.

The effect of unused capacity to achieve long life can be easily observed from the perspective of installed BESS capacity. Against base scenario, there is 11.15% increase in installed BESS capacity on average if allowable range is 5%-95%. If the allowable range is between 10%-90%, the battery capacity has increased 25.12%, on average. Finally, the model yielded 43.13% more installed capacity in case of the allowable range between 15%-85%.

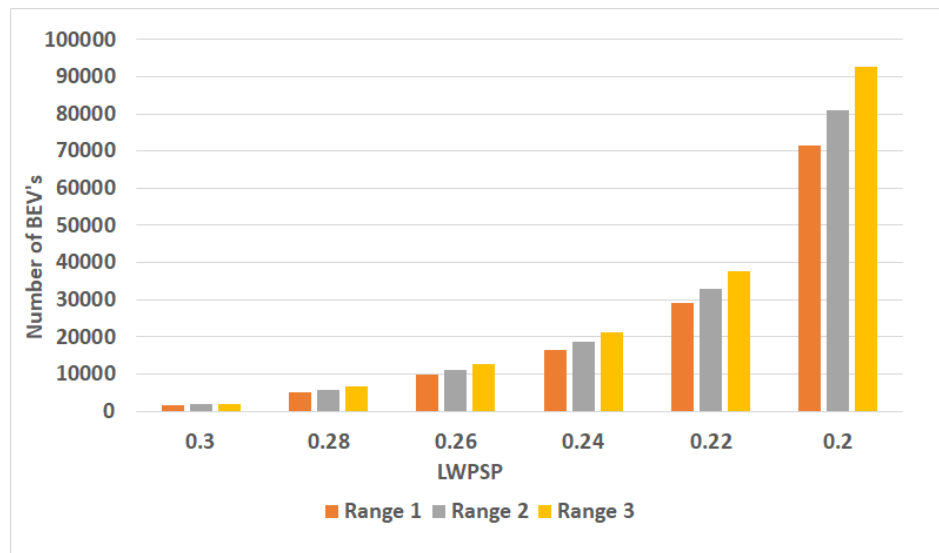


Figure 4.12. Total number of BEV's required for long life scenario under full availability assumption.

Similar comments can be made for the amount of required BEV's to obtain necessary capacity. As long as safety stock and upper bound increases, the level of installed capacity increases. Hence, this means more electric vehicles are needed in the system. For instance, nearly 72,000 BEV's are required if first threshold range were applied under 20% LWSP in the system. This number goes up to 81,000 for second threshold range whereas nearly 93,000 BEV's are required in case of third threshold scenario.

4.4.2. Efficiency Scenario

Battery efficiency parameters indicate the estimated percentage of actual delivered energy, either to or from the battery, during the operation of battery. Regarding efficiency scenario, 2 different efficiency configurations were defined.

Table 4.10. Efficiency configurations for efficiency scenario.

| Scenario | Charging Efficiency | Discharging Efficiency |
|----------------|---------------------|------------------------|
| Low Efficiency | 85% | 85% |
| Ideal Battery | 100% | 100% |

For low efficient battery scenario, the parameters related with battery technology were considered as in undesired form. Charging and discharging efficiency of the storage units were assumed as 85%. Another proposed system setting is called ideal battery scenario. We assumed that charging and discharging efficiencies of batteries are 100%. In simple words, we assumed that there is no inefficiency in the storage units.

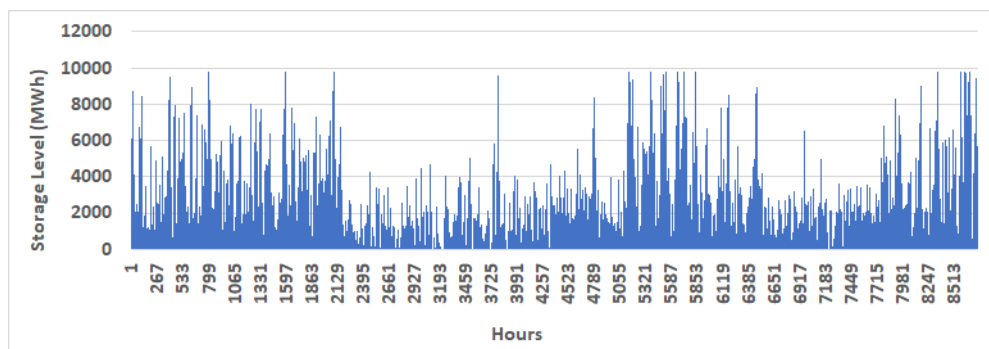


Figure 4.13. Hourly storage level with low efficient battery while LWSP=0.2.

For instance, Figure 4.13 represents the hourly storage level of the storage units with lower efficient batteries while LWSP equals to 20%. The install BESS capacity is 9,767.79 MWh. LCOE resulted as 184.07 \$/MWh while the overall wind energy utilization is 99.05%. The cumulative CO₂ emission is 864.29 kton.

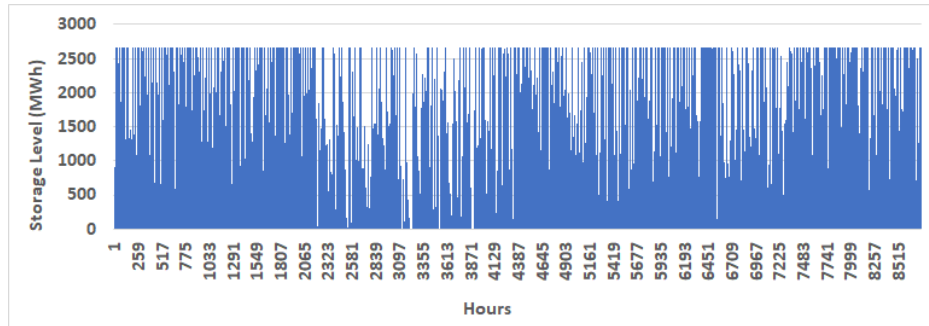


Figure 4.14. Hourly storage level with ideal battery while LWSP=0.2.

For instance, Figure 4.14 represents the hourly storage level of the storage units with lower efficient batteries while LWSP equals to 20%. The install BESS capacity is 2,658.61 MWh. LCOE resulted as 55.18 \$/MWh while the overall wind energy utilization is 94.14%. The cumulative CO₂ emission is 864.29 kton. If we compare with low efficient battery scenario, the installed BESS capacity almost 73% decreased. In case of LCOE, it nearly dropped its half. Renewable energy penetration can not be higher than 84% in the system since 99.24% of wind energy was utilized while LWSP is equal to 16%. After this value, the model yields infeasibility. Different from previous technology scenarios, renewable proportion in the system can be increased up to 84% since there is less amount loss of energy due to high efficiency of the batteries. Therefore, high efficient batteries enable wind energy to be deployed more in the proposed system.

4.5. No LWSP Scenario

As stated previously, constraint 3.23 implied a minimum average level for the wind energy penetration in the system. We limited the total yearly cumulative carbon emission from a different perspective. That's why we did not add carbon tax because it would be meaningless. It will only increase LCOE since the model firstly try to satisfy the wind penetration with certain percentage. To achieve this, it installs specific capacity to compensate the variation between supply and demand. However, for "no LWSP" scenario, we removed this constraint and assess the effect of carbon tax.

Few adjustments were made in the model. Firstly, total penalty cost was defined. The calculation of the total penalty cost is as follows:

$$total_pen_cost = \sum_{t=1}^{8760} carbon_tax * dir_emis_factor * LWPS(t). \quad (4.1)$$

in which

- `total_pen_cost`: total penalty cost (in USD)
- `carbon_tax`: unit carbon tax cost (in \$/ton CO₂)
- `dir_emis_factor`: emission intensity (in ton CO₂/MWh)

We start to apply different amount of carbon tax and find the point where installing BESS would be more beneficial in terms of objective function. For the current cost structure of the model, the turning point resulted as 10,500 \$ per ton CO₂. Generating energy from NGA is more favorable in terms of cost if carbon tax is less than 10,500 \$ per ton CO₂. After this amount, the model decides to install capacity and takes advantage of wind energy more.

Table 4.11. Performance measure results for “no LWPSP” scenario.

| Performance Measure | Minimum | Average | Maximum |
|---------------------|---------|---------|---------|
| Capacity | 41.29 | 81.81 | 142.48 |
| LWPSP | 29.45 | 30.43 | 31.1 |
| LCOE | 82.61 | 84.07 | 85.33 |
| wind_util | 82.26 | 82.64 | 83.13 |
| dir_emis | 1,273.2 | 1,316.4 | 1,347 |

Performance measures regarding “no LWPSP” scenario were listed in Table 4.11. After running 100 runs with each combination of supply and demand pairs, we obtained average capacity as 81.81 MWh, LWPSP as 30.43%, average LCOE as 84.07 MWh and yearly average cumulative emission as 1316.4 kton CO₂.

In addition, the model benefited % 82.64 of the wind energy through the year, on average. Table 4.12 lists the confidence intervals for “No LWSP” scenario.

Table 4.12. 95% confidence interval for “No LWSP” scenario.

| Performance Measures | Lower CI | Average | Upper CI |
|-----------------------------|-----------------|----------------|-----------------|
| Capacity | 77.09 | 81.81 | 86.52 |
| LWSP | 30.34 | 30.43 | 30.51 |
| LCOE | 83.92 | 84.07 | 84.22 |
| wind_util | 82.6 | 82.64 | 82.67 |
| dir_emis | 1312.69 | 1316.4 | 1320.1 |

5. CONCLUSION

The paradigm shift is approaching when it comes to the way of energy is generated. According to many, the spread of renewables in energy systems are inevitable. However, transition to sustainable energy has brought with few challenges for system operators due to undesired characteristics of renewable energy. As stated earlier, intermittency and unavailability aspects due to unstable weather conditions stand as a strong problem against full transition to sustainable and clean energy in nations. Battery energy storage systems can be determining component with their critical role and can accelerate this transformation.

In our setting, we proposed a hypothetical question that considers the effect of battery energy storage system on the uncertainty and efficiency level of renewable energy. Specifically, wind was assumed as the dominant energy provider and lithium-ion batteries were assumed as the main storage units. We aimed to test the efficiency of wind power using storage capacity under different scenarios. To carry out the required analysis, both linear optimization model and a statistical model was developed. National electricity generation and demand data was used to develop the statistical model.

We developed the optimization model that analyzes the system on a hourly basis. Energy kept in storage units were treated as stock which was held in a general inventory setting. To put it another way, we addressed the problem as multi period scheduling problem.

We reported the results by analyzing the system from both technical and economical perspective. In our experiments, we did not take the price competition into consideration by assuming that the energy demand is inelastic. In addition, it must be underlined that our model did not reveal the real energy cost values. Instead, we reported the relative cost values.

Although the cost parameters show the current cost structure, the results reveal the comparative analysis. From this perspective, the results regarding cost values of the system can be considered as a trade-off measure. This is mainly due to the fact that we proposed a fictive system setting in the study.

To capture the stochastic nature of both energy supply and demand, we used Monte Carlo technique by approximating probability distribution functions. We used the wind power and energy demand fluctuation values of Turkey between 2016 and 2019 to be used as input for data fitting purposes. For supply side, the total number of 288 PDF's were obtained for 24 hours on a day through 12 months in a year. For demand side, the first segregation was based on the working day or holiday distinction. Then, the same procedure applied was for both sides by fitting each hour in a day through each month in a year. In summary, we fitted total number of 864 PDF's. The number of data points, Chi-Square test statistic and corresponding p-value and Kolmogorov-Smirnov test statistic and corresponding p-value were listed for each PDF's in the appendix. Then, in order to generate alternative instances demand-supply realizations, we have generated 100 instances using Monte Carlo simulation.

According to the global base scenario, the wind penetration in the system is 70% without any storage capacity. With the help of BESS, this level can be increased up to 80%. After this point, the infeasibility occurs since wind energy is fully utilized. Based on optimization runs, the average installed BESS capacity is between 143 MWh and 6,435 MWh whereas the LCOE is in a wide range from 10 \$/MWh to 123 \$/MWh. Regarding confidence intervals of battery capacity, it is found between 134.73 MWh and 6,090 MWh under different LWSP values. On the other hand, confidence intervals of wind utilization levels are found between 83.15% and 98.04% under different LWSP values. Only 10% increase in wind penetration nearly lead to eleven times higher LCOE in the proposed system, as well as 44 times higher capacity can be required. This situation is mainly due to higher variability in supply side. The model installs higher capacity to compensate the high variability each time when a higher wind efficiency level is forced.

The non-linear relationship can be easily observed between capacity and wind efficiency level. The capacity increases in non-linear manner against higher wind utilization. On the other hand, the efficiency level of wind power increases linearly with the help of storage capacity. Figure 5.1 illustrates this relationship.

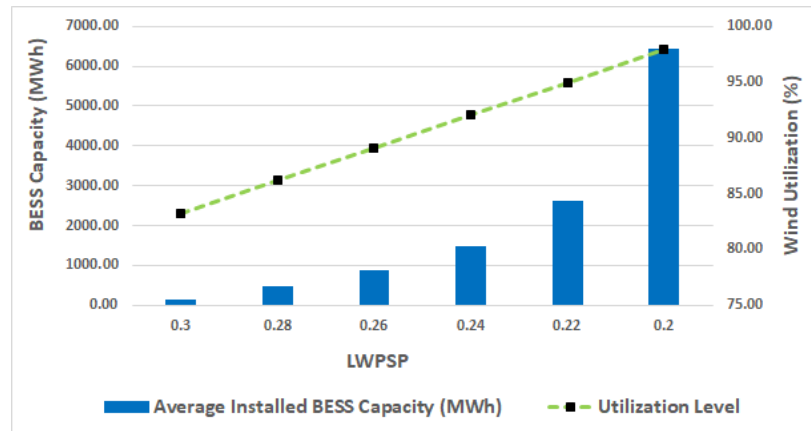


Figure 5.1. Installed BESS capacity and wind efficiency under different LWSP levels.

In long life scenario, we selected 3 different threshold ranges to analyze the extra required capacity if we would like obtain longer operational life of storage units. According to long life scenario with first threshold range, the average installed BESS capacity is between 159 MWh and 7,165 MWh whereas the LCOE is in a wide range from 10 \$/MWh to 136 \$/MWh. If we compare with base scenario, nearly 11.24% increase has been observed. This result is due to unused capacity forced by safety stock and upper bound restriction. For the case of second threshold, the average installed BESS capacity starts from 179 MWh and 8,086 MWh. For his case, the LCOE starts from 10 \$/MWh to 153 \$/MWh. Almost 25% of capacity increase has been observed, comparing with base scenario. Finally, if we apply third threshold values to the model, we reported average capacities beginning from 205 MWh to 9,283 MWh. LCOE starts from 11 \$/MWh to 175 \$/MWh. This case, drastic increment has been observed. Similar to previous cases, safety stock and upper bound restrictions lead to higher capacity requirements in the model.

Regarding the low efficient battery scenario, the average installed BESS capacity is between 152 MWh and 10,133 MWh. LCOE has been resulted as between 10 \$/MWh and 190 \$/MWh. For this case, the model yielded 40 infeasible solutions out of 100 runs while LWSP is 20%. This is simply due to high energy loss occurred in energy exchange. Only 60 out of 100 runs yielded feasible solutions. For some supply-demand pairs, the wind is almost fully utilized but the desired wind penetration was not reached against the demand. Therefore, infeasible solution occurs.

If we assume that the storage units are ideal, the average capacity values have a wide interval beginning from 128 MWh to 119,000 MWh, under different LWSP values. In addition, LCOE starts from 9 \$/MWh and increases up to above 2,000 \$/MWh. Different from other cases, wind penetration level can be increased up to 84% since we have zero loss due to chemical inefficiency. That means more energy can be stored in the batteries and therefore we can utilize wind energy more. However, 36 out of 100 runs yielded infeasible solutions. Only 64 supply and demand combinations yielded feasible solutions while LWSP equals to 16%. Similar to low efficient battery scenario, the wind energy can't satisfy the desired level of LWSP for some certain supply-demand pairs in the system. For those cases, the model yields infeasible solution.

According to the model results, system operators must determine the carbon tax above 10,000 \$/kton CO₂ to make renewable favorable in terms of financial perspective. Considering the fact that average carbon tax is about 120 \$/MWh across Europe, this number is drastically high. This situation is simply because of the current cost structure of LIB technology. It can be said that the cost must decrease drastically in order them to be utilized more.

We have also provided a calculation for the amount of BEV's that are necessary to achieve the total required storage capacity in Turkey. For this calculation, we assumed 3 different availability values. Under the assumption of full availability, the required BEV's is found between 1,400 and 65,000.

If we assume that the 30% of electric vehicles are ready to be used as storage units on average, the total amount of required BEV's is calculated between 4,800 and 214,000. Finally, this number is calculated between 7,000 and 321,000 under 20% availability assumption. Turkey Wind Energy Potential Atlas predicts the total usable potential wind energy capacity as 47,850 MW. For current situation, Turkey utilizes almost 19.56% of its potential capacity, accounting of 9,367.5 MW. With a simple calculation, Turkey can satisfy nearly 40% of its current demand by utilizing the total wind energy potential across the country. Under these setting, the total number of actual BEV's must be multiplied with 5. At this point, domestic production of lithium-ion batteries and governmental incentives may play a critical role to accelerate the spread of storage technologies and green energy in Turkey.

For the future work, the analysis can be extended to model the penetration of other renewable energy systems in Turkey. Based on national data, a similar analysis can be conducted with more detailed perspective where the penetration of hourly solar, geothermal and/or biomass generation can be taken into account. In this thesis, we assumed that wind is the dominant energy provider in the system. The analysis can also be supported with detailed modeling of vehicle to grid mechanisms on a national scale. Considering the expected spread of BEV's as a result of a paradigm shift in auto industry and the national electric car project of Turkey, future researches can mathematically model the vehicle to grid mechanism as batteries in the BEV can be used as stored energy supplies to national grid during on peak demand periods. Similarly, both environmental and economical analysis can be implement on a national scale.

REFERENCES

- Abdin, Z. and K. R. Khalilpour, “Chapter 4 - Single and Polystorage Technologies for Renewable-Based Hybrid Energy Systems”, K. R. Khalilpour (Editor), *Polygeneration with Polystorage for Chemical and Energy Hubs*, pp. 77 – 131, Academic Press, 2019.
- Alex, Z., A. Clark, W. Cheung, L. Zou and J. Kleissl, “Minimizing the Lead-Acid Battery Bank Capacity through a Solar PV - Wind Turbine Hybrid System for a high-altitude village in the Nepal Himalayas”, *Energy Procedia*, Vol. 57, pp. 1516 – 1525, 2014, 2013 ISES Solar World Congress.
- Atwa, Y. M. and E. F. El-Saadany, “Optimal Allocation of ESS in Distribution Systems With a High Penetration of Wind Energy”, *IEEE Transactions on Power Systems*, Vol. 25, No. 4, pp. 1815–1822, 2010.
- Bahmani-Firouzi, B. and R. Azizipanah-Abarghooee, “Optimal sizing of battery energy storage for micro-grid operation management using a new improved bat algorithm”, *International Journal of Electrical Power & Energy Systems*, Vol. 56, pp. 42–54, 2014.
- Bahramirad, S., W. Reder and A. Khodaei, “Reliability-Constrained Optimal Sizing of Energy Storage System in a Microgrid”, *IEEE Transactions on Smart Grid*, Vol. 3, No. 4, pp. 2056–2062, 2012.
- Beltran, H., E. Bilbao, E. Belenguer, I. Etxeberria-Otadui and P. Rodriguez, “Evaluation of Storage Energy Requirements for Constant Production in PV Power Plants”, *IEEE Transactions on Industrial Electronics*, Vol. 60, No. 3, pp. 1225–1234, 2013.
- Bird, L., M. Milligan and D. Lew, *Integrating Variable Renewable Energy: Challenges and Solutions*, Tech. rep., U.S National Renewable Energy Laboratory, 2013.

BNEF, “2023 Türkiye’inde en ucuz elektrik üretim kaynağı rüzgar ve güneş olacak”, <https://yesilekonomi.com/2023-turkiyesinde-en-ucuz-elektrik-uretim-kaynagi-ruzgar-ve-gunes-olacak/>, accessed at July 2020.

Bogdanov, D. and C. Breyer, “North-East Asian Super Grid for 100% renewable energy supply: Optimal mix of energy technologies for electricity, gas and heat supply options”, *Energy Conversion and Management*, Vol. 112, pp. 176–190, 2016.

Brekken, T. K. A., A. Yokochi, A. von Jouanne, Z. Z. Yen, H. M. Hapke and D. A. Halamay, “Optimal Energy Storage Sizing and Control for Wind Power Applications”, *IEEE Transactions on Sustainable Energy*, Vol. 2, pp. 69–77, 2011.

Cabral, C. V. T., D. O. Filho, A. S. A. C. Diniz, J. H. Martins, O. M. Toledo and L. V. M. Neto, “A stochastic method for stand-alone photovoltaic system sizing”, *Solar Energy*, Vol. 84, No. 9, pp. 1628 – 1636, 2010.

Cervone, A., G. Carbone, E. Santini and S. Teodori, “Optimization of the battery size for PV systems under regulatory rules using a Markov-Chains approach”, *Renewable Energy*, Vol. 85, pp. 657–665, 2016.

Chakraborty, S., T. Senjyu, H. Toyama, A. Saber and T. Funabashi, “Determination methodology for optimising the energy storage size for power system”, *IET Generation, Transmission & Distribution*, Vol. 3, pp. 987–999, 2009.

Chen, S. X., H. B. Gooi and M. Q. Wang, “Sizing of Energy Storage for Microgrids”, *IEEE Transactions on Smart Grid*, Vol. 3, No. 1, pp. 142–151, 2012.

Chen, H., T. N. Cong, W. Yang, C. Tan, Y. Li and Y. Ding, “Progress in electrical energy storage system: A critical review”, *Progress in Natural Science*, Vol. 19, No. 3, pp. 291 – 312, 2009.

Child, M., D. Bogdanov and C. Breyer, “The Baltic Sea Region: Storage, grid exchange and flexible electricity generation for the transition to a 100% renewable energy system”, *Energy Procedia*, Vol. 155, pp. 390 – 402, 2018.

Child, M., D. Bogdanov and C. Breyer, “The role of storage technologies for the transition to a 100% renewable energy system in Europe”, *Energy Procedia*, Vol. 155, pp. 44 – 60, 2018, 12th International Renewable Energy Storage Conference, IRES 2018, 13-15 March 2018, Düsseldorf, Germany.

CISO, “Impacts of renewable energy on grid operations”, <https://www.caiso.com/documents/curtailmentfastfacts.pdf>, accessed at June 2020.

Cole, W. and A. W. Frazier, *Cost Projections for Utility-Scale Battery Storage*, Tech. rep., National Renewable Energy Laboratory, 2019.

Condon, M., R. L. Revesz and B. Unel, *Managing the Future of Energy Storage*, Tech. rep., Institute for Policy Integrity, 2018.

CTTRAN, *Brown to green: The G20 transition to a low carbon economy*, Tech. rep., Climate Transparency, 2017.

Diaf, S., D. Diaf, M. Belhamel, M. Haddadi and A. Louche, “A methodology for optimal sizing of autonomous hybrid PV/wind system”, *Energy Policy*, Vol. 35, No. 11, pp. 5708 – 5718, 2007.

Dragičević, T., H. Pandžić, D. Škrlec, I. Kuzle, J. M. Guerrero and D. S. Kirschen, “Capacity Optimization of Renewable Energy Sources and Battery Storage in an Autonomous Telecommunication Facility”, *IEEE Transactions on Sustainable Energy*, Vol. 5, No. 4, pp. 1367–1378, 2014.

EIA, “Wind generation seasonal patterns vary across the United States”, <https://www.eia.gov/todayinenergy/detail.php?id=20112>, accessed at August 2020.

Ekren, O. and B. Y. Ekren, “Size optimization of a PV/wind hybrid energy conversion system with battery storage using simulated annealing”, *Applied Energy*, Vol. 87, No. 2, pp. 592 – 598, 2010.

EP, “Türkiye Elektrik Enerjisi Üretim İstatistikleri: Nisan 2021”, <https://www.enerjiportali.com/turkiye-elektrik-enerjisi-uretim-istatistikleri-nisan-2021/>, accessed at April 2021.

EP, “Yenilenebilir Enerji Kaynakları Destekleme Mekanizması (YEKDEM) Nedir?”, <https://www.enerjiportali.com/yenilenebilir-enerji-kaynaklari-destekleme-mekanizmasi-yekdem-nedir/>, accessed at June 2020.

EPIAS, “Hakkımızda”, <https://www.epias.com.tr>, accessed at April 2020.

EPIAS, “Şeffaflık Platformu”, <https://seffaflik.epias.com.tr/transparency/>, accessed at April 2020.

EUD, “2020 Sonrası Yenilenebilir Enerji Kaynakları Destek İhtiyaçları ve Mekanizma Önerileri Çalışma Grubu Raporu”, , 2018, <http://www.eud.org.tr/wp-content/uploads/2020-sonrasi-yek-tesvikleri-oneri-raporu.pdf>, accessed at June 2020.

Evans, A., V. Strezov and T. J. Evans, “Assessment of utility energy storage options for increased renewable energy penetration”, *Renewable and Sustainable Energy Reviews*, Vol. 16, No. 6, pp. 4141 – 4147, 2012.

Handleman, C., “New NREL Data Suggests Wind Could Replace Coal as Nations Primary Generation Source”, , 2015.

IRENA, *Electricity storage and renewables: costs and markets to 2030*, Tech. rep., International Renewable Energy Agency, Abu Dhabi, 2017.

IRENA, *Electricity Storage Valuation Framework: Assessing system value and ensuring project viability*, Tech. rep., International Renewable Energy Agency, Abu Dhabi, 2020.

Julch, V., “Comparison of electricity storage options using levelized cost of storage method”, *Applied Energy*, Vol. 183, pp. 1594 – 1606, 2016.

Kelton, W., R. Sadowski and N. Zupick, *Simulation with Arena*, McGraw-Hill Publishing, 5th edn., 2010.

Khorramdel, H., J. Aghaei, B. Khorramdel and P. Siano, “Optimal Battery Sizing in Microgrids Using Probabilistic Unit Commitment”, *IEEE Transactions on Industrial Informatics*, Vol. 12, pp. 834–843, 2015.

Kilickaplan, A., D. Bogdanov, O. Peker, U. Caldera, A. Aghahosseini and C. Breyer, “An energy transition pathway for Turkey to achieve 100% renewable energy powered electricity, desalination and non-energetic industrial gas demand sectors by 2050”, *Solar Energy*, Vol. 158, pp. 218 – 235, 2017.

Korpaas, M., A. T. Holen and R. Hildrum, “Operation and sizing of energy storage for wind power plants in a market system”, *International Journal of Electrical Power & Energy Systems*, Vol. 25, No. 8, pp. 599 – 606, 2003, 14th Power Systems Computation Conference.

Li, Y., Y. Li, P. Ji and J. Yang, “Development of energy storage industry in China: A technical and economic point of review”, *Renewable and Sustainable Energy Reviews*, Vol. 49, pp. 805 – 812, 2015.

Liserre, M., T. Sauter and J. Y. Hung, “Future Energy Systems: Integrating Renewable Energy Sources into the Smart Power Grid Through Industrial Electronics”, *IEEE Industrial Electronics Magazine*, Vol. 4, No. 1, pp. 18–37, 2010.

Lockhart, E., X. Li, S. Booth, J. Salasovich, D. Olis, J. Elsworth and L. Lisell, *Comparative Study of Techno-Economics of Lithium-Ion and Lead-Acid Batteries in Microgrid in Sub-Saharan Africa*, Tech. rep., National Renewable Energy Laboratory, 2019.

Lopes, J. A. P., C. L. Moreira and A. G. Madureira, “Defining control strategies for MicroGrids islanded operation”, *IEEE Transactions on Power Systems*, Vol. 21, No. 2, pp. 916–924, 2006.

Luo, Y., L. Shi and G. Tu, “Optimal sizing and control strategy of isolated grid with wind power and energy storage system”, *Energy Conversion and Management*, Vol. 80, pp. 407 – 415, 2014.

Malheiro, A., P. M. Castro, R. M. Lima and A. Estanqueiro, “Integrated sizing and scheduling of wind/PV/diesel/battery isolated systems”, *Renewable Energy*, Vol. 83, pp. 646 – 657, 2015.

Marchi, B., S. Zanoni and M. Pasetti, “Multi-Period Newsvendor Problem for the Management of Battery Energy Storage Systems in Support of Distributed Generation”, *Energies*, Vol. 12, p. 4598, 12 2019.

MENR, *2019-2023 Stratejik Planı*, Tech. rep., Republic of Turkey Ministry of Energy and Natural Resources, 2018, https://sp.enerji.gov.tr/ETKB_2019_2023_Stratejik_Planı.pdf, accessed at August 2020.

MGM, “Türkiye Rüzgar Enerjisi Potansiyeli”, https://www.mgm.gov.tr/FILES/haberler/2010/rets-seminer/2_Mustafa_CALISKAN_RITM.pdf, accessed at August 2020.

Morais, H., P. Kádár, P. Faria, Z. A. Vale and H. Khodr, “Optimal scheduling of a renewable micro-grid in an isolated load area using mixed-integer linear programming”, *Renewable Energy*, Vol. 35, No. 1, pp. 151 – 156, 2010.

Nguyen, T. A., M. L. Crow and A. C. Elmore, “Optimal Sizing of a Vanadium Redox Battery System for Microgrid Systems”, *IEEE Transactions on Sustainable Energy*, Vol. 6, No. 3, pp. 729–737, 2015.

Ozcan, E. and S. Erol, “A Multi-Objective Mixed Integer Linear Programming Model for Electricity Generation Planning in Turkey”, *Gazi University Journal of Science*, Vol. 1, pp. 41–54, 2013.

Palma-Behnke, R., C. Benavides, F. Lanas, B. Severino, L. Reyes, J. Llanos and D. Sáez, “A Microgrid Energy Management System Based on the Rolling Horizon Strategy”, *IEEE Transactions on Smart Grid*, Vol. 4, No. 2, pp. 996–1006, 2013.

Rekioua, D., *Hybrid Renewable Energy Systems*, Springer International Publishing, 2020.

REN21, *Renewables 2017 Global Status Report*, Tech. rep., Renewable Energy Policy Network for the 21st Century, 2017.

Rossetti, M. D., *Simulation Modeling and Arena*, Wiley Publishing, 2nd edn., 2015.

Ru, Y., J. Kleissl and S. Martinez, “Storage Size Determination for Grid-Connected Photovoltaic Systems”, *IEEE Transactions on Sustainable Energy*, Vol. 4, No. 1, pp. 68–81, 2013.

Saboori, H., R. Hemmati and M. A. Jirdehi, “Reliability improvement in radial electrical distribution network by optimal planning of energy storage systems”, *Energy*, Vol. 93, pp. 2299 – 2312, 2015.

Saran, P., J. Goentzel and C. W. Siegert, “Economic analysis of wind plant and battery storage operation using supply chain management techniques”, *IEEE PES General Meeting*, pp. 1–8, 2010.

Schneider, M., K. Biel, S. Pfaller, H. Schaede, S. Rinderknecht and C. H. Glock, “Optimal Sizing of Electrical Energy Storage Systems using Inventory Models”, *Energy Procedia*, Vol. 73, pp. 48 – 58, 2015.

Schneider, M., K. Biel, S. Pfaller, H. Schaede, S. Rinderknecht and C. H. Glock, “Using inventory models for sizing energy storage systems: An interdisciplinary approach”, *Journal of Energy Storage*, Vol. 8, pp. 339 – 348, 2016.

Shang, C., D. Srinivasan and T. Reindl, “An improved particle swarm optimisation algorithm applied to battery sizing for stand-alone hybrid power systems”, *International Journal of Electrical Power & Energy Systems*, Vol. 74, pp. 104–117, 2016.

Silva, I. F., C. Bentz, M. Bouhtou, M. Chardy and S. Kedad-Sidhoum, “Energy storage management with energy curtailing incentives in a telecommunications context”, *10th International Workshop on Lot sizing - IWLS 2019*, Conservatoire national des arts et métiers, Paris, France, 2019.

Sørensen, B., “Chapter 1 - Introduction”, B. Sørensen (Editor), *Renewable Energy Conversion, Transmission and Storage*, p. 1, Academic Press, Burlington, 2007.

Suazo-Martínez, C., E. Pereira-Bonvallet and R. Palma-Behnke, “A Simulation Framework for Optimal Energy Storage Sizing”, *Energies*, Vol. 7, pp. 3033–3055, 2014.

Tan, C. W., T. C. Green and C. A. Hernandez-Aramburo, “A stochastic method for battery sizing with uninterruptible-power and demand shift capabilities in PV (photovoltaic) systems”, *Energy*, Vol. 35, No. 12, pp. 5082 – 5092, 2010.

TUIK, *Turkish Greenhouse Gas Inventory 1990-2018*, Tech. rep., Turkish Statistical Institute, 2020, <https://unfccc.int/documents/223580>, accessed at June 2020.

UNCC, “About the Secretariat”, <https://unfccc.int/about-us/about-the-secretariat>, accessed at June 2020.

Vazquez, S., S. M. Lukic, E. Galvan, L. G. Franquelo and J. M. Carrasco, “Energy Storage Systems for Transport and Grid Applications”, *IEEE Transactions on Industrial Electronics*, Vol. 57, No. 12, pp. 3881–3895, 2010.

Wang, X. Y., D. M. Vilathgamuwa and S. S. Choi, “Determination of Battery Storage Capacity in Energy Buffer for Wind Farm”, *IEEE Transactions on Energy Conversion*, Vol. 23, No. 3, pp. 868–878, 2008.

Wang, W., C. Mao, J. Lu and D. Wang, “An Energy Storage System Sizing Method for Wind Power Integration”, *Energies*, Vol. 6, pp. 3392–3404, 2013.

WB, “Turkey’s Energy Transition Milestones and Challenges”, <http://documents1.worldbank.org/curated/en/249831468189270397/pdf/ACS14951-REVISED-Box393232B-PUBLIC-EnergyVeryFinalEN.pdf>, accessed at June 2020.

WEC, *Turkish Energy Market Outlook: Achievements, Overview and Opportunities*, Tech. rep., World Energy Council, 2016, <https://www.dunyaenerji.org.tr/wp-content/uploads/2017/10/turkish-energy-market-outlook.pdf>, accessed at December 2020.

Wu, J., B. Zhang, H. Li, Z. Li, Y. Chen and X. Miao, “Statistical distribution for wind power forecast error and its application to determine optimal size of energy storage system”, *International Journal of Electrical Power & Energy Systems*, Vol. 55, pp. 100 – 107, 2014.

WWF, “Turkey’s Renewable Power- Alternative Power Supply Scenarios for Turkey”, , 2014, https://wwftr.awsassets.panda.org/downloads/wwf_turkey___bnef___turkey_s_renewable_power___alternative_power_supply_scenarios_until_.pdf?4182, accessed at August 2020.

Yang, Y., S. Bremner, C. Menictas and M. Kay, “Battery energy storage system size determination in renewable energy systems: A review”, *Renewable and Sustainable Energy Reviews*, Vol. 91, pp. 109–125, 2018.

Yang, Y., H. Li, A. Aichhorn, J. Zheng and M. Greenleaf, “Sizing Strategy of Distributed Battery Storage System With High Penetration of Photovoltaic for Voltage Regulation and Peak Load Shaving”, *IEEE Transactions on Smart Grid*, Vol. 5, No. 2, pp. 982–991, 2014.

Yang, H., L. Lu and W. Zhou, “A novel optimization sizing model for hybrid solar-wind power generation system”, *Solar Energy*, Vol. 81, No. 1, pp. 76 – 84, 2007.

Zakaria, A., F. B. Ismail, M. H. Lipu and M. Hannan, “Uncertainty models for stochastic optimization in renewable energy applications”, *Renewable Energy*, Vol. 145, pp. 1543–1571, 2020.

Zheng, Y., Z. Y. Dong, F. J. Luo, K. Meng, J. Qiu and K. P. Wong, “Optimal Allocation of Energy Storage System for Risk Mitigation of DISCOs With High Renewable Penetrations”, *IEEE Transactions on Power Systems*, Vol. 29, No. 1, pp. 212–220, 2014.

APPENDIX A: OPTIMIZATION MODEL ROBUST RESULTS

Table A.1. Minimum, maximum and average capacity results in global base scenario.

| LWPSP | Minimum Capacity | Average Capacity | Maximum Capacity |
|--------------|-------------------------|-------------------------|-------------------------|
| 0.3 | 62.24 | 143.53 | 219.09 |
| 0.28 | 354.12 | 463.76 | 568.26 |
| 0.26 | 713.26 | 878.04 | 1,030.61 |
| 0.24 | 1,204.25 | 1,482.96 | 1,738.92 |
| 0.22 | 2,022.68 | 2,625.52 | 3,191.6 |
| 0.2 | 3,863.55 | 6,435.53 | 9,879.9 |

Table A.2. 3 sigma limits for average capacity results in global base scenario.

| LWPSP | Lower Bound | Average | Upper Bound |
|--------------|--------------------|----------------|--------------------|
| 0.3 | 9.61 | 143.53 | 277.44 |
| 0.28 | 285.94 | 463.76 | 641.59 |
| 0.26 | 619.91 | 878.04 | 1,136.17 |
| 0.24 | 1,044.28 | 1,482.96 | 1,921.63 |
| 0.22 | 1,598.98 | 2,625.52 | 3,652.05 |
| 0.2 | 1,171.56 | 6,435.53 | 11,699.5 |

Table A.3. Minimum, maximum and average capacity results for 1. threshold range.

| LWPSP | Minimum Capacity | Maximum Capacity | Average Capacity |
|--------------|-------------------------|-------------------------|-------------------------|
| 0.3 | 69.16 | 243.44 | 159.47 |
| 0.28 | 393.47 | 631.45 | 515.29 |
| 0.26 | 792.53 | 1,145.24 | 975.58 |
| 0.24 | 1,338.1 | 1,932.51 | 1,647.75 |
| 0.22 | 2,247.57 | 3,547.82 | 2,917.69 |
| 0.2 | 4,294.28 | 10,998.08 | 7,165.78 |

Table A.4. 3 sigma limits of average capacity with 1. threshold in long life scenario.

| LWPSP | Lower Bound | Average | Upper Bound |
|--------------|--------------------|----------------|--------------------|
| 0.3 | 9.9 | 159.48 | 309.05 |
| 0.28 | 316.55 | 515.29 | 714.03 |
| 0.26 | 686.97 | 975.59 | 1,264.21 |
| 0.24 | 1,157.12 | 1,647.75 | 2,138.38 |
| 0.22 | 1,769.28 | 2,917.69 | 4,066.11 |
| 0.2 | 1,248.13 | 7,165.79 | 13,083.44 |

Table A.5. Minimum, maximum and average capacity results for 2. threshold range.

| LWPSP | Minimum Capacity | Maximum Capacity | Average Capacity |
|--------------|-------------------------|-------------------------|-------------------------|
| 0.3 | 77.81 | 273.90 | 179.42 |
| 0.28 | 442.66 | 710.45 | 579.66 |
| 0.26 | 891.62 | 1,288.58 | 1,097.63 |
| 0.24 | 1,505.43 | 2,174.6 | 1,853.99 |
| 0.22 | 2,529.1 | 3,993.57 | 3,283.56 |
| 0.2 | 4,835.02 | 12,439.76 | 8,086.06 |

Table A.6. 3 sigma limits of average capacity with 2. threshold in long life scenario.

| LWPSP | Lower Bound | Average | Upper Bound |
|--------------|--------------------|----------------|--------------------|
| 0.3 | 11.98 | 179.42 | 346.86 |
| 0.28 | 357 | 579.67 | 802.33 |
| 0.26 | 774.46 | 1097.64 | 1420.82 |
| 0.24 | 1304.48 | 1854 | 2403.52 |
| 0.22 | 1996.52 | 3283.57 | 4570.61 |
| 0.2 | 1407.47 | 8086.07 | 14,764.66 |

Table A.7. Minimum, maximum and average capacity results for 3. threshold.

| LWPSP | Minimum Capacity | Maximum Capacity | Average Capacity |
|--------------|-------------------------|-------------------------|-------------------------|
| 0.3 | 88.93 | 313.06 | 205.06 |
| 0.28 | 505.92 | 812.05 | 662.61 |
| 0.26 | 1,019.03 | 1,472.92 | 1,254.59 |
| 0.24 | 1,720.82 | 2,486.03 | 2,119.27 |
| 0.22 | 2,891.47 | 4,567.4 | 3,754.4 |
| 0.2 | 5,531.55 | 14,344.57 | 9,283.6 |

Table A.8. 3 sigma limits of average capacity with 3. threshold in long life scenario.

| LWPSP | Lower Bound | Average | Upper Bound |
|--------------|--------------------|----------------|--------------------|
| 0.3 | 12.72 | 205.07 | 397.41 |
| 0.28 | 406.99 | 662.62 | 918.25 |
| 0.26 | 883.22 | 1,254.59 | 1,625.96 |
| 0.24 | 1,487.63 | 2,119.28 | 2,750.92 |
| 0.22 | 2,274.01 | 3,754.41 | 5,234.81 |
| 0.2 | 1,512.16 | 9,283.61 | 17,055.05 |

Table A.9. Minimum, maximum and average capacity for low efficiency scenario.

| LWPSP | Minimum Capacity | Maximum Capacity | Average Capacity |
|--------------|-------------------------|-------------------------|-------------------------|
| 0.3 | 66.03 | 233.73 | 152.75 |
| 0.28 | 379.05 | 614.59 | 499.65 |
| 0.26 | 775.73 | 1,140.45 | 966.226 |
| 0.24 | 1,354.85 | 2,055.08 | 1,715.02 |
| 0.22 | 2,466.40 | 4,437.94 | 3,475.26 |
| 0.2 | 6,653.21 | 20,582.52 | 10,133.88 |

Table A.10. 3 sigma limits of average capacity in low efficiency scenario

| LWPSP | Lower Bound | Average | Upper Bound |
|--------------|--------------------|----------------|--------------------|
| 0.3 | 8.92 | 152.75 | 296.58 |
| 0.28 | 303.19 | 499.66 | 696.12 |
| 0.26 | 666.66 | 966.23 | 1,265.8 |
| 0.24 | 1,131.04 | 1,715.02 | 2,299.01 |
| 0.22 | 1,670.03 | 3,475.26 | 5,280.49 |
| 0.2 | 1,263.03 | 10,133.89 | 19,004.74 |

Table A.11. Minimum, maximum and average capacity for ideal battery scenario.

| LWPSP | Minimum Capacity | Maximum Capacity | Average Capacity |
|--------------|-------------------------|-------------------------|-------------------------|
| 0.3 | 55.88 | 194.82 | 128.15 |
| 0.28 | 313.23 | 494.89 | 406.73 |
| 0.26 | 618 | 869.32 | 748.73 |
| 0.24 | 1,002.54 | 1,371.82 | 1198.51 |
| 0.22 | 1,544.05 | 2,167.44 | 1875.76 |
| 0.2 | 2,442.14 | 3,687.14 | 3,100.06 |
| 0.18 | 4,269.54 | 8,050.18 | 6,197.81 |
| 0.16 | 12,862.82 | 28,5070 | 119,041.74 |

Table A.12. 3 sigma limits of average capacity in ideal battery scenario.

| LWPSP | Lower Bound | Average | Upper Bound |
|--------------|--------------------|----------------|--------------------|
| 0.3 | 8.76 | 128.15 | 247.56 |
| 0.28 | 254.42 | 406.73 | 559.04 |
| 0.26 | 542.85 | 748.73 | 954.62 |
| 0.24 | 893.73 | 1,198.51 | 1,503.3 |
| 0.22 | 1,347.29 | 1,875.76 | 2,404.23 |
| 0.2 | 1,967.44 | 3,100.07 | 4,232.7 |
| 0.18 | 2,537.62 | 6,197.81 | 9,858 |
| 0.16 | 0 | 119,041.74 | 443,671.55 |

**APPENDIX B: ARENA DISTRIBUTION FITTING
SUMMARIES**

Table B.1. Arena PDF fitting summary for wind energy supply in January.

| Hour | Expression | Sample Size | Chi-Square | p-value | K-S Test | p-value |
|------|--------------------------|-------------|------------|---------|----------|---------|
| 0 | 436+5090*BETA(0.95,1.57) | 124 | 5.41 | 0.38 | 0.038 | 0.15 |
| 1 | 379+5000*BETA(0.98,1.52) | 124 | 2.76 | 0.73 | 0.042 | 0.15 |
| 2 | 425+5110*BETA(0.98,1.62) | 124 | 1.4 | 0.75 | 0.049 | 0.15 |
| 3 | 444+5040*BETA(0.98,1.59) | 124 | 2.56 | 0.75 | 0.0503 | 0.15 |
| 4 | 424+4970*BETA(0.99,1.57) | 124 | 6.8 | 0.24 | 0.059 | 0.15 |
| 5 | 469+4710*BETA(0.92,1.42) | 124 | 9.68 | 0.15 | 0.06 | 0.15 |
| 6 | 479+4710*BETA(0.93,1.48) | 124 | 9.91 | 0.08 | 0.06 | 0.15 |
| 7 | 459+4720*BETA(0.95,1.51) | 124 | 4.42 | 0.49 | 0.045 | 0.15 |
| 8 | 470+4900* BETA(0.98,1.6) | 124 | 1.54 | 0.75 | 0.04 | 0.15 |
| 9 | 343+WEIB(2150,1.48) | 124 | 7.62 | 0.11 | 0.057 | 0.15 |
| 10 | TRIA(233,942,5430) | 124 | 2.91 | 0.71 | 0.064 | 0.15 |
| 11 | TRIA(148,873,5460) | 124 | 2.16 | 0.75 | 0.04 | 0.15 |
| 12 | 126+WEIB(2350,1.6) | 124 | 1.82 | 0.75 | 0.04 | 0.15 |
| 13 | 146+5500*BETA(1.26,2.04) | 124 | 1.33 | 0.75 | 0.044 | 0.15 |
| 14 | 177+5430*BETA(1.23,1.97) | 124 | 5 | 0.42 | 0.037 | 0.15 |
| 15 | 170+WEIB(2310,1.54) | 124 | 3.8 | 0.44 | 0.053 | 0.15 |
| 16 | 198+5510*BETA(1.16,1.92) | 124 | 5.15 | 0.41 | 0.045 | 0.15 |
| 17 | 243+5450*BETA(1.14,1.89) | 124 | 4.14 | 0.53 | 0.045 | 0.15 |
| 18 | 273+5500*BETA(1.17,1.97) | 124 | 4.71 | 0.46 | 0.049 | 0.15 |
| 19 | 271+WEIB(2280,1.49) | 124 | 4.14 | 0.4 | 0.063 | 0.15 |
| 20 | 263+5380*BETA(1.14,1.8) | 124 | 3.42 | 0.63 | 0.045 | 0.15 |
| 21 | 202+5390*BETA(1.19,1.78) | 124 | 2.55 | 0.75 | 0.052 | 0.15 |
| 22 | 211+WEIB(2350,1.53) | 124 | 5.03 | 0.42 | 0.047 | 0.15 |
| 23 | 194+5400*BETA(1.21,1.85) | 124 | 1.54 | 0.75 | 0.045 | 0.15 |

Table B.2. Arena PDF fitting summary for wind energy supply in February.

| Hour | Expression | Sample Size | Chi-Square | p-value | K-S Test | p-value |
|------|------------------------------|-------------|------------|---------|----------|---------|
| 0 | 135+5310* BETA(1.17,1.67) | 113 | 3.83 | 0.57 | 0.042 | 0.15 |
| 1 | 148+5260*BETA(1.16,1.68) | 113 | 2.25 | 0.75 | 0.04 | 0.15 |
| 2 | 118+5280*BETA(1.18,1.69) | 113 | 2.38 | 0.75 | 0.039 | 0.15 |
| 3 | 135+5220*BETA(1.15,1.65) | 113 | 3 | 0.7 | 0.037 | 0.15 |
| 4 | 148+5160*BETA(1.14,1.61) | 113 | 1.52 | 0.75 | 0.049 | 0.15 |
| 5 | 208+5020*BETA(1.08,1.54) | 113 | 3.29 | 0.65 | 0.049 | 0.15 |
| 6 | 235+5080*BETA(1.08,1.54) | 113 | 3.34 | 0.65 | 0.056 | 0.15 |
| 7 | 267+5110*BETA(1.08,1.54) | 113 | 3.43 | 0.49 | 0.069 | 0.15 |
| 8 | 228+5220*BETA(1.04,1.55) | 113 | 1.76 | 0.75 | 0.04 | 0.15 |
| 9 | 171+5170*BETA(0.978,1.41) | 113 | 1.46 | 0.75 | 0.043 | 0.15 |
| 10 | 179+5080*BETA(0.978,1.41) | 113 | 1.69 | 0.75 | 0.042 | 0.15 |
| 11 | 182+5180*BETA(0.875,1.32) | 113 | 0.67 | 0.75 | 0.048 | 0.15 |
| 12 | 154+5250*BETA(0.875,1.32) | 113 | 4.08 | 0.54 | 0.048 | 0.15 |
| 13 | 146+5200*BETA(0.881,1.26) | 113 | 5.33 | 0.39 | 0.055 | 0.15 |
| 14 | 164+5110*BETA(0.881,1.26) | 113 | 9.65 | 0.08 | 0.052 | 0.15 |
| 15 | 163+5040*BETA(0.881,1.26) | 113 | 7.13 | 0.22 | 0.048 | 0.15 |
| 16 | 151+5100*BETA(0.881,1.26) | 113 | 4.86 | 0.44 | 0.056 | 0.15 |
| 17 | 147+5110*BETA(0.881,1.26) | 113 | 7.73 | 0.18 | 0.053 | 0.15 |
| 18 | 107+5150*BETA(0.881,1.26) | 113 | 5.89 | 0.33 | 0.057 | 0.15 |
| 19 | 117+5080*BETA(1.07,1.39) | 113 | 2.4 | 0.75 | 0.04 | 0.15 |
| 20 | 121+4950*BETA(1.07,1.39) | 113 | 2.5 | 0.75 | 0.047 | 0.15 |
| 21 | 109+5190*BETA(1.07,1.39) | 113 | 2.5 | 0.75 | 0.047 | 0.15 |
| 22 | 96+WEIB(2450,1.57) | 113 | 5.68 | 0.14 | 0.067 | 0.15 |
| 23 | 94+5240*BETA(1.21,1.67) | 113 | 4.61 | 0.47 | 0.054 | 0.15 |

Table B.3. Arena PDF fitting summary for wind energy supply in March.

| Hour | Expression | Sample Size | Chi-Square | p-value | K-S Test | p-value |
|------|--------------------------|-------------|------------|---------|----------|---------|
| 0 | 306+5290*BETA(1.21,2.02) | 123 | 1.31 | 0.75 | 0.041 | 0.15 |
| 1 | 349+5160*BETA(1.11,1.89) | 123 | 5.03 | 0.426 | 0.047 | 0.15 |
| 2 | 375+WEIB(2030,1.36) | 123 | 8.1 | 0.0905 | 0.06 | 0.15 |
| 3 | 375+WEIB(2020,1.35) | 123 | 5.92 | 0.216 | 0.064 | 0.15 |
| 4 | TRIA(315,957,5440) | 123 | 7.13 | 0.221 | 0.062 | 0.15 |
| 5 | 245+ERLA(991,2) | 123 | 11.6 | 0.0215 | 0.052 | 0.15 |
| 6 | 167+GAMM(1030,1.99) | 123 | 6.22 | 0.198 | 0.053 | 0.15 |
| 7 | 110+GAMM(1010,2.06) | 123 | 5.38 | 0.161 | 0.055 | 0.15 |
| 8 | 101+ERLA(1050,2) | 123 | 4.66 | 0.211 | 0.046 | 0.15 |
| 9 | 118+ERLA(1000,2) | 123 | 7.14 | 0.14 | 0.06 | 0.15 |
| 10 | 121+GAMM(1190,1.68) | 123 | 3.46 | 0.487 | 0.058 | 0.15 |
| 11 | 122+WEIB(2210,1.4) | 123 | 8.18 | 0.0883 | 0.066 | 0.15 |
| 12 | 156+GAMM(1270,1.62) | 123 | 8.94 | 0.066 | 0.07 | 0.15 |
| 13 | TRIA(216,925,5420) | 123 | 9.09 | 0.108 | 0.091 | 0.15 |
| 14 | TRIA(365,1120,5400) | 123 | 12.4 | 0.0314 | 0.1 | 0.145 |
| 15 | 298+WEIB(2210,1.43) | 123 | 10.1 | 0.0774 | 0.066 | 0.15 |
| 16 | 231+WEIB(2340,1.56) | 123 | 6.27 | 0.194 | 0.058 | 0.15 |
| 17 | 228+WEIB(2360,1.58) | 123 | 7.43 | 0.122 | 0.053 | 0.15 |
| 18 | 253+WEIB(2330,1.58) | 123 | 4.21 | 0.395 | 0.058 | 0.15 |
| 19 | 259+WEIB(2400,1.69) | 123 | 4.86 | 0.315 | 0.069 | 0.15 |
| 20 | 307+WEIB(2340,1.64) | 123 | 5.39 | 0.25 | 0.084 | 0.15 |
| 21 | 345+WEIB(2260,1.56) | 123 | 7.17 | 0.138 | 0.062 | 0.15 |
| 22 | 375+5040*BETA(1.17,1.81) | 123 | 1.55 | 0.75 | 0.058 | 0.15 |
| 23 | 332+5200*BETA(1.19,1.95) | 123 | 1.78 | 0.75 | 0.042 | 0.15 |

Table B.4. Arena PDF fitting summary for wind energy supply in April.

| Hour | Expression | Sample Size | Chi-Square | p-value | K-S Test | p-value |
|------|---------------------------|-------------|------------|---------|----------|---------|
| 0 | 109+4470*BETA(0.99,2.08) | 120 | 2.8 | 0.596 | 0.0608 | 0.15 |
| 1 | 116+4360*BETA(0.99,2.12) | 120 | 1.26 | 0.75 | 0.0521 | 0.15 |
| 2 | 113+4310*BETA(0.99,2.17) | 120 | 0.721 | 0.75 | 0.0442 | 0.15 |
| 3 | 110+WEIB(1440,1.29) | 120 | 4.67 | 0.21 | 0.0517 | 0.15 |
| 4 | 110+WEIB(1430,1.29) | 120 | 2.81 | 0.436 | 0.0491 | 0.15 |
| 5 | 139+3980*BETA(0.86,1.77) | 120 | 5.63 | 0.234 | 0.0514 | 0.15 |
| 6 | 152+4080*BETA(0.88,1.9) | 120 | 2.45 | 0.657 | 0.0663 | 0.15 |
| 7 | 159+4180*BETA(0.915,2.16) | 120 | 4.72 | 0.207 | 0.0598 | 0.15 |
| 8 | 113+4270*BETA(0.914,2.27) | 120 | 5.03 | 0.185 | 0.0669 | 0.15 |
| 9 | 70+GAMM(931,1.3) | 120 | 3.59 | 0.324 | 0.0629 | 0.15 |
| 10 | 68+4320*BETA(0.75,1.88) | 120 | 1.37 | 0.716 | 0.0944 | 0.15 |
| 11 | 74+4390*BETA(0.72,1.55) | 120 | 4.69 | 0.336 | 0.0865 | 0.15 |
| 12 | 118+EXPO(1310) | 120 | 3.48 | 0.485 | 0.0582 | 0.15 |
| 13 | 135+EXPO(1370) | 120 | 6.54 | 0.178 | 0.0641 | 0.15 |
| 14 | 158+EXPO(1430) | 120 | 5.87 | 0.219 | 0.059 | 0.15 |
| 15 | 178+EXPO(1490) | 120 | 5.78 | 0.225 | 0.0783 | 0.15 |
| 16 | 160+4780*BETA(0.83,1.67) | 120 | 3.09 | 0.546 | 0.0831 | 0.15 |
| 17 | 238+4750*BETA(0.81,1.68) | 120 | 5.22 | 0.27 | 0.0704 | 0.15 |
| 18 | 185+GAMM(1020,1.57) | 120 | 7.27 | 0.0674 | 0.0603 | 0.15 |
| 19 | 213+GAMM(969,1.63) | 120 | 11.8 | 0.00835 | 0.0619 | 0.15 |
| 20 | 224+GAMM(964,1.62) | 120 | 14.8 | 0.005 | 0.0705 | 0.15 |
| 21 | 222+GAMM(1010,1.48) | 120 | 7.63 | 0.0559 | 0.0805 | 0.15 |
| 22 | 210+4880*BETA(0.97,2.35) | 120 | 7.59 | 0.0573 | 0.0943 | 0.15 |
| 23 | 156+4670*BETA(1.01,2.37) | 120 | 4.53 | 0.22 | 0.094 | 0.15 |

Table B.5. Arena PDF fitting summary for wind energy supply in May.

| Hour | Expression | Sample Size | Chi-Square | p-value | K-S Test | p-value |
|------|---------------------------|-------------|------------|---------|----------|---------|
| 0 | 247+ERLA(637,2) | 124 | 3.67 | 0.462 | 0.0574 | 0.15 |
| 1 | 245+GAMM(761,1.61) | 124 | 4.45 | 0.365 | 0.0444 | 0.15 |
| 2 | 242+GAMM(734,1.62) | 124 | 4.95 | 0.303 | 0.0429 | 0.15 |
| 3 | 264+WEIB(1.240,1.33) | 124 | 3.03 | 0.556 | 0.0475 | 0.15 |
| 4 | 291+WEIB(1.160,1.22) | 124 | 8.61 | 0.0758 | 0.0443 | 0.15 |
| 5 | 201+ERLA(579,2) | 124 | 3.49 | 0.483 | 0.0598 | 0.15 |
| 6 | 126+ERLA(603,2) | 124 | 4.94 | 0.305 | 0.05 | 0.15 |
| 7 | 65+ERLA(594,2) | 124 | 7.78 | 0.0999 | 0.0515 | 0.15 |
| 8 | 43+ERLA(572,2) | 124 | 2.48 | 0.653 | 0.0644 | 0.15 |
| 9 | 43+GAMM(759,1.48) | 124 | 7.09 | 0.143 | 0.0619 | 0.15 |
| 10 | 65+GAMM(832,1.38) | 124 | 6.08 | 0.206 | 0.0553 | 0.15 |
| 11 | 138+GAMM(1000,1.23) | 93 | 4.67 | 0.0978 | 0.0801 | 0.15 |
| 12 | 220+EXPO(1.270) | 93 | 6.1 | 0.11 | 0.0817 | 0.15 |
| 13 | 179+WEIB(1.490,1.33) | 124 | 9.22 | 0.0578 | 0.0681 | 0.15 |
| 14 | 237+ERLA(738,2) | 124 | 9 | 0.0644 | 0.0792 | 0.15 |
| 15 | 333+GAMM(927,1.62) | 124 | 7.06 | 0.145 | 0.0635 | 0.15 |
| 16 | 450+WEIB(1.620,1.35) | 124 | 8.41 | 0.0815 | 0.057 | 0.15 |
| 17 | 547+4250*BETA(0.907,1.65) | 124 | 8.91 | 0.119 | 0.0949 | 0.15 |
| 18 | 546+GAMM(981,1.4) | 124 | 13.1 | 0.0114 | 0.0608 | 0.15 |
| 19 | 480+ERLA(691,2) | 124 | 3.82 | 0.443 | 0.0629 | 0.15 |
| 20 | 395+ERLA(719,2) | 124 | 3.23 | 0.522 | 0.0528 | 0.15 |
| 21 | 327+ERLA(712,2) | 124 | 2.69 | 0.616 | 0.0615 | 0.15 |
| 22 | 352+ERLA(650,2) | 124 | 5.6 | 0.236 | 0.0587 | 0.15 |
| 23 | 284+GAMM(762,1.64) | 124 | 5.47 | 0.244 | 0.0497 | 0.15 |

Table B.6. Arena PDF fitting summary for wind energy supply in June.

| Hour | Expression | Sample Size | Chi-Square | p-value | K-S Test | p-value |
|------|----------------------|-------------|------------|---------|----------|---------|
| 0 | 371+ERLA(679,2) | 120 | 2.71 | 0.45 | 0.0506 | 0.15 |
| 1 | 377+WEIB(1.340,1.22) | 120 | 2.13 | 0.552 | 0.0581 | 0.15 |
| 2 | 343+WEIB(1.350,1.25) | 120 | 2.4 | 0.495 | 0.0489 | 0.15 |
| 3 | 339+WEIB(1.330,1.22) | 120 | 1.6 | 0.461 | 0.05 | 0.15 |
| 4 | 290+WEIB(1.390,1.31) | 120 | 0.245 | 0.75 | 0.0301 | 0.15 |
| 5 | 244+WEIB(1.440,1.37) | 120 | 0.726 | 0.75 | 0.0357 | 0.15 |
| 6 | 217+WEIB(1.430,1.34) | 120 | 4.08 | 0.254 | 0.0493 | 0.15 |
| 7 | 156+GAMM(774,1.62) | 120 | 1.24 | 0.545 | 0.047 | 0.15 |
| 8 | 108+GAMM(815,1.51) | 120 | 0.856 | 0.66 | 0.0527 | 0.15 |
| 9 | 84+GAMM(846,1.42) | 120 | 0.855 | 0.664 | 0.0517 | 0.15 |
| 10 | 94+GAMM(879,1.39) | 120 | 2.32 | 0.332 | 0.0518 | 0.15 |
| 11 | 117+GAMM(842,1.51) | 120 | 1.53 | 0.474 | 0.0537 | 0.15 |
| 12 | 158+GAMM(815,1.66) | 120 | 1.8 | 0.426 | 0.0455 | 0.15 |
| 13 | 272+WEIB(1.510,1.36) | 120 | 3.15 | 0.387 | 0.0571 | 0.15 |
| 14 | 423+WEIB(1.540,1.37) | 120 | 4.59 | 0.217 | 0.0516 | 0.15 |
| 15 | 564+GAMM(869,1.66) | 120 | 4.49 | 0.223 | 0.0518 | 0.15 |
| 16 | 635+WEIB(1.610,1.33) | 120 | 4 | 0.265 | 0.0612 | 0.15 |
| 17 | 631+ERLA(796,2) | 120 | 5.32 | 0.165 | 0.0715 | 0.15 |
| 18 | 652+ERLA(802,2) | 120 | 7.75 | 0.052 | 0.0525 | 0.15 |
| 19 | 648+ERLA(785,2) | 120 | 12.6 | 0.0059 | 0.059 | 0.15 |
| 20 | 657+ERLA(763,2) | 120 | 3.79 | 0.295 | 0.0523 | 0.15 |
| 21 | 573+ERLA(760,2) | 120 | 5.56 | 0.148 | 0.0621 | 0.15 |
| 22 | 490+ERLA(746,2) | 120 | 4.01 | 0.264 | 0.0629 | 0.15 |
| 23 | 434+WEIB(1.540,1.39) | 120 | 3.95 | 0.273 | 0.0433 | 0.15 |

Table B.7. Arena PDF fitting summary for wind energy supply in July.

| Hour | Expression | Sample Size | Chi-Square | p-value | K-S Test | p-value |
|------|---------------------------|-------------|------------|---------|----------|---------|
| 0 | 709+3970*BETA(1.26,1.58) | 124 | 11.3 | 0.0473 | 0.0751 | 0.15 |
| 1 | 618+4040*BETA(1.07,1.41) | 124 | 13.5 | 0.0384 | 0.0969 | 0.15 |
| 2 | 602+3990*BETA(1.22,1.63) | 124 | 12.7 | 0.0481 | 0.0705 | 0.15 |
| 3 | 580+4070*BETA(1.22,1.72) | 124 | 11.2 | 0.0847 | 0.0687 | 0.15 |
| 4 | 513+4210*BETA(1.25,1.8) | 124 | 16.1 | 0.0146 | 0.0972 | 0.15 |
| 5 | 415+420*BETA(1.29,1.7) | 124 | 14 | 0.0305 | 0.0779 | 0.15 |
| 6 | 302+4090*BETA(1.35,1.56) | 124 | 4.29 | 0.64 | 0.0476 | 0.15 |
| 7 | 298+3850*BETA(1.24,1.46) | 124 | 7.31 | 0.303 | 0.0479 | 0.15 |
| 8 | 316+380*BETA(1.03,1.34) | 124 | 11.1 | 0.0876 | 0.0439 | 0.15 |
| 9 | 301+3820*BETA(0.944,1.29) | 124 | 8.84 | 0.197 | 0.0519 | 0.15 |
| 10 | 323+3870*BETA(0.955,1.35) | 124 | 5.01 | 0.545 | 0.0525 | 0.15 |
| 11 | 365+3870*BETA(1.01,1.41) | 124 | 4.65 | 0.592 | 0.0641 | 0.15 |
| 12 | 427+3870*BETA(1.1,1.47) | 124 | 4.13 | 0.661 | 0.0731 | 0.15 |
| 13 | 503+WEIB(1.880,1.64) | 124 | 19.1 | 0.005 | 0.0821 | 0.15 |
| 14 | 601+4060*BETA(1.45,1.89) | 124 | 9.99 | 0.0796 | 0.0503 | 0.15 |
| 15 | 737+4210*BETA(1.53,2.08) | 124 | 1.81 | 0.75 | 0.0518 | 0.15 |
| 16 | 808+4330*BETA(1.67,2.18) | 124 | 4.33 | 0.503 | 0.0407 | 0.15 |
| 17 | 940+4310*BETA(1.58,2.02) | 124 | 2.27 | 0.75 | 0.0497 | 0.15 |
| 18 | 976+4330*BETA(1.54,1.9) | 124 | 5.6 | 0.363 | 0.0605 | 0.15 |
| 19 | 957+4250*BETA(1.5,1.73) | 124 | 6.51 | 0.384 | 0.0536 | 0.15 |
| 20 | 965+4110*BETA(1.44,1.58) | 124 | 8.68 | 0.205 | 0.0667 | 0.15 |
| 21 | 843+4130*BETA(1.46,1.51) | 124 | 5.7 | 0.464 | 0.0542 | 0.15 |
| 22 | 742+4090*BETA(1.44,1.45) | 124 | 6.44 | 0.391 | 0.0534 | 0.15 |
| 23 | 764+3920*BETA(1.3,1.48) | 124 | 5.94 | 0.441 | 0.056 | 0.15 |

Table B.8. Arena PDF fitting summary for wind energy supply in August.

| Hour | Expression | Sample Size | Chi-Square | p-value | K-S Test | p-value |
|------|-------------------------------|-------------|------------|---------|----------|---------|
| 0 | 970+4210*BETA(1.36,1.38) | 124 | 11.4 | 0.0805 | 0.0653 | 0.15 |
| 1 | 789+4320*BETA(1.49,1.53) | 124 | 6.5 | 0.385 | 0.0706 | 0.15 |
| 2 | 694+4330*BETA(1.57,1.57) | 124 | 5.1 | 0.533 | 0.0624 | 0.15 |
| 3 | 705+4140*BETA(1.49,1.41) | 124 | 6.27 | 0.408 | 0.0575 | 0.15 |
| 4 | 674+4120*BETA(1.55,1.41) | 124 | 8.21 | 0.23 | 0.0566 | 0.15 |
| 5 | 699+3990*BETA(1.51,1.31) | 124 | 8.25 | 0.228 | 0.0564 | 0.15 |
| 6 | 647+4020*BETA(1.61,1.35) | 124 | 7.19 | 0.217 | 0.0523 | 0.15 |
| 7 | 586+3900*BETA(1.65,1.36) | 124 | 9.94 | 0.0807 | 0.0656 | 0.15 |
| 8 | 555+3770*BETA(1.43,1.17) | 124 | 10.3 | 0.118 | 0.0742 | 0.15 |
| 9 | TRIA(491,3120,4350) | 124 | 10.7 | 0.0991 | 0.0985 | 0.15 |
| 10 | NORM(2560,1020) | 124 | 7.7 | 0.188 | 0.081 | 0.15 |
| 11 | 4740+4070* BETA(1.48,1.39) | 124 | 11.1 | 0.087 | 0.0628 | 0.15 |
| 12 | UNIF(617,4540) | 124 | 12.1 | 0.287 | 0.121 | 0.0479 |
| 13 | UNIF(756,4570) | 124 | 17 | 0.0771 | 0.106 | 0.117 |
| 14 | 891+3980*BETA(1.42,1.4) | 124 | 9.12 | 0.182 | 0.0527 | 0.15 |
| 15 | 1090+3990*BETA(1.38,1.38) | 124 | 7.63 | 0.271 | 0.0615 | 0.15 |
| 16 | 1250+3920*BETA(1.33,1.23) | 124 | 6.57 | 0.377 | 0.0673 | 0.15 |
| 17 | TRIA(1490,4220,5380) | 93 | 9.05 | 0.0628 | 0.0931 | 0.15 |
| 18 | NORM(3520,1050) | 124 | 8.95 | 0.117 | 0.069 | 0.15 |
| 19 | NORM(3540,1050) | 124 | 5.18 | 0.276 | 0.0825 | 0.15 |
| 20 | TRIA(1270,4320,5740) | 124 | 10.9 | 0.0927 | 0.114 | 0.15 |
| 21 | 1260+4320*BETA(1.59,1.48) | 124 | 10.6 | 0.102 | 0.0819 | 0.15 |
| 22 | NORM(3390,1070) | 124 | 19.3 | 0.005 | 0.0921 | 0.15 |
| 23 | TRIA(1170,3940,5220) | 93 | 3.16 | 0.534 | 0.108 | 0.15 |

Table B.9. Arena PDF fitting summary for wind energy supply in September.

| Hour | Expression | Sample Size | Chi-Square | p-value | K-S Test | p-value |
|------|--------------------------|-------------|------------|---------|----------|---------|
| 0 | 260+GAMM(1060,1.81) | 120 | 7.43 | 0.0623 | 0.0695 | 0.15 |
| 1 | 192+ERLA(946,2) | 120 | 4.25 | 0.24 | 0.0645 | 0.15 |
| 2 | 137+GAMM(1010,1.88) | 120 | 6.82 | 0.0819 | 0.0515 | 0.15 |
| 3 | 103+GAMM(1020,1.86) | 120 | 6.82 | 0.0819 | 0.0515 | 0.15 |
| 4 | 90+GAMM(1080,1.75) | 120 | 6.98 | 0.0768 | 0.0615 | 0.15 |
| 5 | 95+5530*BETA(1.05,2.03) | 120 | 3.8 | 0.445 | 0.074 | 0.15 |
| 6 | 87+5490*BETA(1.04,1.99) | 120 | 3.08 | 0.548 | 0.062 | 0.15 |
| 7 | TRIA(88,179,5460) | 120 | 2.46 | 0.75 | 0.0556 | 0.15 |
| 8 | 75+5400*BETA(0.955,2.01) | 120 | 4.02 | 0.419 | 0.0584 | 0.15 |
| 9 | 33+5330*BETA(0.896,1.95) | 120 | 5.24 | 0.267 | 0.0565 | 0.15 |
| 10 | 24+GAMM(1280,1.31) | 120 | 6.3 | 0.0983 | 0.0829 | 0.15 |
| 11 | 31+5.580*BETA(0.95,2.16) | 120 | 4.39 | 0.23 | 0.0581 | 0.15 |
| 12 | 71+WEIB(1860,1.32) | 120 | 4.12 | 0.249 | 0.0552 | 0.15 |
| 13 | 147+WEIB(1880,1.35) | 120 | 2.55 | 0.474 | 0.0525 | 0.15 |
| 14 | 236+WEIB(1950,1.4) | 120 | 1.74 | 0.637 | 0.0503 | 0.15 |
| 15 | 310+ERLA(938,2) | 120 | 4.39 | 0.23 | 0.0507 | 0.15 |
| 16 | 384+ERLA(976,2) | 120 | 3.32 | 0.363 | 0.0549 | 0.15 |
| 17 | 511+WEIB(2120,1.43) | 120 | 5.61 | 0.145 | 0.0546 | 0.15 |
| 18 | 558+ERLA(979,2) | 120 | 7.51 | 0.0599 | 0.0662 | 0.15 |
| 19 | TRIA(699,944,5990) | 120 | 7.31 | 0.211 | 0.0756 | 0.15 |
| 20 | TRIA(581,1180,5830) | 120 | 8.95 | 0.117 | 0.0729 | 0.15 |
| 21 | 481+GAMM(1230,1.59) | 120 | 8.31 | 0.0845 | 0.0812 | 0.15 |
| 22 | 389+ERLA(971,2) | 120 | 3.86 | 0.286 | 0.0803 | 0.15 |
| 23 | 307+ERLA(943,2) | 120 | 5.9 | 0.125 | 0.0759 | 0.15 |

Table B.10. Arena PDF fitting summary for wind energy supply in October.

| Hour | Expression | Sample Size | Chi-Square | p-value | K-S Test | p-value |
|------|--------------------------|-------------|------------|---------|----------|---------|
| 0 | 71+4250*BETA(0.93,1.39) | 124 | 6.38 | 0.396 | 0.0401 | 0.15 |
| 1 | 98+4090*BETA(0.86,1.3) | 124 | 2.45 | 0.75 | 0.0481 | 0.15 |
| 2 | 102+4130*BETA(0.87,1.4) | 124 | 1.21 | 0.75 | 0.0398 | 0.15 |
| 3 | 118+4160*BETA(0.86,1.45) | 124 | 2.3 | 0.75 | 0.0377 | 0.15 |
| 4 | 95+4300*BETA(0.91,1.57) | 124 | 6.09 | 0.309 | 0.0437 | 0.15 |
| 5 | TRIA(95,150,4810) | 124 | 9.05 | 0.111 | 0.0629 | 0.15 |
| 6 | 89+4250*BETA(0.93,1.55) | 124 | 9.33 | 0.0974 | 0.0605 | 0.15 |
| 7 | TRIA(67,636,4290) | 124 | 11.2 | 0.0481 | 0.0792 | 0.15 |
| 8 | TRIA(56,426,4380) | 124 | 11.5 | 0.0785 | 0.0691 | 0.15 |
| 9 | 44+4320*BETA(0.97,1.89) | 124 | 8.81 | 0.124 | 0.059 | 0.15 |
| 10 | 42+4680*BETA(0.76,1.64) | 124 | 7.19 | 0.137 | 0.0546 | 0.15 |
| 11 | 50+4950*BETA(0.91,2.28) | 124 | 6.04 | 0.209 | 0.0656 | 0.15 |
| 12 | 70+4740*BETA(0.85,2) | 93 | 4.8 | 0.202 | 0.0604 | 0.15 |
| 13 | 59+4580*BETA(0.86,1.76) | 124 | 7.45 | 0.203 | 0.0601 | 0.15 |
| 14 | 52+4360*BETA(0.84,1.46) | 124 | 3.62 | 0.609 | 0.0614 | 0.15 |
| 15 | 80+WEIB(1800,1.31) | 124 | 6.44 | 0.184 | 0.0793 | 0.15 |
| 16 | 96+4740*BETA(0.98,1.66) | 124 | 7.12 | 0.221 | 0.0617 | 0.15 |
| 17 | 131+4790*BETA(0.99,1.63) | 124 | 4.71 | 0.461 | 0.0593 | 0.15 |
| 18 | 139+4900*BETA(1.1,1.74) | 124 | 3.47 | 0.632 | 0.0464 | 0.15 |
| 19 | 114+4860*BETA(1.16,1.72) | 124 | 2.69 | 0.748 | 0.0416 | 0.15 |
| 20 | 86+4840*BETA(1.18,1.72) | 124 | 2.34 | 0.75 | 0.045 | 0.15 |
| 21 | 45+4680*BETA(1.14,1.58) | 124 | 3.85 | 0.698 | 0.0485 | 0.15 |
| 22 | 30+4480*BETA(1.08,1.47) | 124 | 7.08 | 0.327 | 0.0453 | 0.15 |
| 23 | 43+4410*BETA(1.05,1.52) | 124 | 5.14 | 0.413 | 0.0422 | 0.15 |

Table B.11. Arena PDF fitting summary for wind energy supply in November.

| Hour | Expression | Sample Size | Chi-Square | p-value | K-S Test | p-value |
|------|--------------------------|-------------|------------|---------|----------|---------|
| 0 | 155+5350*BETA(0.93,1.73) | 120 | 4.3 | 0.384 | 0.0523 | 0.15 |
| 1 | 156+5390*BETA(0.93,1.81) | 120 | 1.94 | 0.747 | 0.0448 | 0.15 |
| 2 | 156+5540*BETA(0.96,1.95) | 120 | 1.7 | 0.75 | 0.0427 | 0.15 |
| 3 | 169+5400*BETA(0.95,1.87) | 120 | 2.34 | 0.677 | 0.0559 | 0.15 |
| 4 | 156+WEIB(2000,1.38) | 120 | 2.23 | 0.53 | 0.0532 | 0.15 |
| 5 | 152+WEIB(2040,1.41) | 120 | 4.14 | 0.403 | 0.0586 | 0.15 |
| 6 | 212+WEIB(1970,1.35) | 120 | 2.29 | 0.687 | 0.0527 | 0.15 |
| 7 | 155+ERLA(935,2) | 120 | 1.74 | 0.636 | 0.0625 | 0.15 |
| 8 | 150+ERLA(948,2) | 120 | 1.66 | 0.653 | 0.0449 | 0.15 |
| 9 | 126+WEIB(2030,1.44) | 120 | 2.91 | 0.422 | 0.0461 | 0.15 |
| 10 | 94+WEIB(1970,1.37) | 120 | 2.28 | 0.518 | 0.0464 | 0.15 |
| 11 | TRIA(74,298,5340) | 120 | 3.83 | 0.577 | 0.0582 | 0.15 |
| 12 | 77+5310*BETA(0.87,1.65) | 120 | 3.76 | 0.451 | 0.0883 | 0.15 |
| 13 | 99+5330*BETA(0.83,1.59) | 120 | 3.5 | 0.482 | 0.0816 | 0.15 |
| 14 | 116+5250*BETA(0.81,1.51) | 120 | 5.4 | 0.249 | 0.0802 | 0.15 |
| 15 | 147+5270*BETA(0.79,1.52) | 120 | 4.41 | 0.37 | 0.0716 | 0.15 |
| 16 | 149+5230*BETA(0.81,1.5) | 120 | 2.04 | 0.73 | 0.0652 | 0.15 |
| 17 | 182+5170*BETA(0.83,1.5) | 120 | 1.9 | 0.75 | 0.0459 | 0.15 |
| 18 | 176+5160*BETA(0.87,1.44) | 120 | 0.33 | 0.75 | 0.0462 | 0.15 |
| 19 | 200+5140*BETA(0.9,1.45) | 120 | 1.97 | 0.75 | 0.0372 | 0.15 |
| 20 | 188+5190*BETA(0.91,1.47) | 120 | 4.5 | 0.484 | 0.0406 | 0.15 |
| 21 | 180+5340*BETA(0.93,1.59) | 120 | 1.26 | 0.75 | 0.0502 | 0.15 |
| 22 | 208+5210*BETA(0.86,1.49) | 120 | 5.96 | 0.214 | 0.0445 | 0.15 |
| 23 | 189+5180*BETA(0.86,1.52) | 120 | 7.71 | 0.104 | 0.0468 | 0.15 |

Table B.12. Arena PDF fitting summary for wind energy supply in December.

| Hour | Expression | Sample Size | Chi-Square | p-value | K-S Test | p-value |
|------|---------------------------|-------------|------------|---------|----------|---------|
| 0 | TRIA(330,1070,5770) | 124 | 6.82 | 0.239 | 0.0954 | 0.15 |
| 1 | 324+5350*BETA(1.05,1.49) | 124 | 3.37 | 0.75 | 0.0521 | 0.15 |
| 2 | 346+5310*BETA(1.04,1.48) | 124 | 6.58 | 0.376 | 0.0504 | 0.15 |
| 3 | 371+5290*BETA(1.03,1.49) | 124 | 3.88 | 0.57 | 0.056 | 0.15 |
| 4 | 422+5310*BETA(1.03,1.49) | 124 | 6.1 | 0.308 | 0.0591 | 0.15 |
| 5 | TRIA(436,1290,5830) | 124 | 7.8 | 0.182 | 0.0701 | 0.15 |
| 6 | TRIA(455,1310,5780) | 124 | 9.75 | 0.086 | 0.0818 | 0.15 |
| 7 | 447+WEIB(2250,1.45) | 124 | 6.27 | 0.195 | 0.069 | 0.15 |
| 8 | 446+WEIB(2300,1.48) | 124 | 2.86 | 0.586 | 0.078 | 0.15 |
| 9 | 432+WEIB(2250,1.41) | 124 | 5.88 | 0.219 | 0.0756 | 0.15 |
| 10 | 398+5480*BETA(0.949,1.6) | 124 | 6.78 | 0.241 | 0.05 | 0.15 |
| 11 | 359+5350*BETA(0.856,1.42) | 124 | 2.18 | 0.75 | 0.0589 | 0.15 |
| 12 | 316+5510*BETA(0.856,1.42) | 124 | 2.35 | 0.75 | 0.057 | 0.15 |
| 13 | 275+5680*BETA(0.894,1.58) | 124 | 2.8 | 0.732 | 0.0531 | 0.15 |
| 14 | 288+5690*BETA(0.897,1.62) | 124 | 5.09 | 0.419 | 0.0537 | 0.15 |
| 15 | 299+5770*BETA(0.912,1.7) | 124 | 4.11 | 0.536 | 0.0578 | 0.15 |
| 16 | 333+5750*BETA(0.906,1.7) | 124 | 2.61 | 0.75 | 0.0716 | 0.15 |
| 17 | TRIA(424,774,5990) | 124 | 8.47 | 0.144 | 0.117 | 0.0637 |
| 18 | 466+GAMM(1390,1.51) | 124 | 12.5 | 0.0061 | 0.0918 | 0.15 |
| 19 | TRIA(383,1080,6040) | 124 | 10.1 | 0.0757 | 0.0938 | 0.15 |
| 20 | TRIA(283,1070,6080) | 124 | 6.26 | 0.29 | 0.0774 | 0.15 |
| 21 | TRIA(271,1050,5990) | 124 | 5.93 | 0.327 | 0.0694 | 0.15 |
| 22 | TRIA(297,1060,5900) | 124 | 7.85 | 0.18 | 0.0692 | 0.15 |
| 23 | 291+WEIB(2410,1.5) | 124 | 4.71 | 0.334 | 0.0725 | 0.15 |

Table B.13. Arena PDF fitting summary for weekday energy demand in January.

| Hour | Expression | Sample Size | Chi-Square | p-value | K-S Test | p-value |
|------|---------------------------|-------------|------------|---------|----------|---------|
| 0 | TRIA(1980,2400,2560) | 86 | 2.72 | 0.61 | 0.102 | 0.15 |
| 1 | 1880+531*BETA(2.06,1.45) | 86 | 3.34 | 0.36 | 0.0678 | 0.15 |
| 2 | 1810+477*BETA(1.77,1.15) | 86 | 9.11 | 0.0612 | 0.0801 | 0.15 |
| 3 | 1790+445*BETA(1.68,1.12) | 86 | 9.02 | 0.0636 | 0.0754 | 0.15 |
| 4 | 1780+426*BETA(1.64,1.06) | 86 | 10.8 | 0.0305 | 0.0807 | 0.15 |
| 5 | NORM(2060,104) | 86 | 19.7 | 0.005 | 0.109 | 0.15 |
| 6 | 1900+410*BETA(1.46,1.03) | 86 | 7.84 | 0.0982 | 0.0892 | 0.15 |
| 7 | 2040+482*BETA(1.51,1.1) | 86 | 6.64 | 0.172 | 0.0588 | 0.15 |
| 8 | 2440+404*BETA(1.11,0.943) | 86 | 4.82 | 0.448 | 0.0931 | 0.15 |
| 9 | 2620+477*BETA(2.02,1.49) | 86 | 6.06 | 0.113 | 0.0605 | 0.15 |
| 10 | TRIA(2670,3050,3180) | 86 | 8.58 | 0.0765 | 0.0795 | 0.15 |
| 11 | TRIA(2330,2650,2800) | 86 | 1.54 | 0.75 | 0.0527 | 0.15 |
| 12 | TRIA(2560,2930,3170) | 86 | 3.74 | 0.452 | 0.101 | 0.15 |
| 13 | NORM(2910,134) | 86 | 5.56 | 0.149 | 0.0571 | 0.15 |
| 14 | NORM(2940,130) | 86 | 4.2 | 0.243 | 0.0548 | 0.15 |
| 15 | NORM(2920,126) | 86 | 3.04 | 0.404 | 0.052 | 0.15 |
| 16 | NORM(2940,109) | 86 | 1.35 | 0.721 | 0.0589 | 0.15 |
| 17 | NORM(2940,109) | 86 | 2.18 | 0.541 | 0.0405 | 0.15 |
| 18 | NORM(2930,117) | 86 | 1.64 | 0.657 | 0.0723 | 0.15 |
| 19 | TRIA(2540,2940,3040) | 86 | 4.6 | 0.347 | 0.0713 | 0.15 |
| 20 | 2480+462*BETA(1.68,1.1) | 86 | 3.82 | 0.443 | 0.0686 | 0.15 |
| 21 | 2420+455*BETA(1.75,1.21) | 86 | 5.06 | 0.291 | 0.0832 | 0.15 |
| 22 | NORM(2650,91.4) | 86 | 5.29 | 0.167 | 0.0638 | 0.15 |
| 23 | NORM(2550,98) | 86 | 4.32 | 0.235 | 0.0858 | 0.15 |

Table B.14. Arena PDF fitting summary for weekday energy demand in February.

| Hour | Expression | Sample Size | Chi-Square | p-value | K-S Test | p-value |
|------|---------------------------|-------------|------------|---------|----------|---------|
| 0 | TRIA(1900,2470,2510) | 81 | 15.8 | 0.005 | 0.124 | 0.15 |
| 1 | TRIA(1800,2330,2360) | 81 | 4.99 | 0.188 | 0.143 | 0.0686 |
| 2 | 1720+546*BETA(1.76,0.893) | 81 | 7.78 | 0.0512 | 0.107 | 0.15 |
| 3 | 1690+520*BETA(1.76,0.881) | 81 | 6.01 | 0.117 | 0.101 | 0.15 |
| 4 | 1690+476*BETA(1.43,0.628) | 81 | 4.16 | 0.246 | 0.0726 | 0.15 |
| 5 | 1730+462*BETA(1.47,0.644) | 81 | 2.62 | 0.463 | 0.0603 | 0.15 |
| 6 | 1770+558*BETA(1.75,0.859) | 81 | 3.77 | 0.298 | 0.115 | 0.15 |
| 7 | 1920+544*BETA(1.27,0.666) | 81 | 9.49 | 0.0239 | 0.129 | 0.125 |
| 8 | NORM(2700,55.3) | 60 | 1.58 | 0.222 | 0.0669 | 0.15 |
| 9 | TRIA(2440,2960,3040) | 81 | 7.87 | 0.0972 | 0.0914 | 0.15 |
| 10 | TRIA(2460,2940,3120) | 81 | 3.24 | 0.52 | 0.066 | 0.15 |
| 11 | TRIA(2480,2920,3160) | 81 | 1.11 | 0.75 | 0.0592 | 0.15 |
| 12 | TRIA(2330,2840,3030) | 81 | 1.35 | 0.75 | 0.07 | 0.15 |
| 13 | NORM(2730,170) | 81 | 3.52 | 0.334 | 0.06 | 0.15 |
| 14 | NORM(2760,167) | 81 | 3.14 | 0.388 | 0.0714 | 0.15 |
| 15 | 2370+671*BETA(1.62,1.28) | 81 | 5.43 | 0.381 | 0.0753 | 0.15 |
| 16 | 2380+651*BETA(1.78,1.27) | 81 | 3.83 | 0.442 | 0.0557 | 0.15 |
| 17 | 2440+568*BETA(1.87,1.2) | 81 | 11.9 | 0.0197 | 0.0852 | 0.15 |
| 18 | TRIA(2470,2920,2990) | 81 | 10.7 | 0.0152 | 0.107 | 0.15 |
| 19 | TRIA(2700,2910,2990) | 60 | 10.5 | 0.0162 | 0.116 | 0.15 |
| 20 | TRIA(2620,2840,2930) | 60 | 5.08 | 0.182 | 0.101 | 0.15 |
| 21 | TRIA(2570,2760,2860) | 60 | 9.29 | 0.0259 | 0.105 | 0.15 |
| 22 | TRIA(2530,2730,2760) | 60 | 0.442 | 0.75 | 0.0763 | 0.15 |
| 23 | 2420+227*BETA(1.82,0.891) | 60 | 3.71 | 0.173 | 0.0766 | 0.15 |

Table B.15. Arena PDF fitting summary for weekday energy demand in March.

| Hour | Expression | Sample Size | Chi-Square | p-value | K-S Test | p-value |
|------|----------------------|-------------|------------|---------|----------|---------|
| 0 | TRIA(1890,2310,2480) | 89 | 1.38 | 0.75 | 0.0715 | 0.15 |
| 1 | TRIA(1770,2200,2330) | 89 | 1.49 | 0.75 | 0.0807 | 0.15 |
| 2 | TRIA(1690,2150,2240) | 89 | 3.15 | 0.536 | 0.0588 | 0.15 |
| 3 | TRIA(1690,2100,2180) | 89 | 2.51 | 0.647 | 0.0697 | 0.15 |
| 4 | TRIA(1690,2070,2170) | 89 | 1.01 | 0.75 | 0.0514 | 0.15 |
| 5 | TRIA(1720,2100,2200) | 89 | 1.18 | 0.75 | 0.0691 | 0.15 |
| 6 | TRIA(1750,2160,2310) | 89 | 5.83 | 0.222 | 0.111 | 0.15 |
| 7 | TRIA(1920,2250,2460) | 89 | 10.5 | 0.035 | 0.111 | 0.15 |
| 8 | TRIA(2280,2520,2770) | 89 | 3.62 | 0.32 | 0.105 | 0.15 |
| 9 | NORM(2660,122) | 89 | 2.22 | 0.532 | 0.0496 | 0.15 |
| 10 | NORM(2680,125) | 89 | 4.1 | 0.251 | 0.0534 | 0.15 |
| 11 | NORM(2700,133) | 89 | 3.58 | 0.326 | 0.0555 | 0.15 |
| 12 | NORM(2560,147) | 89 | 10.7 | 0.0146 | 0.0745 | 0.15 |
| 13 | 2270+WEIB(330,2.18) | 89 | 1.9 | 0.601 | 0.0856 | 0.15 |
| 14 | NORM(2610,136) | 89 | 2.99 | 0.41 | 0.0533 | 0.15 |
| 15 | 2320+WEIB(302,2) | 89 | 3.72 | 0.306 | 0.0809 | 0.15 |
| 16 | 2340+WEIB(287,1.97) | 89 | 6.51 | 0.0918 | 0.0891 | 0.15 |
| 17 | 2370+WEIB(259,1.91) | 89 | 6.48 | 0.0925 | 0.077 | 0.15 |
| 18 | NORM(2610,110) | 89 | 0.984 | 0.624 | 0.067 | 0.15 |
| 19 | TRIA(2370,2730,2950) | 89 | 4.83 | 0.318 | 0.066 | 0.15 |
| 20 | TRIA(2320,2740,2890) | 89 | 3.36 | 0.499 | 0.0752 | 0.15 |
| 21 | TRIA(2250,2670,2810) | 89 | 6.46 | 0.183 | 0.0848 | 0.15 |
| 22 | TRIA(2260,2570,2760) | 89 | 2.46 | 0.656 | 0.0694 | 0.15 |
| 23 | TRIA(2130,2460,2670) | 89 | 2.21 | 0.699 | 0.0822 | 0.15 |

Table B.16. Arena PDF fitting summary for weekday energy demand in April.

| Hour | Expression | Sample Size | Chi-Square | p-value | K-S Test | p-value |
|------|--------------------------|-------------|------------|---------|----------|---------|
| 0 | 1880+514*BETA(1.63,0.97) | 82 | 11.3 | 0.01 | 0.0997 | 0.15 |
| 1 | 1800+483*BETA(1.84,1.22) | 82 | 7.77 | 0.101 | 0.0899 | 0.15 |
| 2 | 1720+475*BETA(1.92,1.24) | 82 | 11.3 | 0.0237 | 0.0876 | 0.15 |
| 3 | NORM(1970,109) | 82 | 15.2 | 0.005 | 0.085 | 0.15 |
| 4 | 1700+443*BETA(1.85,1.23) | 82 | 7.49 | 0.118 | 0.0826 | 0.15 |
| 5 | 1710+456*BETA(1.9,1.27) | 82 | 6.6 | 0.174 | 0.083 | 0.15 |
| 6 | NORM(1980,110) | 82 | 6.89 | 0.0794 | 0.0713 | 0.15 |
| 7 | 1830+446*BETA(2.62,1.6) | 82 | 3.67 | 0.461 | 0.0493 | 0.15 |
| 8 | TRIA(2220,2500,2570) | 82 | 1.88 | 0.75 | 0.0647 | 0.15 |
| 9 | TRIA(2420,2610,2720) | 82 | 10.7 | 0.0318 | 0.0997 | 0.15 |
| 10 | NORM(2610,66.8) | 82 | 7.68 | 0.0544 | 0.0769 | 0.15 |
| 11 | 2440+WEIB(214,2.81) | 82 | 20.2 | 0.005 | 0.102 | 0.15 |
| 12 | 2320+362*BETA(2.71,2.6) | 82 | 4.57 | 0.218 | 0.0532 | 0.15 |
| 13 | TRIA(2290,2540,2700) | 82 | 2.61 | 0.631 | 0.0594 | 0.15 |
| 14 | NORM(2570,76) | 82 | 3.05 | 0.402 | 0.0488 | 0.15 |
| 15 | NORM(2560,72.6) | 82 | 2.58 | 0.47 | 0.0847 | 0.15 |
| 16 | NORM(2560,81.2) | 82 | 6.15 | 0.202 | 0.0639 | 0.15 |
| 17 | 2340+377*BETA(1.31,1.14) | 82 | 2.33 | 0.75 | 0.0477 | 0.15 |
| 18 | UNIF(2300,2690) | 82 | 10.6 | 0.23 | 0.105 | 0.15 |
| 19 | 2350+470*BETA(1.19,1.21) | 82 | 8.76 | 0.0712 | 0.0813 | 0.15 |
| 20 | 2440+383*BETA(0.85,0.69) | 82 | 1.37 | 0.717 | 0.0477 | 0.15 |
| 21 | 2390+352*BETA(0.72,0.66) | 82 | 1.65 | 0.655 | 0.0809 | 0.15 |
| 22 | UNIF(2370,2.670) | 82 | 10.4 | 0.243 | 0.107 | 0.15 |
| 23 | 2210+361*BETA(1.42,1.18) | 82 | 12.4 | 0.0311 | 0.0844 | 0.15 |

Table B.17. Arena PDF fitting summary for weekday energy demand in May.

| Hour | Expression | Sample Size | Chi-Square | p-value | K-S Test | p-value |
|------|--------------------------|-------------|------------|---------|----------|---------|
| 0 | NORM(2240,160) | 86 | 0.961 | 0.75 | 0.0488 | 0.15 |
| 1 | NORM(2130,165) | 86 | 1.73 | 0.638 | 0.092 | 0.15 |
| 2 | NORM(2070,170) | 86 | 15 | 0.005 | 0.108 | 0.15 |
| 3 | NORM(2020,158) | 86 | 8.95 | 0.0658 | 0.1 | 0.15 |
| 4 | 1660+WEIB(362,2.3) | 86 | 6.32 | 0.191 | 0.101 | 0.15 |
| 5 | TRIA(1630,2000,2160) | 86 | 8.55 | 0.0774 | 0.0565 | 0.15 |
| 6 | TRIA(1660,1950,2130) | 86 | 1.46 | 0.75 | 0.0684 | 0.15 |
| 7 | NORM(2050,83.5) | 86 | 1.96 | 0.587 | 0.048 | 0.15 |
| 8 | NORM(2370,77.7) | 86 | 5.91 | 0.124 | 0.056 | 0.15 |
| 9 | NORM(2530,84.7) | 86 | 3.21 | 0.379 | 0.0708 | 0.15 |
| 10 | NORM(2580,86.1) | 86 | 1.56 | 0.469 | 0.0515 | 0.15 |
| 11 | NORM(2620,84.8) | 86 | 4.17 | 0.246 | 0.0595 | 0.15 |
| 12 | NORM(2500,84.5) | 86 | 1.52 | 0.684 | 0.0544 | 0.15 |
| 13 | NORM(2540,98.1) | 86 | 0.717 | 0.682 | 0.0606 | 0.15 |
| 14 | NORM(2620,93.1) | 86 | 5.83 | 0.13 | 0.0656 | 0.15 |
| 15 | NORM(2620,96.2) | 86 | 1.59 | 0.464 | 0.0534 | 0.15 |
| 16 | NORM(2620,99.9) | 86 | 3.14 | 0.22 | 0.065 | 0.15 |
| 17 | 2410+486*BETA(1.27,2.18) | 86 | 3.77 | 0.448 | 0.0689 | 0.15 |
| 18 | 2310+537*BETA(1.38,1.89) | 86 | 5.44 | 0.246 | 0.0597 | 0.15 |
| 19 | NORM(2550,133) | 86 | 4.48 | 0.224 | 0.0581 | 0.15 |
| 20 | TRIA(2370,2570,2820) | 86 | 6.92 | 0.154 | 0.0855 | 0.15 |
| 21 | NORM(2580,111) | 86 | 3.77 | 0.299 | 0.0695 | 0.15 |
| 22 | NORM(2540,104) | 86 | 2.67 | 0.456 | 0.0599 | 0.15 |
| 23 | NORM(2420,121) | 86 | 1.8 | 0.624 | 0.0632 | 0.15 |

Table B.18. Arena PDF fitting summary for weekday energy demand in June.

| Hour | Expression | Sample Size | Chi-Square | p-value | K-S Test | p-value |
|------|-------------------------|-------------|------------|---------|----------|---------|
| 0 | TRIA(1920,2470,2750) | 79 | 2.8 | 0.438 | 0.0767 | 0.15 |
| 1 | NORM(2280,172) | 79 | 2.49 | 0.301 | 0.081 | 0.15 |
| 2 | NORM(2200,159) | 79 | 1.98 | 0.394 | 0.0886 | 0.15 |
| 3 | NORM(2130,155) | 79 | 4.07 | 0.144 | 0.0831 | 0.15 |
| 4 | TRIA(1670,2150,2380) | 79 | 0.488 | 0.75 | 0.0603 | 0.15 |
| 5 | TRIA(1590,2020,2300) | 79 | 3.63 | 0.466 | 0.0523 | 0.15 |
| 6 | NORM(1960,153) | 79 | 1.31 | 0.522 | 0.0495 | 0.15 |
| 7 | NORM(2080,161) | 79 | 0.593 | 0.744 | 0.0582 | 0.15 |
| 8 | TRIA(2200,2270,2820) | 79 | 2.02 | 0.732 | 0.0906 | 0.15 |
| 9 | TRIA(2380,2490,3030) | 79 | 3.09 | 0.397 | 0.0823 | 0.15 |
| 10 | NORM(2690,216) | 79 | 3.58 | 0.0616 | 0.107 | 0.15 |
| 11 | NORM(2750,220) | 79 | 10.8 | 0.005 | 0.107 | 0.15 |
| 12 | 2430+WEIB(289,1.4) | 79 | 6.62 | 0.0883 | 0.0735 | 0.15 |
| 13 | NORM(2720,225) | 79 | 5.09 | 0.0243 | 0.0772 | 0.15 |
| 14 | NORM(2810,233) | 79 | 8.17 | 0.005 | 0.1 | 0.15 |
| 15 | NORM(280,235) | 79 | 5.98 | 0.0161 | 0.0928 | 0.15 |
| 16 | NORM(2790,234) | 79 | 0.965 | 0.353 | 0.0714 | 0.15 |
| 17 | NORM(2730,223) | 79 | 8.63 | 0.0147 | 0.0827 | 0.15 |
| 18 | NORM(2660,200) | 79 | 2.07 | 0.377 | 0.0806 | 0.15 |
| 19 | NORM(2630,182) | 79 | 1.18 | 0.75 | 0.0722 | 0.15 |
| 20 | 2230+WEIB(442,1.82) | 79 | 5.14 | 0.0807 | 0.0977 | 0.15 |
| 21 | 2270+863*BETA(1.75,2.1) | 79 | 7.57 | 0.0579 | 0.103 | 0.15 |
| 22 | NORM(2650,174) | 79 | 2.59 | 0.283 | 0.0647 | 0.15 |
| 23 | NORM(2550,170) | 79 | 2.47 | 0.304 | 0.0541 | 0.15 |

Table B.19. Arena PDF fitting summary for weekday energy demand in July.

| Hour | Expression | Sample Size | Chi-Square | p-value | K-S Test | p-value |
|------|----------------------------|-------------|------------|---------|----------|---------|
| 0 | 1960+916*BETA(2.88,0.885) | 83 | 3.26 | 0.21 | 0.0645 | 0.15 |
| 1 | 1870+879*BETA(2.91,0.9) | 83 | 6.06 | 0.0488 | 0.0698 | 0.15 |
| 2 | 1770+871*BETA(3.17,0.977) | 83 | 4.55 | 0.105 | 0.0667 | 0.15 |
| 3 | 1710+873*BETA(3.21,0.97) | 83 | 3.27 | 0.209 | 0.0618 | 0.15 |
| 4 | 1680+852*BETA(2.88,0.867) | 83 | 3.06 | 0.227 | 0.073 | 0.15 |
| 5 | 2000+473*BETA(1.4,0.973) | 80 | 4.97 | 0.301 | 0.069 | 0.15 |
| 6 | 1580+834*BETA(2.71,0.805) | 83 | 3.49 | 0.191 | 0.0793 | 0.15 |
| 7 | 1700+857*BETA(2.57,0.648) | 83 | 2.69 | 0.102 | 0.0883 | 0.15 |
| 8 | 2410+541*BETA(2.49,1.02) | 81 | 3.06 | 0.227 | 0.0913 | 0.15 |
| 9 | 2670+554*BETA(2.72,1.54) | 81 | 6.34 | 0.0972 | 0.0988 | 0.15 |
| 10 | TRIA(2750,3230,3.320) | 80 | 7.15 | 0.0713 | 0.118 | 0.15 |
| 11 | TRIA(2820,3250,3.420) | 81 | 6.84 | 0.159 | 0.0761 | 0.15 |
| 12 | TRIA(2730,3140,3.350) | 80 | 6.88 | 0.0798 | 0.0721 | 0.15 |
| 13 | 2170+1300*BETA(5.78,2.19) | 83 | 9.1 | 0.0109 | 0.121 | 0.15 |
| 14 | 2170+1360*BETA(5.92,1.84) | 83 | 12.3 | 0.005 | 0.122 | 0.15 |
| 15 | TRIA(2890,3280,3510) | 80 | 1.94 | 0.747 | 0.0525 | 0.15 |
| 16 | TRIA(2870,3310,3480) | 80 | 1.65 | 0.655 | 0.0516 | 0.15 |
| 17 | 2110+1240*BETA(4.2,0.987) | 82 | 6.94 | 0.00879 | 0.12 | 0.15 |
| 18 | 2110+1120*BETA(3.81,1.01) | 82 | 4.48 | 0.11 | 0.0916 | 0.15 |
| 19 | 2140+1060*BETA(3.62,1.08) | 82 | 4.01 | 0.149 | 0.11 | 0.15 |
| 20 | 2150+1130*BETA(3.59,1.01) | 82 | 4.59 | 0.101 | 0.0852 | 0.15 |
| 21 | 2200+1060*BETA(3.36,0.898) | 82 | 1.43 | 0.492 | 0.0925 | 0.15 |
| 22 | 2190+997*BETA(3.6,0.916) | 82 | 2.86 | 0.243 | 0.09 | 0.15 |
| 23 | 2120+941*BETA(3.52,0.929) | 82 | 1.25 | 0.543 | 0.0754 | 0.15 |

Table B.20. Arena PDF fitting summary for weekday energy demand in August.

| Hour | Expression | Sample Size | Chi-Square | p-value | K-S Test | p-value |
|------|--------------------------|-------------|------------|---------|----------|---------|
| 0 | 2250+663*BETA(1.97,1.29) | 78 | 10.1 | 0.019 | 0.0693 | 0.15 |
| 1 | TRIA(2150,2670,2780) | 79 | 3.13 | 0.391 | 0.128 | 0.141 |
| 2 | 2070+603*BETA(1.9,1.24) | 79 | 11.4 | 0.0231 | 0.105 | 0.15 |
| 3 | 2010+599*BETA(2.03,1.3) | 79 | 7.31 | 0.0661 | 0.0691 | 0.15 |
| 4 | TRIA(1980,2460,2570) | 79 | 3.11 | 0.393 | 0.0708 | 0.15 |
| 5 | TRIA(1970,2430,2510) | 79 | 1.92 | 0.597 | 0.0834 | 0.15 |
| 6 | TRIA(1930,2360,2460) | 79 | 2.78 | 0.6 | 0.0624 | 0.15 |
| 7 | 2080+518*BETA(1.84,1.26) | 78 | 6.22 | 0.198 | 0.0687 | 0.15 |
| 8 | NORM(2770,121) | 78 | 1.76 | 0.433 | 0.065 | 0.15 |
| 9 | 2710+516*BETA(1.82,1.37) | 78 | 3.19 | 0.53 | 0.0717 | 0.15 |
| 10 | 2800+WEIB(332,2.38) | 78 | 17.2 | 0.005 | 0.079 | 0.15 |
| 11 | 2850+564*BETA(2.02,1.67) | 78 | 11 | 0.0127 | 0.0766 | 0.15 |
| 12 | TRIA(2850,2980,3420) | 77 | 11.3 | 0.0242 | 0.113 | 0.15 |
| 13 | TRIA(2850,3100,3420) | 78 | 2.82 | 0.246 | 0.0883 | 0.15 |
| 14 | NORM(3230,134) | 78 | 2.17 | 0.359 | 0.0596 | 0.15 |
| 15 | 2880+WEIB(388,2.59) | 78 | 5.8 | 0.0569 | 0.089 | 0.15 |
| 16 | 2900+550*BETA(1.57,1.21) | 78 | 6.17 | 0.0469 | 0.09 | 0.15 |
| 17 | 2800+571*BETA(1.6,1.17) | 78 | 3.68 | 0.46 | 0.0988 | 0.15 |
| 18 | 2640+628*BETA(1.86,1.33) | 78 | 8.14 | 0.0896 | 0.0701 | 0.15 |
| 19 | 2650+590*BETA(1.43,1.09) | 78 | 8.75 | 0.0716 | 0.0608 | 0.15 |
| 20 | 2690+611*BETA(1.69,1.12) | 78 | 1.18 | 0.75 | 0.0552 | 0.15 |
| 21 | 2630+647*BETA(1.8,1.3) | 78 | 2.19 | 0.703 | 0.0549 | 0.15 |
| 22 | 2620+577*BETA(1.82,1.32) | 78 | 5.69 | 0.231 | 0.0583 | 0.15 |
| 23 | 2500+563*BETA(1.82,1.29) | 78 | 3.21 | 0.526 | 0.0558 | 0.15 |

Table B.21. Arena PDF fitting summary for weekday energy demand in September.

| Hour | Expression | Sample Size | Chi-Square | p-value | K-S Test | p-value |
|------|-------------------------|-------------|------------|---------|----------|---------|
| 0 | TRIA(1870,2450,2730) | 77 | 1.08 | 0.75 | 0.0769 | 0.15 |
| 1 | TRIA(1780,2360,2600) | 77 | 1.9 | 0.601 | 0.0707 | 0.15 |
| 2 | TRIA(1740,2280,2510) | 77 | 1.13 | 0.75 | 0.0759 | 0.15 |
| 3 | NORM(2120,162) | 77 | 3.25 | 0.211 | 0.0973 | 0.15 |
| 4 | TRIA(1700,2220,2410) | 77 | 2.12 | 0.554 | 0.0795 | 0.15 |
| 5 | TRIA(1720,2180,2400) | 77 | 5.6 | 0.146 | 0.0967 | 0.15 |
| 6 | TRIA(1750,2200,2320) | 77 | 2.01 | 0.578 | 0.134 | 0.117 |
| 7 | TRIA(1880,2300,2420) | 77 | 6.44 | 0.094 | 0.0941 | 0.15 |
| 8 | NORM(2540,135) | 77 | 4.65 | 0.0984 | 0.0839 | 0.15 |
| 9 | NORM(2720,149) | 77 | 5.79 | 0.132 | 0.0756 | 0.15 |
| 10 | UNIF(2480,3070) | 77 | 7.05 | 0.434 | 0.069 | 0.15 |
| 11 | UNIF(2520,3120) | 77 | 4.77 | 0.689 | 0.0524 | 0.15 |
| 12 | UNIF(2400,3060) | 77 | 5.39 | 0.614 | 0.0588 | 0.15 |
| 13 | UNIF(2400,3150) | 77 | 3.94 | 0.75 | 0.065 | 0.15 |
| 14 | UNIF(2510,3230) | 77 | 8.09 | 0.338 | 0.0799 | 0.15 |
| 15 | NORM(2870,208) | 77 | 8.32 | 0.0418 | 0.0638 | 0.15 |
| 16 | NORM(2870,200) | 77 | 6.19 | 0.104 | 0.0928 | 0.15 |
| 17 | TRIA(2400,2860,3220) | 77 | 11.5 | 0.0228 | 0.1 | 0.15 |
| 18 | 2680+457*BETA(1.1,1.82) | 60 | 0.253 | 0.75 | 0.078 | 0.15 |
| 19 | NORM(2830,172) | 77 | 6.31 | 0.0443 | 0.11 | 0.15 |
| 20 | NORM(2870,131) | 77 | 3.26 | 0.21 | 0.091 | 0.15 |
| 21 | TRIA(2330,2720,3090) | 77 | 8.89 | 0.0676 | 0.109 | 0.15 |
| 22 | TRIA(2300,2690,3000) | 77 | 3.23 | 0.522 | 0.0997 | 0.15 |
| 23 | TRIA(2180,2570,2880) | 77 | 5 | 0.297 | 0.0969 | 0.15 |

Table B.22. Arena PDF fitting summary for weekday energy demand in October.

| Hour | Expression | Sample Size | Chi-Square | p-value | K-S Test | p-value |
|------|---------------------------|-------------|------------|---------|----------|---------|
| 0 | TRIA(1860,2180,2290) | 87 | 0.811 | 0.677 | 0.201 | 0.01 |
| 1 | TRIA(1760,2150,2190) | 87 | 3.61 | 0.181 | 0.159 | 0.023 |
| 2 | 1720+388*BETA(1.5,0.812) | 87 | 1.29 | 0.53 | 0.144 | 0.0495 |
| 3 | 1670+395*BETA(1.76,0.939) | 87 | 5.1 | 0.0823 | 0.15 | 0.0378 |
| 4 | TRIA(1670,2040,2050) | 87 | 3.67 | 0.312 | 0.153 | 0.0313 |
| 5 | TRIA(1690,2060,2080) | 87 | | | | |
| 6 | TRIA(1730,2090,2120) | 87 | | | | |
| 7 | TRIA(1880,2160,2250) | 87 | 1.84 | 0.614 | 0.117 | 0.15 |
| 8 | NORM(2420,45.7) | 87 | 6.43 | 0.185 | 0.128 | 0.108 |
| 9 | TRIA(2430,2500,2710) | 86 | 2.69 | 0.454 | 0.0997 | 0.15 |
| 10 | TRIA(2430,2480,2740) | 86 | 1.85 | 0.75 | 0.0588 | 0.15 |
| 11 | 2440+302*BETA(1.35,1.6) | 86 | 4.76 | 0.204 | 0.0747 | 0.15 |
| 12 | 2300+WEIB(152,1.82) | 86 | 3.79 | 0.295 | 0.0703 | 0.15 |
| 13 | NORM(2.490,81) | 86 | 1.3 | 0.731 | 0.0682 | 0.15 |
| 14 | 2410+WEIB(183,2.72) | 86 | 5.95 | 0.121 | 0.0716 | 0.15 |
| 15 | NORM(2590,52.7) | 86 | 3.92 | 0.277 | 0.0468 | 0.15 |
| 16 | NORM(2630,43) | 65 | 5.21 | 0.0783 | 0.106 | 0.15 |
| 17 | TRIA(2580,2610,2780) | 65 | 3.2 | 0.38 | 0.0713 | 0.15 |
| 18 | 2620+194*BETA(1.51,2.12) | 65 | 4.3 | 0.237 | 0.0755 | 0.15 |
| 19 | 2630+WEIB(61.3,1.37) | 65 | 2.64 | 0.274 | 0.0597 | 0.15 |
| 20 | 2550+WEIB(74.8,1.83) | 65 | 5.88 | 0.054 | 0.0677 | 0.15 |
| 21 | NORM(2540,35.3) | 65 | 1.59 | 0.221 | 0.0924 | 0.15 |
| 22 | 2430+WEIB(57.8,1.69) | 65 | 4.37 | 0.231 | 0.0925 | 0.15 |
| 23 | NORM(2360,30.8) | 65 | 3.68 | 0.311 | 0.0776 | 0.15 |

Table B.23. Arena PDF fitting summary for weekday energy demand in November.

| Hour | Expression | Sample Size | Chi-Square | p-value | K-S Test | p-value |
|------|--------------------------|-------------|------------|---------|----------|---------|
| 0 | TRIA(1940,2350,2450) | 87 | 2.75 | 0.605 | 0.092 | 0.15 |
| 1 | TRIA(1850,2240,2310) | 87 | 2.73 | 0.61 | 0.0848 | 0.15 |
| 2 | 1770+459*BETA(2.22,1.27) | 87 | 10.1 | 0.0192 | 0.0873 | 0.15 |
| 3 | TRIA(1770,2080,2230) | 87 | 7.11 | 0.0725 | 0.0948 | 0.15 |
| 4 | TRIA(1740,2090,2170) | 87 | 5.82 | 0.13 | 0.144 | 0.0502 |
| 5 | TRIA(1770,2090,2190) | 87 | 8.61 | 0.0149 | 0.0918 | 0.15 |
| 6 | TRIA(1870,2190,2300) | 87 | 12.3 | 0.0166 | 0.0946 | 0.15 |
| 7 | TRIA(2030,2300,2460) | 87 | 4.32 | 0.382 | 0.0538 | 0.15 |
| 8 | NORM(2550,95.8) | 87 | 3.27 | 0.37 | 0.0531 | 0.15 |
| 9 | 2460+508*BETA(1.66,1.84) | 87 | 10.8 | 0.0301 | 0.106 | 0.15 |
| 10 | NORM(2720,136) | 87 | 5.04 | 0.185 | 0.0561 | 0.15 |
| 11 | NORM(2730,144) | 87 | 6.92 | 0.154 | 0.0552 | 0.15 |
| 12 | NORM(2580,150) | 87 | 4.74 | 0.329 | 0.0502 | 0.15 |
| 13 | 2310+WEIB(335,1.93) | 87 | 2.55 | 0.474 | 0.0769 | 0.15 |
| 14 | 2420+WEIB(294,1.87) | 87 | 5.62 | 0.144 | 0.0871 | 0.15 |
| 15 | 2440+ERLA(83.5,3) | 87 | 13.8 | 0.005 | 0.0752 | 0.15 |
| 16 | 2520+WEIB(249,1.73) | 87 | 20.7 | 0.005 | 0.0859 | 0.15 |
| 17 | 2570+490*BETA(1.57,1.39) | 87 | 13.4 | 0.00959 | 0.116 | 0.15 |
| 18 | NORM(2840,96.7) | 87 | 18.4 | 0.005 | 0.0992 | 0.15 |
| 19 | NORM(2760,89.8) | 87 | 8.69 | 0.0358 | 0.101 | 0.15 |
| 20 | NORM(2700,89.3) | 87 | 8.41 | 0.0403 | 0.0957 | 0.15 |
| 21 | NORM(2630,89.1) | 87 | 3.83 | 0.291 | 0.0766 | 0.15 |
| 22 | NORM(2570,85.7) | 87 | 1.17 | 0.75 | 0.0627 | 0.15 |
| 23 | NORM(2460,83) | 87 | 1.48 | 0.483 | 0.0513 | 0.15 |

Table B.24. Arena PDF fitting summary for weekday energy demand in December.

| Hour | Expression | Sample Size | Chi-Square | p-value | K-S Test | p-value |
|------|---------------------------|-------------|------------|---------|----------|---------|
| 0 | 2100+395*BETA(1.74,0.928) | 82 | 5.59 | 0.0646 | 0.112 | 0.15 |
| 1 | TRIA(1970,2330,2370) | 82 | 1.09 | 0.593 | 0.111 | 0.15 |
| 2 | TRIA(1900,2230,2280) | 82 | 3.32 | 0.364 | 0.0905 | 0.15 |
| 3 | TRIA(1850,2190,2230) | 82 | 5.93 | 0.122 | 0.0764 | 0.15 |
| 4 | 1850+345*BETA(1.44,0.854) | 82 | 5.15 | 0.177 | 0.118 | 0.15 |
| 5 | TRIA(1.880,2200,2230) | 82 | 2.92 | 0.577 | 0.0789 | 0.15 |
| 6 | TRIA(1.960,2270,2340) | 82 | 2.03 | 0.574 | 0.0646 | 0.15 |
| 7 | TRIA(2.140,2470,2530) | 82 | 4 | 0.421 | 0.0803 | 0.15 |
| 8 | 2410+436*BETA(3.62,1.61) | 82 | 1.42 | 0.706 | 0.084 | 0.15 |
| 9 | NORM(2910,76.2) | 82 | 3.58 | 0.326 | 0.0819 | 0.15 |
| 10 | NORM(2950,87.4) | 82 | 2.76 | 0.443 | 0.0782 | 0.15 |
| 11 | NORM(2970,99.5) | 82 | 3.61 | 0.321 | 0.0811 | 0.15 |
| 12 | NORM(2840,113) | 82 | 2.18 | 0.541 | 0.0701 | 0.15 |
| 13 | TRIA(2540,2940,3090) | 82 | 2.86 | 0.587 | 0.0648 | 0.15 |
| 14 | TRIA(2570,3010,3110) | 82 | 2.28 | 0.689 | 0.0946 | 0.15 |
| 15 | 2560+530*BETA(2.72,1.59) | 82 | 2.13 | 0.715 | 0.0594 | 0.15 |
| 16 | 2590+511*BETA(2.99,1.34) | 82 | 5.72 | 0.0599 | 0.0689 | 0.15 |
| 17 | 2590+511*BETA(2.99,1.34) | 82 | 4.64 | 0.469 | 0.0502 | 0.15 |
| 18 | NORM(3000,55.4) | 82 | 4.55 | 0.219 | 0.0846 | 0.15 |
| 19 | NORM(2900,55.5) | 82 | 6.66 | 0.0869 | 0.0906 | 0.15 |
| 20 | 2660+274*BETA(2.77,1.7) | 82 | 6.8 | 0.0823 | 0.0913 | 0.15 |
| 21 | TRIA(2610,2810,2870) | 82 | 3.47 | 0.486 | 0.064 | 0.15 |
| 22 | NORM(2700,49.8) | 82 | 11.9 | 0.005 | 0.0737 | 0.15 |
| 23 | TRIA(2480,2610,2690) | 82 | 4.32 | 0.381 | 0.0946 | 0.15 |

Table B.25. Arena PDF fitting summary for weekend energy demand in January.

| Hour | Expression | Sample Size | Chi-Square | p-value | K-S Test | p-value |
|------|--------------------------|-------------|------------|---------|----------|---------|
| 0 | TRIA(1970,2400,2540) | 35 | 0.808 | 0.678 | 0.0808 | 0.15 |
| 1 | UNIF(1850,2390) | 35 | 7.14 | 0.14 | 0.249 | 0.0222 |
| 2 | TRIA(1760,2110,2270) | 38 | 2.89 | 0.24 | 0.117 | 0.15 |
| 3 | 1680+523*BETA(1.28,1.03) | 38 | 1.92 | 0.404 | 0.12 | 0.15 |
| 4 | NORM(1950,143) | 38 | 2.19 | 0.156 | 0.124 | 0.15 |
| 5 | 1650+546*BETA(1.31,1.04) | 38 | 1.6 | 0.461 | 0.126 | 0.15 |
| 6 | UNIF(1670,2230) | 38 | 4.95 | 0.434 | 0.186 | 0.131 |
| 7 | NORM(2000,195) | 38 | 1.77 | 0.202 | 0.117 | 0.15 |
| 8 | UNIF(1690,2550) | 38 | 11.9 | 0.0383 | 0.135 | 0.15 |
| 9 | 1790+992*BETA(0.71,0.71) | 38 | 14.9 | 0.005 | 0.157 | 0.15 |
| 10 | UNIF(1930,2870) | 38 | 9.05 | 0.111 | 0.166 | 0.15 |
| 11 | UNIF(2040,2900) | 38 | 8.86 | 0.0685 | 0.173 | 0.15 |
| 12 | UNIF(2100,2860) | 38 | 2.74 | 0.741 | 0.127 | 0.15 |
| 13 | 2150+712*BETA(0.58,0.72) | 38 | 2.92 | 0.421 | 0.065 | 0.15 |
| 14 | UNIF(2120,2820) | 38 | 1.47 | 0.75 | 0.096 | 0.15 |
| 15 | UNIF(2100,2780) | 38 | 0.842 | 0.75 | 0.074 | 0.15 |
| 16 | UNIF(2150,2770) | 38 | 0.526 | 0.75 | 0.0953 | 0.15 |
| 17 | 2280+559*BETA(0.93,1.09) | 38 | 1.14 | 0.75 | 0.0696 | 0.15 |
| 18 | 2320+WEIB(312,1.58) | 38 | 3.04 | 0.228 | 0.128 | 0.15 |
| 19 | 2280+559*BETA(1.19,1.06) | 38 | 0.575 | 0.75 | 0.0961 | 0.15 |
| 20 | 2250+517*BETA(1.22,1.08) | 38 | 0.496 | 0.75 | 0.0914 | 0.15 |
| 21 | 2210+477*BETA(1.13,0.94) | 38 | 0.914 | 0.645 | 0.0907 | 0.15 |
| 22 | UNIF(2190,2660) | 38 | 3.68 | 0.599 | 0.138 | 0.15 |
| 23 | NORM(2350,125) | 38 | 0.547 | 0.473 | 0.0621 | 0.15 |

Table B.26. Arena PDF fitting summary for weekend energy demand in February.

| Hour | Expression | Sample Size | Chi-Square | p-value | K-S Test | p-value |
|------|--------------------------|-------------|------------|---------|----------|---------|
| 0 | TRIA(1990,2430,2480) | 32 | 1.91 | 0.405 | 0.12 | 0.15 |
| 1 | TRIA(1880,2280,2340) | 32 | 1.21 | 0.553 | 0.113 | 0.15 |
| 2 | TRIA(1780,2170,2220) | 32 | 0.419 | 0.75 | 0.135 | 0.15 |
| 3 | TRIA(1730,2110,2160) | 32 | 0.239 | 0.75 | 0.137 | 0.15 |
| 4 | TRIA(1710,2100,2140) | 32 | 0.574 | 0.75 | 0.126 | 0.15 |
| 5 | 1730+431*BETA(1.27,0.86) | 32 | 1.79 | 0.199 | 0.094 | 0.15 |
| 6 | 1670+538*BETA(1.3,0.77) | 32 | 1.15 | 0.301 | 0.136 | 0.15 |
| 7 | 1650+631*BETA(1.14,0.79) | 32 | 17.4 | 0.005 | 0.196 | 0.15 |
| 8 | 1720+775*BETA(0.69,0.58) | 32 | 5.79 | 0.0179 | 0.149 | 0.15 |
| 9 | 1840+895*BETA(0.64,0.6) | 32 | 8.24 | 0.005 | 0.137 | 0.15 |
| 10 | UNIF(1940,2840) | 32 | 8 | 0.0935 | 0.151 | 0.15 |
| 11 | UNIF(1990,2880) | 32 | 9.25 | 0.057 | 0.136 | 0.15 |
| 12 | UNIF(1970,2780) | 32 | 4.25 | 0.39 | 0.15 | 0.15 |
| 13 | UNIF(1980,2780) | 32 | 4.56 | 0.351 | 0.154 | 0.15 |
| 14 | UNIF(1950,2760) | 32 | 8 | 0.0935 | 0.169 | 0.15 |
| 15 | 1930+777*BETA(0.85,0.65) | 32 | 6 | 0.0499 | 0.14 | 0.15 |
| 16 | UNIF(1940,2700) | 32 | 7.69 | 0.106 | 0.182 | 0.15 |
| 17 | NORM(2420,180) | 32 | 4.48 | 0.0364 | 0.154 | 0.15 |
| 18 | 2200+WEIB(372,1.86) | 32 | 7.65 | 0.00592 | 0.135 | 0.15 |
| 19 | TRIA(2190,2690,2840) | 32 | 2.01 | 0.387 | 0.114 | 0.15 |
| 20 | TRIA(2160,2660,2760) | 32 | 1.3 | 0.527 | 0.111 | 0.15 |
| 21 | TRIA(2120,2590,2690) | 32 | 2.38 | 0.32 | 0.107 | 0.15 |
| 22 | TRIA(2140,2570,2610) | 32 | 0.384 | 0.75 | 0.134 | 0.15 |
| 23 | TRIA(2020,2480,2530) | 32 | 5.1 | 0.0823 | 0.147 | 0.15 |

Table B.27. Arena PDF fitting summary for weekend energy demand in March.

| Hour | Expression | Sample Size | Chi-Square | p-value | K-S Test | p-value |
|------|--------------------------|-------------|------------|---------|----------|---------|
| 0 | NORM(2250,119) | 34 | 1.86 | 0.192 | 0.098 | 0.15 |
| 1 | TRIA(1860,2190,2310) | 34 | 1.12 | 0.582 | 0.131 | 0.15 |
| 2 | 1770+443*BETA(1.54,1.17) | 34 | 0.79 | 0.403 | 0.0924 | 0.15 |
| 3 | NORM(1970,110) | 34 | 0.735 | 0.419 | 0.103 | 0.15 |
| 4 | NORM(1950,107) | 34 | 1.03 | 0.334 | 0.097 | 0.15 |
| 5 | TRIA(1720,1950,2170) | 34 | 0.691 | 0.432 | 0.181 | 0.15 |
| 6 | 1650+527*BETA(1.31,0.98) | 34 | 1.24 | 0.275 | 0.0977 | 0.15 |
| 7 | UNIF(1650,2210) | 34 | 6.29 | 0.193 | 0.189 | 0.15 |
| 8 | UNIF(1730,2450) | 34 | 8.06 | 0.0918 | 0.18 | 0.15 |
| 9 | 1860+802*BETA(0.58,0.64) | 34 | 5.12 | 0.0815 | 0.138 | 0.15 |
| 10 | UNIF(1910,2740) | 34 | 7.18 | 0.138 | 0.144 | 0.15 |
| 11 | UNIF(1940,2760) | 34 | 4.53 | 0.355 | 0.118 | 0.15 |
| 12 | UNIF(1890,2670) | 34 | 1 | 0.75 | 0.0928 | 0.15 |
| 13 | UNIF(1890,2640) | 34 | 0.706 | 0.75 | 0.122 | 0.15 |
| 14 | UNIF(1880,2600) | 34 | 1.29 | 0.75 | 0.124 | 0.15 |
| 15 | 1890+671*BETA(0.84,0.77) | 34 | 0.376 | 0.75 | 0.0624 | 0.15 |
| 16 | 1940+589*BETA(0.71,0.71) | 34 | 4.88 | 0.09 | 0.108 | 0.15 |
| 17 | UNIF(2010,2560) | 34 | 2.18 | 0.706 | 0.101 | 0.15 |
| 18 | NORM(2380,141) | 34 | 3.26 | 0.0758 | 0.11 | 0.15 |
| 19 | UNIF(2220,2760) | 34 | 3.94 | 0.428 | 0.14 | 0.15 |
| 20 | TRIA(2190,2550,2710) | 34 | 0.356 | 0.57 | 0.144 | 0.15 |
| 21 | TRIA(2140,2500,2630) | 34 | 0.792 | 0.403 | 0.122 | 0.15 |
| 22 | 2120+435*BETA(1.49,1.04) | 34 | 1.47 | 0.234 | 0.0938 | 0.15 |
| 23 | 2010+442*BETA(1.46,0.91) | 34 | 0.932 | 0.363 | 0.0978 | 0.15 |

Table B.28. Arena PDF fitting summary for weekend energy demand in April.

| Hour | Expression | Sample Size | Chi-Square | p-value | K-S Test | p-value |
|------|--------------------------|-------------|------------|---------|----------|---------|
| 0 | UNIF(1990,2400) | 38 | 5.58 | 0.365 | 0.131 | 0.15 |
| 1 | NORM(2080,102) | 38 | 2.05 | 0.172 | 0.104 | 0.15 |
| 2 | UNIF(1800,2170) | 38 | 2.11 | 0.75 | 0.118 | 0.15 |
| 3 | NORM(1930,103) | 38 | 0.492 | 0.489 | 0.0683 | 0.15 |
| 4 | NORM(1920,103) | 38 | 0.438 | 0.512 | 0.107 | 0.15 |
| 5 | NORM(1910,110) | 38 | 0.946 | 0.359 | 0.064 | 0.15 |
| 6 | NORM(1850,120) | 38 | 0.985 | 0.347 | 0.0709 | 0.15 |
| 7 | UNIF(1610,2100) | 38 | 3.37 | 0.647 | 0.123 | 0.15 |
| 8 | 1690+670*BETA(0.63,0.57) | 38 | 5.42 | 0.158 | 0.106 | 0.15 |
| 9 | 1780+715*BETA(0.59,0.47) | 38 | 1.88 | 0.19 | 0.131 | 0.15 |
| 10 | 1860+725*BETA(0.67,0.61) | 38 | 8.32 | 0.0173 | 0.106 | 0.15 |
| 11 | UNIF(1880,2640) | 38 | 16.3 | 0.0063 | 0.168 | 0.15 |
| 12 | UNIF(1870,2600) | 38 | 7.16 | 0.219 | 0.1 | 0.15 |
| 13 | 1860+734*BETA(1.11,1.03) | 38 | 5.18 | 0.175 | 0.13 | 0.15 |
| 14 | 1820+770*BETA(1.19,1.09) | 38 | 1.79 | 0.427 | 0.0841 | 0.15 |
| 15 | 1810+724*BETA(1.25,1.06) | 38 | 1.76 | 0.432 | 0.1 | 0.15 |
| 16 | 1820+703*BETA(1.31,1.18) | 38 | 2.13 | 0.366 | 0.0793 | 0.15 |
| 17 | UNIF(1850,2540) | 38 | 2.74 | 0.741 | 0.104 | 0.15 |
| 18 | NORM(2240,170) | 38 | 0.969 | 0.352 | 0.0756 | 0.15 |
| 19 | TRIA(2040,2410,2680) | 38 | 2.9 | 0.24 | 0.124 | 0.15 |
| 20 | TRIA(2150,2470,2730) | 38 | 2.85 | 0.243 | 0.106 | 0.15 |
| 21 | TRIA(2120,2410,2670) | 38 | 1.7 | 0.444 | 0.0991 | 0.15 |
| 22 | TRIA(2100,2370,2580) | 38 | 1.24 | 0.545 | 0.0994 | 0.15 |
| 23 | NORM(2240,112) | 38 | 0.591 | 0.461 | 0.0806 | 0.15 |

Table B.29. Arena PDF fitting summary for weekend energy demand in May.

| Hour | Expression | Sample Size | Chi-Square | p-value | K-S Test | p-value |
|------|--------------------------|-------------|------------|---------|----------|---------|
| 0 | TRIA(1940,2100,2520) | 38 | 0.935 | 0.639 | 0.0672 | 0.15 |
| 1 | NORM(2080,140) | 38 | 0.384 | 0.55 | 0.11 | 0.15 |
| 2 | TRIA(1750,1910,2370) | 38 | 0.197 | 0.75 | 0.0913 | 0.15 |
| 3 | 1710+WEIB(258,1.48) | 38 | 1.48 | 0.233 | 0.1 | 0.15 |
| 4 | 1690+526*BETA(1.24,1.73) | 38 | 1.14 | 0.577 | 0.0986 | 0.15 |
| 5 | 1630+460*BETA(1.35,1.61) | 38 | 0.48 | 0.75 | 0.0944 | 0.15 |
| 6 | TRIA(1570,1730,2030) | 38 | 0.591 | 0.745 | 0.118 | 0.15 |
| 7 | UNIF(1610,2060) | 38 | 1.79 | 0.75 | 0.122 | 0.15 |
| 8 | UNIF(1690,2350) | 38 | 8.11 | 0.165 | 0.179 | 0.15 |
| 9 | UNIF(1750,2540) | 38 | 5.89 | 0.33 | 0.16 | 0.15 |
| 10 | UNIF(1820,2620) | 38 | 8.42 | 0.147 | 0.131 | 0.15 |
| 11 | UNIF(1880,2650) | 38 | 8.42 | 0.147 | 0.173 | 0.15 |
| 12 | 1880+777*BETA(1.15,1.54) | 38 | 4.3 | 0.125 | 0.117 | 0.15 |
| 13 | UNIF(1930,2570) | 38 | 8.74 | 0.129 | 0.132 | 0.15 |
| 14 | 1960+634*BETA(0.76,0.91) | 38 | 5.14 | 0.178 | 0.104 | 0.15 |
| 15 | UNIF(1960,2590) | 38 | 3.37 | 0.647 | 0.143 | 0.15 |
| 16 | 1960+634*BETA(1.07,1.48) | 38 | 4.44 | 0.227 | 0.0778 | 0.15 |
| 17 | UNIF(1960,2530) | 38 | 2.42 | 0.75 | 0.112 | 0.15 |
| 18 | NORM(2250,158) | 38 | 0.277 | 0.626 | 0.0831 | 0.15 |
| 19 | TRIA(2010,2260,2670) | 38 | 0.381 | 0.75 | 0.0764 | 0.15 |
| 20 | NORM(2380,116) | 38 | 1.35 | 0.247 | 0.156 | 0.15 |
| 21 | TRIA(2160,2360,2650) | 38 | 0.753 | 0.695 | 0.166 | 0.15 |
| 22 | TRIA(2140,2270,2570) | 38 | 1.65 | 0.452 | 0.0696 | 0.15 |
| 23 | NORM(2220,109) | 38 | 0.218 | 0.668 | 0.062 | 0.15 |

Table B.30. Arena PDF fitting summary for weekend energy demand in June.

| Hour | Expression | Sample Size | Chi-Square | p-value | K-S Test | p-value |
|------|---------------------------|-------------|------------|---------|----------|---------|
| 0 | TRIA(1740,2450,2690) | 41 | 2.12 | 0.369 | 0.114 | 0.15 |
| 1 | TRIA(1640,2250,2590) | 41 | 4.85 | 0.0913 | 0.142 | 0.15 |
| 2 | TRIA(1560,2240,2470) | 41 | 5.88 | 0.0539 | 0.157 | 0.15 |
| 3 | TRIA(1500,2110,2390) | 41 | 4.39 | 0.118 | 0.176 | 0.15 |
| 4 | UNIF(1470,2350) | 41 | 7.15 | 0.22 | 0.147 | 0.15 |
| 5 | TRIA(1400,1940,2240) | 41 | 3.37 | 0.201 | 0.145 | 0.15 |
| 6 | NORM(1790,221) | 41 | 0.475 | 0.494 | 0.107 | 0.15 |
| 7 | NORM(1820,235) | 41 | 0.571 | 0.467 | 0.0687 | 0.15 |
| 8 | UNIF(1440,2570) | 41 | 3.34 | 0.651 | 0.118 | 0.15 |
| 9 | UNIF(1510,2720) | 41 | 3.93 | 0.563 | 0.113 | 0.15 |
| 10 | UNIF(1520,2830) | 41 | 11.5 | 0.0434 | 0.0987 | 0.15 |
| 11 | 1500+1430*BETA(1.37,1.29) | 41 | 4.62 | 0.0996 | 0.108 | 0.15 |
| 12 | NORM(2220,340) | 41 | 2.17 | 0.158 | 0.0884 | 0.15 |
| 13 | NORM(2260,349) | 41 | 2.09 | 0.167 | 0.081 | 0.15 |
| 14 | NORM(2280,354) | 41 | 0.858 | 0.384 | 0.0802 | 0.15 |
| 15 | NORM(2270,343) | 41 | 0.399 | 0.54 | 0.0797 | 0.15 |
| 16 | TRIA(1580,2340,2890) | 41 | 0.623 | 0.735 | 0.0955 | 0.15 |
| 17 | TRIA(1650,2370,2810) | 41 | 1.69 | 0.445 | 0.107 | 0.15 |
| 18 | NORM(2300,288) | 41 | 1.84 | 0.194 | 0.0667 | 0.15 |
| 19 | UNIF(1810,2790) | 41 | 4.51 | 0.482 | 0.13 | 0.15 |
| 20 | NORM(2370,250) | 41 | 0.575 | 0.465 | 0.0699 | 0.15 |
| 21 | NORM(2400,248) | 41 | 0.726 | 0.422 | 0.0783 | 0.15 |
| 22 | NORM(2370,246) | 41 | 0.72 | 0.424 | 0.0799 | 0.15 |
| 23 | TRIA(1830,2340,2660) | 41 | 1.43 | 0.492 | 0.111 | 0.15 |

Table B.31. Arena PDF fitting summary for weekend energy demand in July.

| Hour | Expression | Sample Size | Chi-Square | p-value | K-S Test | p-value |
|------|--------------------------|-------------|------------|---------|----------|---------|
| 0 | TRIA(2190,2780,2880) | 37 | 0.921 | 0.643 | 0.132 | 0.15 |
| 1 | 2050+674*BETA(2.34,1.26) | 37 | 1.3 | 0.256 | 0.123 | 0.15 |
| 2 | NORM(2390,143) | 37 | 1.22 | 0.28 | 0.116 | 0.15 |
| 3 | NORM(2320,143) | 37 | 2.48 | 0.124 | 0.113 | 0.15 |
| 4 | NORM(2260,151) | 37 | 1.24 | 0.273 | 0.105 | 0.15 |
| 5 | TRIA(1750,2240,2400) | 37 | 2.29 | 0.337 | 0.149 | 0.15 |
| 6 | 1710+646*BETA(1.88,1.18) | 37 | 1.45 | 0.488 | 0.0835 | 0.15 |
| 7 | NORM(2170,168) | 37 | 0.982 | 0.348 | 0.0954 | 0.15 |
| 8 | 1450+1120*BETA(1.48,1.4) | 37 | 4.25 | 0.129 | 0.167 | 0.15 |
| 9 | UNIF(2060,2930) | 37 | 7.92 | 0.176 | 0.131 | 0.15 |
| 10 | UNIF(2170,3040) | 37 | 8.89 | 0.12 | 0.138 | 0.15 |
| 11 | UNIF(2260,3110) | 37 | 5 | 0.429 | 0.126 | 0.15 |
| 12 | UNIF(2250,3030) | 37 | 3.05 | 0.693 | 0.0993 | 0.15 |
| 13 | UNIF(2280,3080) | 37 | 3.7 | 0.597 | 0.121 | 0.15 |
| 14 | UNIF(2300,3110) | 37 | 3.7 | 0.597 | 0.126 | 0.15 |
| 15 | UNIF(2290,3070) | 37 | 8.24 | 0.157 | 0.13 | 0.15 |
| 16 | UNIF(2280,3050) | 37 | 2.08 | 0.75 | 0.131 | 0.15 |
| 17 | 2190+825*BETA(1.61,1.14) | 37 | 2.81 | 0.247 | 0.0916 | 0.15 |
| 18 | TRIA(2170,2700,2990) | 37 | 1.39 | 0.499 | 0.171 | 0.15 |
| 19 | TRIA(2180,2670,3010) | 37 | 2.77 | 0.25 | 0.178 | 0.15 |
| 20 | NORM(2760,200) | 37 | 1.9 | 0.187 | 0.0845 | 0.15 |
| 21 | NORM(2780,198) | 37 | 1.99 | 0.178 | 0.109 | 0.15 |
| 22 | TRIA(2340,2770,3020) | 37 | 3.83 | 0.163 | 0.174 | 0.15 |
| 23 | TRIA(2200,2730,2910) | 37 | 2.34 | 0.328 | 0.153 | 0.15 |

Table B.32. Arena PDF fitting summary for weekend energy demand in August.

| Hour | Expression | Sample Size | Chi-Square | p-value | K-S Test | p-value |
|------|--------------------------|-------------|------------|---------|----------|---------|
| 0 | TRIA(2010,2580,2900) | 44 | 0.893 | 0.652 | 0.117 | 0.15 |
| 1 | NORM(2370,217) | 44 | 0.897 | 0.373 | 0.118 | 0.15 |
| 2 | TRIA(1830,2330,2670) | 44 | 0.998 | 0.62 | 0.106 | 0.15 |
| 3 | TRIA(1770,2260,2620) | 44 | 0.392 | 0.75 | 0.108 | 0.15 |
| 4 | UNIF(1750,2570) | 44 | 8.09 | 0.166 | 0.15 | 0.15 |
| 5 | NORM(2130,204) | 44 | 2.58 | 0.114 | 0.107 | 0.15 |
| 6 | TRIA(1630,2100,2430) | 44 | 0.789 | 0.684 | 0.099 | 0.15 |
| 7 | TRIA(1640,2150,2510) | 44 | 2.02 | 0.385 | 0.105 | 0.15 |
| 8 | NORM(2240,305) | 44 | 0.675 | 0.437 | 0.0706 | 0.15 |
| 9 | NORM(2380,360) | 44 | 1.51 | 0.23 | 0.0794 | 0.15 |
| 10 | NORM(2470,380) | 44 | 0.574 | 0.466 | 0.0635 | 0.15 |
| 11 | NORM(2530,389) | 44 | 0.395 | 0.543 | 0.0586 | 0.15 |
| 12 | TRIA(1670,2720,3140) | 44 | 3.73 | 0.171 | 0.15 | 0.15 |
| 13 | NORM(2550,361) | 44 | 2.09 | 0.167 | 0.0865 | 0.15 |
| 14 | TRIA(1790,2760,3210) | 44 | 0.988 | 0.623 | 0.0873 | 0.15 |
| 15 | NORM(2580,340) | 44 | 1.34 | 0.248 | 0.0709 | 0.15 |
| 16 | NORM(2590,316) | 44 | 0.463 | 0.498 | 0.076 | 0.15 |
| 17 | TRIA(1960,2670,3060) | 44 | 3.08 | 0.225 | 0.156 | 0.15 |
| 18 | 2040+1000*BETA(1.6,1.3) | 44 | 0.735 | 0.701 | 0.0778 | 0.15 |
| 19 | TRIA(2140,2730,3060) | 44 | 0.972 | 0.628 | 0.106 | 0.15 |
| 20 | 2260+894*BETA(1.65,1.46) | 44 | 0.315 | 0.315 | 0.0657 | 0.15 |
| 21 | 2240+881*BETA(1.64,1.59) | 44 | 0.426 | 0.75 | 0.082 | 0.15 |
| 22 | NORM(2640,207) | 44 | 1.56 | 0.225 | 0.0728 | 0.15 |
| 23 | 2110+810*BETA(1.67,1.46) | 44 | 1.29 | 0.53 | 0.0662 | 0.15 |

Table B.33. Arena PDF fitting summary for weekend energy demand in September.

| Hour | Expression | Sample Size | Chi-Square | p-value | K-S Test | p-value |
|------|---------------------------|-------------|------------|---------|----------|---------|
| 0 | TRIA(1630,2300,2680) | 43 | 9.46 | 0.0091 | 0.132 | 0.15 |
| 1 | 1520+1040*BETA(1.33,1.12) | 43 | 7.01 | 0.0316 | 0.113 | 0.15 |
| 2 | 1460+1000*BETA(1.28,1.06) | 43 | 7.08 | 0.0303 | 0.122 | 0.15 |
| 3 | TRIA(1400,2150,2390) | 43 | 4.41 | 0.116 | 0.109 | 0.15 |
| 4 | TRIA(1390,2140,2350) | 43 | 5.93 | 0.0523 | 0.113 | 0.15 |
| 5 | TRIA(1360,2140,2320) | 43 | 4.05 | 0.258 | 0.124 | 0.15 |
| 6 | TRIA(1330,2040,2230) | 43 | 8.9 | 0.0324 | 0.137 | 0.15 |
| 7 | 1350+929*BETA(1.24,1.01) | 43 | 4.12 | 0.249 | 0.101 | 0.15 |
| 8 | UNIF(1460,2540) | 43 | 2.07 | 0.75 | 0.081 | 0.15 |
| 9 | UNIF(1520,2760) | 43 | 2.63 | 0.75 | 0.0897 | 0.15 |
| 10 | 1540+1330*BETA(1.4,1.29) | 43 | 0.498 | 0.75 | 0.097 | 0.15 |
| 11 | 1550+WEIB(808,1.97) | 43 | 1.48 | 0.233 | 0.0951 | 0.15 |
| 12 | NORM(2260,315) | 43 | 1.53 | 0.227 | 0.0706 | 0.15 |
| 13 | NORM(2300,320) | 43 | 2.37 | 0.137 | 0.0642 | 0.15 |
| 14 | NORM(2310,330) | 43 | 1.62 | 0.218 | 0.0646 | 0.15 |
| 15 | 1620+1310*BETA(1.54,1.42) | 43 | 0.319 | 0.75 | 0.0692 | 0.15 |
| 16 | 1630+1290*BETA(1.59,1.47) | 43 | 0.653 | 0.726 | 0.0747 | 0.15 |
| 17 | NORM(2300,312) | 43 | 4.85 | 0.0286 | 0.106 | 0.15 |
| 18 | TRIA(1660,2590,2910) | 43 | 3.19 | 0.216 | 0.0854 | 0.15 |
| 19 | TRIA(1820,2570,2980) | 43 | 1.51 | 0.477 | 0.112 | 0.15 |
| 20 | TRIA(1850,2530,3010) | 43 | 2.42 | 0.313 | 0.0973 | 0.15 |
| 21 | TRIA(1810,2460,2930) | 43 | 1.35 | 0.511 | 0.1 | 0.15 |
| 22 | TRIA(1790,2410,2850) | 43 | 2.41 | 0.315 | 0.0744 | 0.15 |
| 23 | TRIA(1720,2310,2740) | 43 | 0.588 | 0.746 | 0.0782 | 0.15 |

Table B.34. Arena PDF fitting summary for weekend energy demand in October.

| Hour | Expression | Sample Size | Chi-Square | p-value | K-S Test | p-value |
|------|--------------------------|-------------|------------|---------|----------|---------|
| 0 | UNIF(1920,2270) | 37 | 7.27 | 0.213 | 0.153 | 0.15 |
| 1 | UNIF(1980,2310) | 37 | 3.19 | 0.0785 | 0.119 | 0.15 |
| 2 | TRIA(1730,1930, 2080) | 37 | 4.9 | 0.0894 | 0.224 | 0.0429 |
| 3 | 1700+319*BETA(1.11,0.85) | 37 | 9.5 | 0.00896 | 0.158 | 0.15 |
| 4 | 1980+330*BETA(1.25,1.34) | 37 | 12 | 0.005 | 0.159 | 0.15 |
| 5 | UNIF(1660,2010) | 37 | 2.03 | 0.573 | 0.184 | 0.145 |
| 6 | UNIF(1660,2020) | 37 | 14.1 | 0.0167 | 0.174 | 0.15 |
| 7 | UNIF(1630,2060) | 37 | 7.27 | 0.213 | 0.166 | 0.15 |
| 8 | 1730+599*BETA(0.51,0.67) | 37 | 6.96 | 0.00871 | 0.162 | 0.15 |
| 9 | 1770+725*BETA(0.55,0.63) | 37 | 6.19 | 0.0141 | 0.135 | 0.15 |
| 10 | UNIF(1820,2560) | 37 | 11.5 | 0.0441 | 0.155 | 0.15 |
| 11 | UNIF(1830,2600) | 37 | 4.03 | 0.548 | 0.109 | 0.15 |
| 12 | UNIF(1800,2500) | 37 | 3.05 | 0.693 | 0.0854 | 0.15 |
| 13 | 1800+669*BETA(1.1,0.84) | 37 | 3.3 | 0.207 | 0.121 | 0.15 |
| 14 | 1820+718*BETA(1.28,1.2) | 37 | 5.43 | 0.0701 | 0.112 | 0.15 |
| 15 | 1840+658*BETA(1.31,1.17) | 37 | 4.89 | 0.0897 | 0.114 | 0.15 |
| 16 | UNIF(1920,2460) | 37 | 9.54 | 0.0917 | 0.109 | 0.15 |
| 17 | UNIF(1990,2480) | 37 | 11.2 | 0.0487 | 0.175 | 0.15 |
| 18 | NORM(2380,131) | 37 | 10.3 | 0.005 | 0.156 | 0.15 |
| 19 | 2190+402*BETA(1.16,0.98) | 37 | 13.6 | 0.005 | 0.153 | 0.15 |
| 20 | 2120+408*BETA(1.43,1.06) | 37 | 5.7 | 0.0605 | 0.143 | 0.15 |
| 21 | TRIA(2090,2260,2480) | 37 | 3.9 | 0.0487 | 0.149 | 0.15 |
| 22 | UNIF(2070,2420) | 37 | 2.41 | 0.75 | 0.127 | 0.15 |
| 23 | UNIF(1980,2310) | 37 | 2.41 | 0.75 | 0.143 | 0.15 |

Table B.35. Arena PDF fitting summary for weekend energy demand in November.

| Hour | Expression | Sample Size | Chi-Square | p-value | K-S Test | p-value |
|------|--------------------------|-------------|------------|---------|----------|---------|
| 0 | TRIA(2060,2220,2460) | 33 | 0.0622 | 0.75 | 0.104 | 0.15 |
| 1 | TRIA(1940,2140,2290) | 33 | 1.28 | 0.262 | 0.13 | 0.15 |
| 2 | TRIA(1830,2030,2220) | 33 | 0.619 | 0.453 | 0.117 | 0.15 |
| 3 | UNIF(1790,2160) | 33 | 3.52 | 0.481 | 0.125 | 0.15 |
| 4 | 1770+362*BETA(1.49,1.4) | 33 | 0.355 | 0.571 | 0.0683 | 0.15 |
| 5 | 1780+379*BETA(1.46,1.42) | 33 | 0.0244 | 0.75 | 0.0722 | 0.15 |
| 6 | 1780+430*BETA(1.37,1.37) | 33 | 0.62 | 0.736 | 0.0814 | 0.15 |
| 7 | UNIF(1750,2270) | 33 | 3.21 | 0.525 | 0.0755 | 0.15 |
| 8 | 1790+727*BETA(0.58,0.67) | 33 | 0.399 | 0.54 | 0.131 | 0.15 |
| 9 | UNIF(1830,2710) | 33 | 4.12 | 0.406 | 0.194 | 0.15 |
| 10 | UNIF(1870,2770) | 33 | 2.61 | 0.631 | 0.102 | 0.15 |
| 11 | 1890+895*BETA(0.81,0.81) | 38 | 2.18 | 0.539 | 0.067 | 0.15 |
| 12 | 1870+792*BETA(0.87,0.86) | 38 | 3.14 | 0.389 | 0.12 | 0.15 |
| 13 | UNIF(1900,2660) | 38 | 1.79 | 0.75 | 0.102 | 0.15 |
| 14 | UNIF(1920,2660) | 38 | 0.842 | 0.75 | 0.0675 | 0.15 |
| 15 | 1960+679*BETA(0.85,0.92) | 38 | 1.59 | 0.667 | 0.0864 | 0.15 |
| 16 | 2060+613*BETA(0.74,0.9) | 38 | 1.51 | 0.477 | 0.0692 | 0.15 |
| 17 | UNIF(2150,2780) | 38 | 1.79 | 0.75 | 0.122 | 0.15 |
| 18 | NORM(2570,141) | 38 | 2.08 | 0.168 | 0.0872 | 0.15 |
| 19 | 2260+511*BETA(1.73,1.49) | 38 | 3.14 | 0.22 | 0.119 | 0.15 |
| 20 | TRIA(2240,2510,2720) | 38 | 2.61 | 0.279 | 0.122 | 0.15 |
| 21 | TRIA(2200,2520,2660) | 38 | 1.36 | 0.507 | 0.123 | 0.15 |
| 22 | NORM(2380,104) | 38 | 3.83 | 0.0504 | 0.0949 | 0.15 |
| 23 | NORM(2280,104) | 38 | 1.2 | 0.286 | 0.0839 | 0.15 |

Table B.36. Arena PDF fitting summary for weekend energy demand in December.

| Hour | Expression | Sample Size | Chi-Square | p-value | K-S Test | p-value |
|------|---------------------------|-------------|------------|---------|----------|---------|
| 0 | UNIF(2240,2510) | 38 | 6.53 | 0.261 | 0.129 | 0.15 |
| 1 | UNIF(2080,2370) | 38 | 3.05 | 0.694 | 0.114 | 0.15 |
| 2 | UNIF(1970,2250) | 38 | 3.68 | 0.599 | 0.0953 | 0.15 |
| 3 | 1920+294*BETA(0.94,1.17) | 38 | 1.47 | 0.485 | 0.0764 | 0.15 |
| 4 | UNIF(1890,2180) | 38 | 2.42 | 0.75 | 0.0976 | 0.15 |
| 5 | UNIF(1870,2210) | 38 | 3.37 | 0.647 | 0.111 | 0.15 |
| 6 | 1910+335*BETA(0.7,0.87) | 38 | 2.94 | 0.418 | 0.0747 | 0.15 |
| 7 | 1850+505*BETA(1.12,1.04) | 38 | 5.8 | 0.132 | 0.149 | 0.15 |
| 8 | 1900+691*BETA(0.45,0.532) | 38 | 0.839 | 0.389 | 0.14 | 0.15 |
| 9 | 1980+813*BETA(0.44,0.48) | 38 | 1.56 | 0.225 | 0.138 | 0.15 |
| 10 | UNIF(2050,2890) | 38 | 7.53 | 0.116 | 0.178 | 0.15 |
| 11 | UNIF(2110,2940) | 38 | 10.9 | 0.0533 | 0.154 | 0.15 |
| 12 | UNIF(2120,2880) | 38 | 6.53 | 0.261 | 0.0956 | 0.15 |
| 13 | 2130+750*BETA(0.91,0.99) | 38 | 1.65 | 0.655 | 0.0839 | 0.15 |
| 14 | UNIF(2140,2870) | 38 | 4 | 0.552 | 0.0964 | 0.15 |
| 15 | UNIF(2150,2830) | 38 | 7.47 | 0.201 | 0.112 | 0.15 |
| 16 | UNIF(2230,2790) | 38 | 3.37 | 0.647 | 0.106 | 0.15 |
| 17 | UNIF(2390,2840) | 38 | 8.11 | 0.165 | 0.125 | 0.15 |
| 18 | UNIF(2480,2910) | 38 | 3.37 | 0.647 | 0.0905 | 0.15 |
| 19 | TRIA(2420,2740,2840) | 38 | 3.11 | 0.223 | 0.162 | 0.15 |
| 20 | TRIA(2310,2700,2770) | 38 | 0.963 | 0.63 | 0.0863 | 0.15 |
| 21 | NORM(2540,111) | 38 | 2.62 | 0.109 | 0.108 | 0.15 |
| 22 | NORM(2490,105) | 38 | 3.26 | 0.0756 | 0.107 | 0.15 |
| 23 | TRIA(2110,2510,2560) | 38 | 3.28 | 0.369 | 0.113 | 0.15 |